Technische Universität München

Quantum effects on right-handed neutrino parameters and phenomenological implications

Dissertation

by

Patrick Strobl

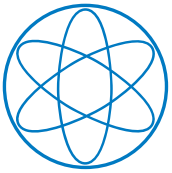

Physics Department, T30d

&

Collaborative Research Center SFB 1258

"Neutrinos and Dark Matter in Astro- and Particle Physics"

Technische Universität München

Physik-Department T30d

Quantum effects on right-handed neutrino parameters and phenomenological implications

Patrick Strobl

Vollständiger Abdruck der von der Fakultät für Physik der Technischen Universität München zur Erlangung des akademischen Grades eines

Doktors der Naturwissenschaften

genehmigten Dissertation.

Vorsitzender:		Prof. Dr. Lothar Oberauer
Prüfende der Dissertation:	1.	Prof. Dr. Alejandro Ibarra
	2.	Prof. Dr. Nora Brambilla

Die Dissertation wurde am 24.03.2021 bei der Technischen Universität München eingereicht und durch die Fakultät für Physik am 03.05.2021 angenommen.

Abstract

According to the Standard Model (SM) of Particle Physics neutrinos are massless. But accumulating evidence from neutrino oscillation experiments shows that at least two neutrinos have a non-zero mass. One way to account for the light, but non-zero left-handed neutrino (LHN) masses, is through the type-I seesaw mechanism in which right-handed neutrinos (RHNs) are added to the SM. The resulting LHN masses are inversely proportional to the RHN masses $m_\nu = (Y_\nu \langle \Phi \rangle)^2 / M$, where Y_ν denotes the neutrino Yukawa coupling and $\langle \Phi \rangle$ the Higgs VEV. For a sizable coupling $Y_\nu \sim \mathcal{O}(1)$, the RHN Majorana masses should be $M \sim \mathcal{O}(10^{14})\,\text{GeV}$ to explain the observed neutrino mass scale $m_\nu \sim \mathcal{O}(0.1)\,\text{eV}$. Even though this seesaw mechanism provides a simple, qualitative scenario in which the active LHN masses are explained by the existence of a heavy seesaw mass scale, it does not explain its origin. In this work, the idea of using quantum effects to generate the RHN mass scales is explored. Using the conjecture that lepton number violation by the RHN mass term occurs at Planck-scale, it is possible to generate the seesaw scale via two-loop effects. Irrespective of the exact mass scale at which the RHNs are introduced, using quantum effects to generate some RHN masses is an interesting possibility to reduce the number of free parameters in neutrino mass models and thus increase predictivity. The studied two-loop quantum effects can alter the RHN mass spectrum due to sizable or dominant contributions and thus significantly affect the low-energy phenomenology of neutrinos. Several realizations of neutrino mass models that incorporate radiative generation of RHN masses are investigated. In detail, the SM extended with two and three RHNs is explored as well as extensions of the scalar sector of the SM, comprising of a two-Higgs doublet model and an inert scalar variant. It is shown how lepton violation at the Planck scale is phenomenologically viable by exploiting two-loop effects and how it can reproduce the observed neutrino parameters in the considered scenarios.

Zusammenfassung

Gemäß dem Standardmodell (SM) der Teilchenphysik sind Neutrinos masselos. Dennoch gibt es zunehmend Belege aus Neutrinooszillationsexperimenten, dass mindestens zwei der Neutrinos eine nicht verschwindende Masse haben. Eine Möglichkeit, um die leichten, aber nicht verschwindenden linkshändigen Neutrinomassen zu erklären, ist der Typ-I Seesaw-Mechanismus, in dem rechtshändige Neutrinos (RHNs) zum SM hinzugefügt werden. Die resultierenden leichten Neutrinomassen sind umgekehrt proportional zu den RHN-Massen $m_\nu = (Y_\nu \langle\Phi\rangle)^2/M$ wobei Y_ν die Neutrino-Yukawa-Kopplung und $\langle\Phi\rangle$ den Vakuumerwartungswert des Higgs-Bosons bezeichnet. Für eine Kopplung von beträchtlicher Größe $Y_\nu \sim \mathcal{O}(1)$ sollten die RHN-Majoranamassen von der Größenordnung $M \sim \mathcal{O}(10^{14})\,\mathrm{GeV}$ sein, um die beobachtete Neutrinomassenskala von $m_\nu \sim \mathcal{O}(0.1)\,\mathrm{eV}$ zu erklären. Obwohl dieser Seesaw-Mechanismus ein einfaches qualitatives Szenario beschreibt, in dem die nicht verschwindenden aktiven Neutrinomassen durch die Anwesenheit von einer schweren Seesaw-Massenskala erklärt werden, wird ihr Ursprung selbst nicht erklärt. In dieser Arbeit wird der Ansatz untersucht, Quanteneffekte zu nutzen, um die RHN-Massenskala zu erzeugen. Nutzt man die Vermutung, dass die Leptonenzahlverletzung durch den RHN-Massenterm auf der Planck-Skala stattfindet, ist es möglich, die bekannte Seesaw-Skala durch Zweischleifeneffekte zu generieren. Ungeachtet der exakten Massenskala, auf welcher die RHNs eingeführt werden, ist das Ausnutzen von Quanteneffekten, um einige RHN-Massen zu erzeugen eine interessante Möglichkeit, um die Anzahl an freien Parametern in Neutrinomassenmodellen zu reduzieren und dadurch ihre Vorhersagbarkeit zu erhöhen. Die untersuchten von RHNs veranlassten Zweischleifen-Quanteneffekte, können das Massenspektrum der RHNs aufgrund von beträchtlichen oder sogar dominanten Beiträgen signifikant ändern und damit die Phänomenologie bei niedrigen Energien der leichten Neutrinos beeinflussen. Verschiedene Realisierungen von Neutrinomassenmodellen, die die radiative Erzeugung von rechtshändigen Neutrinomassen beinhalten, werden untersucht. Im Einzelnen wird das SM erweitert mit zwei und drei RHNs betrachtet sowie Erweiterungen des Skalarsektors wie ein Modell mit zwei Higgs-Dubletts und eine Variante mit inerten Skalaren. Es wird gezeigt, dass Leptonenzahlverletzung auf der Planck-Skala durch das Ausnutzen von Zweischleifen-Quanteneffekten phänomenologisch sinnvoll ist und wie es damit möglich ist, die beobachteten Neutrinoparameter in den betrachteten Szenarien zu reproduzieren.

This dissertation builds on studies presented in

- **Mechanism of Neutrino Mass Generation by Planck-Scale Lepton Number Breaking.** [1]
  Patrick Strobl.
  Master's thesis, Technical University of Munich (2018)

In the context of this dissertation the following works have been published:

- **Neutrino Masses from Planck-Scale Lepton Number Breaking.** [2]
  Alejandro Ibarra, Patrick Strobl, and Takashi Toma.
  Physical Review Letters **122**, no. 8 (2019)
- **Two-Loop Renormalization Group Equations for Right-Handed Neutrino Masses and Phenomenological Implications.** [3]
  Alejandro Ibarra, Patrick Strobl, and Takashi Toma.
  Physical Review D **102**, no. 5 (2020)
- **Neutrino Parameters in the Planck-Scale Lepton Number Breaking Scenario with Extended Scalar Sectors.** [4]
  César Bonilla, Johannes Herms, Alejandro Ibarra, and Patrick Strobl.
  Physical Review D **103**, no. 3 (2021)

Contents

Chapter 1

Introduction

The origin of neutrino masses remains one of the biggest puzzles in Particle Physics. Although the Standard Model (SM) of Particle Physics is showing great success in describing particles as well as their interactions, it predicts neutrinos to be massless particles. From the experimental observation of neutrino oscillations, we know that at least two of the three active neutrinos are massive. Neutrino oscillations experiments have also shown that the mass scale of the neutrinos is by many orders of magnitude smaller than of the other known fermions, as well as that the neutrino mass hierarchies are much milder than those of other fermions in the SM.

Neutrino masses may give a hint about high-scale physics and the theoretical structures underlying the Standard Model. They may be the key to grand unifying theories (GUTs), supersymmetric models [5–7] or models involving extra space-dimensions [8–10]. Many open questions in Fundamental Physics like the nature of dark matter [11, 12] and dark energy [13, 14], the baryon asymmetry of the Universe [15, 16] and the strong CP problem [17, 18], *etc.* may be linked to the mechanism behind the generation of light neutrino masses.

Even though a multitude of mechanisms to include massive neutrinos in the SM have been proposed, the origin of neutrino masses still remains unknown. One of the most popular and theoretically well-motivated models to introduce neutrino masses into the SM is the so-called seesaw mechanism (see [19–22]).

In the simplest realization of the seesaw mechanism (type-I seesaw), the SM is extended with a number of right-handed neutrinos coupling to the left-handed SM lepton doublet via a Yukawa interaction. The newly introduced right-handed neutrinos are singlets under the gauge group of the SM, allowing a Majorana mass term for right-handed neutrinos and a mass scale which can be far above the scale of the electroweak symmetry breaking (EWSB). Introducing a Yukawa interaction between the left-handed doublet and right-handed neutrinos, the neutrinos participating in weak interactions obtain tiny masses, as observed, when the right-handed neutrino (RHN) masses are far above the EWSB scale, reminiscent of a seesaw.

One of the major drawbacks of the seesaw mechanism is the large number of unknown parameters introduced by the model, reducing its predictive power. The Yukawa couplings between the left- and right-handed fields and the Majorana masses of the right-handed neutrinos are unknown *a priori*, facing only the constraint to reproduce the observed neutrino oscillations parameters. The problem of many free parameters can be approached by choosing the most minimal set-up which is still able to reproduce the observed data.

In this thesis, quantum effects on the right-handed neutrino parameters are explored and

it is investigated how these effects can be applied in different neutrino mass models. We will show that in some scenarios quantum effects play an important role in the low-energy phenomenology and specifically in enhancing the predictive power of the seesaw model.

This work is structured as follows: In chapter 2 a short review of the Standard Model of Particle Physics and neutrino physics is given. Since the studied effects will significantly affect the low-energy neutrino parameters through the seesaw mechanism, chapter 3 is dedicated to a review of the type-I seesaw. Chapter 4 investigates how quantum effects can be used to generate right-handed neutrino masses in the Standard Model extended with RHNs, prior to exploring the low-energy phenomenology of a minimally extended Standard Model. As concrete examples, extensions by two and three right-handed neutrinos are considered in chapter 5. The minimally extended SM scenario requires non-generic assumptions on the high-scale parameters to be phenomenologically viable. Even though the observed neutrino mass scale can be reproduced, the neutrino mass hierarchy is typically too large. This can be circumvented if the scalar sector is minimally extended. In chapters 6 and 7, RHN mass generation in models with an extended scalar sector are explored in which low-energy quantum effects are also considered. It is shown how the observed neutrino mass scale and mild neutrino mass hierarchy can be reproduced by making generic assumptions on the high-energy parameters. As extended scalar sector models, a two-Higgs doublet model and a scotogenic variant with two inert doublets are investigated, respectively. The results of this work are summarized in the final chapter 8.

Chapter 2

Massive Neutrinos and the Standard Model

2.1 The Standard Model

The Standard Model (SM) of Particle Physics is an instance of a quantum field theory which only contains renormalizable operators. It correctly describes the known strong, weak and electromagnetic interactions. It is based on the gauge principle and constructed to show invariance under the Standard Model gauge symmetry group $G_{123} = U(1)_Y \times SU(2)_L \times SU(3)_c$. All fundamental interactions are mediated by spin-1 gauge bosons as force carriers. Corresponding to the electromagnetic, weak and strong force, there is the photon γ, the $W^{\pm}$, Z bosons, and the eight gluons g. The particle spectrum of the SM is summarized in Table 2.1. The SM is an example of a chiral gauge theory, which means that left- and right-handed chiralities have different transformation properties under the gauge group. Left-handed particles are organized into three isospin doublets, charged under $SU(2)_L$ while right-handed particles are $SU(2)_L$-singlets. The different fermion types or flavors of charged leptons (e, μ, τ), neutral leptons $(\nu_e, \nu_\mu, \nu_\tau)$, up-type quarks (u, c, t) and down-type quarks (d, s, b) are thus arranged into three generations or families. Right-handed neutrinos are absent in the SM and would be neutral under the gauge group G_{123} if added to the SM particle content.

The Standard Model Lagrangian is the most general, renormalizable Lagrangian invariant under the $U(1)_Y \times SU(2)_L \times SU(3)_c$ gauge group, and can be split up into the following parts (for a review, see [23]):

$$\mathcal{L}_{\text{SM}} = \mathcal{L}_{Dirac} + \mathcal{L}_{Yukawa} + \mathcal{L}_{Gauge} + \mathcal{L}_{Scalar}. \tag{2.1}$$

Here, the gauge part contains all of the gauge boson self-interactions

$$\mathcal{L}_{Gauge} = -\frac{1}{4} B_{\mu\nu} B^{\mu\nu} - \frac{1}{2} W^i_{\mu\nu} W_i^{\mu\nu} - \frac{1}{2} G^a_{\mu\nu} G_a^{\mu\nu}, \tag{2.2}$$

with the field strength tensors $B_{\mu\nu}, W^i_{\mu\nu}$ and $G^a_{\mu\nu}$ of the $U(1)_Y, SU(2)_L$ and $SU(3)_c$ gauge groups respectively defined as

$$\begin{aligned} B_{\mu\nu} &= \partial_\mu B_\nu - \partial_\nu B_\mu, \\ W^i_{\mu\nu} &= \partial_\mu W^i_\nu - \partial_\nu W^i_\mu + g_2 \varepsilon^{ijk} W^j_\rho W^k_\sigma, \\ G^a_{\mu\nu} &= \partial_\mu G^a_\nu - \partial_\nu G^a_\mu + g_s f^{abc} G^b_\mu G^c_\nu, \end{aligned} \tag{2.3}$$

where ε^{ijk} (with $i,j,k = 1,2,3$) and f^{abc} (with $a,b,c = 1,...,8$) are the corresponding group structure constants of $SU(2)_L$ and $SU(3)_c$. The Dirac part of the Lagrangian $\mathcal{L}_{Dirac}$ contains the kinetic terms and their interactions with the gauge bosons through the covariant derivative:

$$\mathcal{L}_{Dirac} = i\overline{L_i}\not{D}L_i + i\overline{e_{Ri}}\not{D}e_{Ri} + i\overline{Q_i}\not{D}Q_i + i\overline{u_{Ri}}\not{D}u_{Ri} + i\overline{d_{Ri}}\not{D}d_{Ri} + \text{h.c.}, \tag{2.4}$$

where $\not{D} = \gamma^\mu D_\mu$ with the covariant derivative according to the transformation property of the fermion field under the SM gauge group (see Table 2.1). For a quark field, the covariant derivative reads $D_\mu = \partial_\mu - iYg_1B_\mu - ig_2W_\mu^i\sigma^i - ig_sG_\mu^a\lambda^a$. Here σ^i and λ^a are the generators of the $SU(2)_L$ and $SU(3)_c$ gauge groups (the three Pauli and eight Gell-Mann matrices respectively) and Y denotes the hypercharge of the quark field. g_1, g_2 and g_s denote the respective gauge couplings of $U(1)_Y$, $SU(2)_L$ and $SU(3)_c$. Similarly, the covariant derivative for a leptonic field would be $D_\mu = \partial_\mu - iYg_1B_\mu - ig_2W_\mu^i\sigma^i$, where Y is the hypercharge of the leptonic field. The scalar sector of the SM contains the spin-0 Higgs field

$$\mathcal{L}_{Scalar} = D_\mu\Phi^\dagger D^\mu\Phi - \mu^2\Phi^\dagger\Phi - \frac{\lambda}{2}\left(\Phi^\dagger\Phi\right)^2, \tag{2.5}$$

with μ being the Higgs mass parameter and λ is the dimensionless Higgs quartic coupling, where $\mu^2 < 0$ such that the complex scalar field Φ acquires a non-zero *vacuum expectation value* (VEV) in its neutral direction, breaking the electroweak $U(1)_Y \times SU(2)_L$ group down to the residual electromagnetic $U(1)_{\text{em}}$ group. The VEV of the neutral component of the Higgs equals $\langle\Phi\rangle = v/\sqrt{2} = 174\,\text{GeV}$. The Higgs doublet can be parametrized in the following way

$$\Phi = \begin{pmatrix} \Phi^+ \\ \frac{1}{\sqrt{2}}(v + h + iA) \end{pmatrix}, \tag{2.6}$$

where h denotes the physical Higgs boson. In the broken phase, the three fields $\Phi^\pm$ and A are Nambu-Goldstone bosons which correspond to the three broken generators of $U(1)_Y \times SU(2)_L$ and get eaten by the three gauge bosons $W^\pm$ and Z^0 which thereby acquire a mass. Due to the residual electromagnetic $U(1)_{\text{em}}$ symmetry, the photon stays massless. The fields $W_\mu^\pm$, Z_μ and A_μ are linear combinations of the $W_\mu^{1,2,3}$ and the B_μ fields:

$$\begin{aligned} W_\mu^\pm &= \frac{1}{2}\left(W_\mu^1 \mp W_\mu^2\right), \\ Z_\mu &= \frac{g_2W_\mu^3 - g_1B_\mu}{\sqrt{g_1^2 + g_2^2}}, \\ A_\mu &= \frac{g_2W_\mu^3 + g_1B_\mu}{\sqrt{g_1^2 + g_2^2}}. \end{aligned} \tag{2.7}$$

Finally, the Yukawa sector in the Standard Model reads

$$\mathcal{L}_{Yukawa} = -\left(Y_e\right)_{ij}\overline{L_i}\Phi e_{Rj} - \left(Y_u\right)_{ij}\overline{Q_i}\widetilde{\Phi}u_{Rj} - \left(Y_d\right)_{ij}\overline{Q_i}\Phi d_{Rj} + \text{h.c.}, \tag{2.8}$$

with the charge conjugated Higgs field $\widetilde{\Phi} = i\sigma_2\Phi^*$ (where σ_2 is the second Pauli matrix) and the dimensionless Yukawa coupling matrices $\left(Y_{e,u,d}\right)_{ij}$. As consequence of electroweak

Symbol	Fields	$U(1)_Y$	$SU(2)_L$	$SU(3)_c$
L_i	$\begin{pmatrix}\nu_e\\ e^-\end{pmatrix}_L, \begin{pmatrix}\nu_\mu\\ \mu^-\end{pmatrix}_L, \begin{pmatrix}\nu_\tau\\ \tau^-\end{pmatrix}_L$	$-\frac{1}{2}$	$\underline{\mathbf{2}}$	$\underline{\mathbf{1}}$
e_{Ri}	e_R^-, μ_R^-, τ_R^-	-1	$\underline{\mathbf{1}}$	$\underline{\mathbf{1}}$
Q_i	$\begin{pmatrix}u\\ d\end{pmatrix}_L, \begin{pmatrix}c\\ s\end{pmatrix}_L, \begin{pmatrix}t\\ b\end{pmatrix}_L$	$\frac{1}{6}$	$\underline{\mathbf{2}}$	$\underline{\mathbf{3}}$
u_{Ri}	u_R, c_R, t_R	$\frac{2}{3}$	$\underline{\mathbf{1}}$	$\underline{\mathbf{3}}$
d_{Ri}	d_R, s_R, b_R	$-\frac{1}{3}$	$\underline{\mathbf{1}}$	$\underline{\mathbf{3}}$
Φ	$\begin{pmatrix}\Phi^+\\ \Phi^0\end{pmatrix}$	$\frac{1}{2}$	$\underline{\mathbf{2}}$	$\underline{\mathbf{1}}$
B	B	0	$\underline{\mathbf{1}}$	$\underline{\mathbf{1}}$
W	$\begin{pmatrix}W_1\\ W_2\\ W_3\end{pmatrix}$	0	$\underline{\mathbf{3}}$	$\underline{\mathbf{1}}$
g	g	0	$\underline{\mathbf{1}}$	$\underline{\mathbf{8}}$

Table 2.1: Overview of all Standard Model particles and their transformation behavior under the gauge groups of the SM

symmetry breaking (EWSB), the Yukawa sector generates Dirac masses for quarks and charged leptons, such that $(M_{e,u,d})_{ij} = v\,(Y_{e,u,d})_{ij}/\sqrt{2}$. The individual Yukawa coupling matrices are diagonalized by bi-unitary transformations of the type $Y_a = U_{La} D_a U_{Ra}^\dagger$, with $a = e, u, d$. The mismatch between the diagonalizations of Y_u and Y_d leads to a mixing among different quark flavors which is captured in the Cabbibo-Kobayashi-Maskawa (CKM) mixing matrix $U_{\text{CKM}} = U_{Lu}^\dagger U_{Ld}$.

2.2 Neutrino Oscillations

From the observation of neutrino flavor oscillations,[1] it follows that at least two neutrinos are massive particles (see [25–28]). Neutrino mass terms cannot be included in the Standard

[1] For the (im)possibility of charged lepton oscillations, see [24].

Model introduced above in a renormalizable manner. The mixing between the different neutrino flavors is captured in the Pontecorvo-Maki-Nakagawa-Sakata (PMNS) matrix $U_{\text{PMNS}} = U_e^\dagger U_\nu$. Mixing between the different mass eigenstates (ν_1, ν_2, ν_3 with the corresponding masses m_1, m_2, m_3) and flavor eigenstates (ν_e, ν_μ, ν_τ) of the neutrinos is characterized by the unitary transformation

$$|\nu_\alpha\rangle = (U_{\text{PMNS}})_{\alpha i}|\nu_i\rangle, \tag{2.9}$$

where $\alpha = e, \mu, \tau$ and $i = 1, 2, 3$. Neutrinos are produced and interact as flavor eigenstates, which are superpositions of the mass eigenstates. A neutrino with energy E in the flavor state $|\nu_\alpha\rangle$ oscillates into a flavor state $|\nu_\beta\rangle$ after propagating the distance L in vacuum[2] with the transition probability [30]

$$P_{\nu_\alpha \to \nu_\beta}(L/E) = \left|\langle \nu_\beta | \nu_\alpha, L\rangle\right|^2 = \left| \sum_{i=1}^{3} U_{\beta i} U_{\alpha i}^* e^{-i m_i^2 \frac{L}{2E}} \right|^2, \tag{2.10}$$

valid for ultra-relativistic neutrinos (like in neutrino oscillations experiments), where $U \equiv U_{\text{PMNS}}$ is used as shorthand in this chapter. For antineutrino oscillations the replacement $U \to U^*$ is used, which leads to the identity: $P_{\nu_\alpha \to \nu_\beta} = P_{\overline{\nu_\beta} \to \overline{\nu_\alpha}}$. From the transition probability several properties can be deduced:

- Oscillations depend on the mass squared differences $\Delta m^2_{31} = m^2_3 - m^2_1$, $\Delta m^2_{21} = m^2_2 - m^2_1$, not the individual masses.
- The transition probability oscillates with the parameter L/E.
- Mass squared differences must be non-vanishing in order to have a non-vanishing transition amplitude.
- For oscillations between flavor states to occur, neutrino mass eigenstates must not be degenerate and there must be non-vanishing mixing, which means U_{PMNS} is not a diagonal matrix.
- Oscillation probability is invariant under the phase transformation $U_{\alpha i} \to e^{i\varphi_\alpha} U_{\alpha i} e^{i\varphi_i}$ (or $U \to IUJ$, where I, J are diagonal phase matrices with $e^{i\varphi_i}$ on the main diagonal), which means so-called Majorana phases have no influence on neutrino oscillations. Only a Dirac phase δ can enter into the oscillation probability, which leads to CP violation for $\delta \neq \{0, \pi\}$, such that $P_{\nu_\alpha \to \nu_\beta} \neq P_{\overline{\nu_\alpha} \to \overline{\nu_\beta}}$.

The leptonic mixing matrix U_{PMNS} is usually parametrized in the PDG convention [31] with the three mixing angles (θ_{12}, θ_{13}, θ_{23}) and the three CP violating phases (δ, α, β) and is expressed as a product of three successive rotations

$$U_{\text{PMNS}} = \begin{pmatrix} c_{12}c_{13} & s_{12}c_{13} & s_{13}e^{-i\delta} \\ -s_{12}c_{23} - c_{12}s_{23}s_{13}e^{i\delta} & c_{12}c_{23} - s_{12}s_{23}s_{13}e^{i\delta} & s_{23}c_{13} \\ s_{12}s_{23} - c_{12}c_{23}s_{13}e^{i\delta} & -c_{12}s_{23} - s_{12}c_{23}s_{13}e^{i\delta} & c_{23}c_{13} \end{pmatrix} \times \text{diag}(e^{i\alpha}, e^{i\beta}, 1), \tag{2.11}$$

[2] In medium with varying density neutrino propagation is correctly described by the MSW (Mikheyev-Smirnov-Wolfenstein) effect. Through coherent forward scattering of neutrinos with the surrounding medium, neutrinos experience refraction which influences the evolution of the neutrino states. The MSW effect is key in solving the solar neutrino problem. For more details see [29].

where the shorthand $c_{ij} = \cos\theta_{ij}$ and $s_{ij} = \sin\theta_{ij}$ with $\theta_{ij} \in [0, \pi/2]$ and $\delta, \alpha, \beta \in [0, 2\pi]$ is used. In case of Dirac neutrinos we have only δ as CP violating phase (sometimes referred to as Dirac phase), for Majorana neutrinos we have in addition the CP violating Majorana phases α and β. The angles and the Dirac phase can be extracted from the mixing matrix by using

$$\begin{aligned}
\theta_{12} &= \begin{cases} \arctan\left(\left|\frac{U_{12}}{U_{11}}\right|\right), & \text{for } U_{11} \neq 0, \\ \frac{\pi}{2}, & \text{else,} \end{cases} \\
\theta_{13} &= \arcsin\left(|U_{13}|\right), \\
\theta_{23} &= \begin{cases} \arctan\left(\left|\frac{U_{23}}{U_{33}}\right|\right), & \text{for } U_{33} \neq 0, \\ \frac{\pi}{2}, & \text{else,} \end{cases} \\
\delta &= -\arg\left(\frac{s_{13}c_{12}c_{23} + \frac{U_{11}^* U_{13} U_{31} U_{33}^*}{s_{13}c_{12}c_{13}^2 c_{23}}}{s_{12}s_{23}}\right),
\end{aligned} \tag{2.12}$$

where U_{ij} are the entries of the U_{PMNS} matrix.

From Eq. (2.10) we see that neutrino oscillations are sensitive to the following six independent observables: θ_{12}, θ_{13}, θ_{23}, δ, $\Delta m^2_{21} \equiv \Delta m^2_{\odot}$ and $\Delta m^2_{31} \equiv \Delta m^2_{\text{atm}}$. Through the observation of enhanced oscillations in matter by the MSW effect, the sign of Δm^2_{21} can be determined experimentally and turns out to be positive $\Delta m^2_{21} > 0$ for the standard convention that ν_1 is the dominant component in ν_e. The sign of Δm^2_{31} (or Δm^2_{32}) is yet unknown and allows for two orderings of the neutrinos mass spectrum. The two possible arrangements[3] explaining the oscillation data are

$$\begin{aligned}
m_1 < m_2 < m_3 \qquad & \text{normal ordering (NO)}, \\
m_3 < m_1 < m_2 \qquad & \text{inverted ordering (IO)},
\end{aligned}$$

and can be seen in Fig. (2.1). Current fits to global neutrino oscillation data for the six neutrino observables for normal and inverted ordering are summarized in Table 2.2 [32,33], where in case of normal ordering $\Delta m^2_{3l} \equiv \Delta m^2_{31} > 0$ and correspondingly for inverted ordering $\Delta m^2_{3l} \equiv \Delta m^2_{32} < 0$. Normal ordering provides the best fit to the data, while inverted ordering with $\Delta\chi^2 = 10.4$ (with respect to the global minimum of χ^2) is somewhat disfavored [32,33].

As neutrino oscillations are only sensitive to the mass squared differences, the absolute neutrino mass scale cannot be determined from oscillation experiments, but a lower bound can be set by $m_{\text{upper}} \geq \sqrt{|\Delta m^2_{31}|}$. Since the experimental data indicates non-vanishing atmospheric Δm^2_{31} and solar Δm^2_{21} mass square differences, at least two neutrinos must be massive, allowing for a massless lightest neutrino. In case of the lightest neutrino being almost massless $m_1 \simeq 0$, the other two neutrino masses become equal to the solar and atmospheric mass scale $m_2 = \sqrt{\Delta m^2_{21}} \simeq 0.0086\,\text{eV}$ and $m_3 = \sqrt{\Delta m^2_{31}} \simeq 0.0503\,\text{eV}$ respectively (taking values at $1\,\sigma$ CL).

For the absolute values of the PMNS matrix elements $|U_{\text{PMNS}}|$, current global fits find at $3\,\sigma$ CL [32]

$$|U_{\text{PMNS}}| = \begin{pmatrix} 0.797 - 0.842 & 0.518 - 0.585 & 0.143 - 0.156 \\ 0.243 - 0.490 & 0.473 - 0.674 & 0.651 - 0.772 \\ 0.295 - 0.525 & 0.493 - 0.688 & 0.618 - 0.744 \end{pmatrix}, \tag{2.13}$$

[3] Quasi-degenerate neutrino masses with $m_1 \approx m_2 \approx m_3$ (QD) are excluded by experiment.

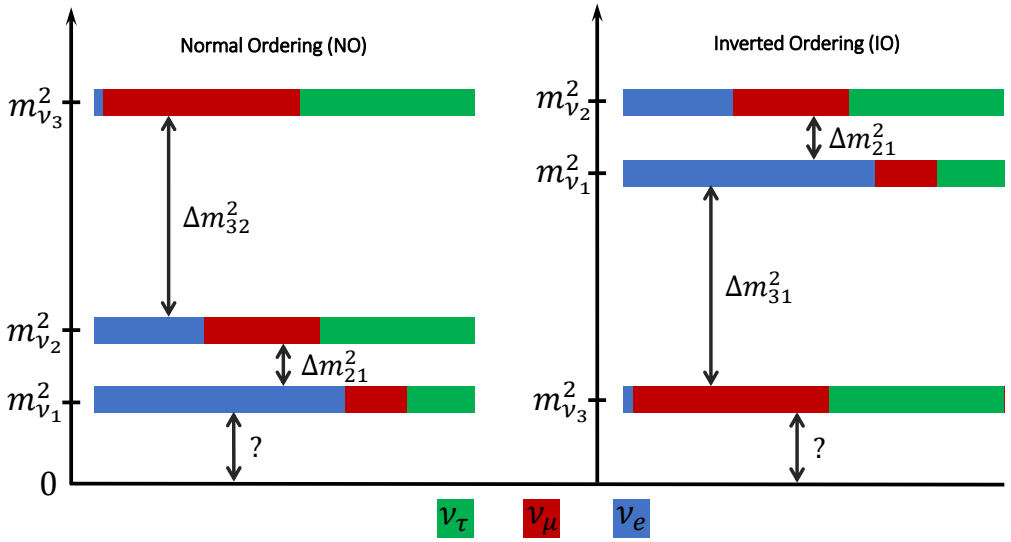

Figure 2.1: Possible orderings of the neutrino mass spectrum and flavor content of the different neutrino mass eigenstates.

	Normal Ordering		**Inverted Ordering**	
	bfp $\pm 1\,\sigma$	$3\,\sigma$ range	bfp $\pm 1\,\sigma$	$3\,\sigma$ range
$\sin^2\theta_{12}$	$0.310^{+0.013}_{-0.012}$	$0.275 - 0.350$	$0.310^{+0.013}_{-0.012}$	$0.275 - 0.350$
$\sin^2\theta_{23}$	$0.563^{+0.018}_{-0.024}$	$0.433 - 0.609$	$0.565^{+0.017}_{-0.022}$	$0.436 - 0.610$
$\sin^2\theta_{13}$	$0.02237^{+0.00066}_{-0.00065}$	$0.02044 - 0.02435$	$0.02259^{+0.00065}_{-0.00065}$	$0.02064 - 0.02457$
$\delta_{\mathrm{CP}}/^\circ$	221^{+39}_{-28}	$144 - 357$	282^{+23}_{-25}	$205 - 348$
$\frac{\Delta m^2_{21}}{10^{-5}\,\mathrm{eV}^2}$	$7.39^{+0.21}_{-0.20}$	$6.79 - 8.01$	$7.39^{+0.21}_{-0.20}$	$6.79 - 8.01$
$\frac{\Delta m^2_{3l}}{10^{-3}\,\mathrm{eV}^2}$	$+2.528^{+0.029}_{-0.031}$	$(+2.436) - (+2.618)$	$-2.510^{+0.030}_{-0.031}$	$(-2.601) - (-2.419)$

Table 2.2: Global neutrino oscillation data for the six neutrino observables, showing the best fit parameters (bfp) and the corresponding $1\,\sigma$ and $3\,\sigma$ CL range for normal and inverted ordering of neutrino masses [32, 33].

where the same parametrization as in Eq. (2.11) is used.

The magnitude of CP violation in neutrino oscillations is characterized by the Jarlskog invariant[4] [34]:

$$\begin{aligned} J_\nu^{CP} &= \mathrm{Im}\left(U_{\alpha i} U^*_{\alpha j} U^*_{\beta i} U_{\beta j}\right) \\ &= \frac{1}{8}\cos\theta_{13}\sin 2\theta_{12}\sin 2\theta_{13}\sin\delta, \end{aligned} \tag{2.14}$$

[4]Where *invariant* means that J_ν^{CP} is independent of the phase convention used for the PMNS matrix, *i.e.* invariant under phase transformations of the following form: $U_{\mathrm{PMNS}} \to \mathrm{diag}(e^{i\varphi_1}, e^{i\varphi_2}, e^{i\varphi_3})\, U_{\mathrm{PMNS}}\, \mathrm{diag}(e^{i\phi_1}, e^{i\phi_2}, e^{i\phi_3})$.

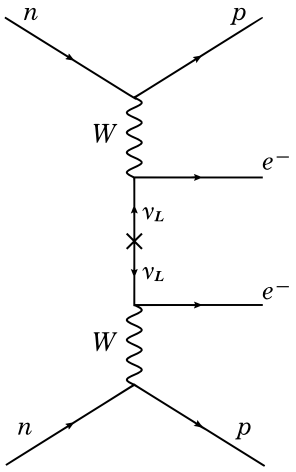

Figure 2.2: Neutrinoless double beta decay ($0\nu2\beta$) which is only possible if the left-handed neutrinos have a Majorana mass term. At the cross vertex the effective Majorana neutrino mass is inserted.

with $\alpha, \beta = e, \mu, \tau$, and $i, j = 1, 2, 3$. Defining the quantity $\Delta^{CP}_{\alpha\beta} := P(\nu_\alpha \to \nu_\beta) - P(\overline{\nu_\alpha} \to \overline{\nu_\beta})$ to measure the CP violation, it is possible to write

$$\Delta^{CP}_{\nu} = \pm 16\, J^{CP}_{\nu} \sin\left(\frac{\Delta m^2_{21} L}{4E}\right) \sin\left(\frac{\Delta m^2_{31} L}{4E}\right) \sin\left(\frac{\Delta m^2_{32} L}{4E}\right), \tag{2.15}$$

where "+" corresponds to even permutations of $(\alpha, \beta, \gamma) = (e, \mu, \tau)$ with $\gamma \neq \alpha, \beta$ and "−" to odd permutations. CP violation occurs only for $\Delta^{CP}_{\nu} \neq 0$, which means that $J^{CP}_{\nu} \neq 0$ (or equivalently $\theta_{ij} \neq 0, \delta \neq \{0, \pi\}$) and no two mass eigenstates are degenerate $m_i \neq m_j$ [35]. Current global fit analysis finds

$$J^{CP}_{\nu} = (0.0333 \pm 0.0019) \times \sin\delta \tag{2.16}$$

at the $3\,\sigma$ CL for both orderings [32]. Compared to the CP violation in the quark sector $J^{CP}_{q} = (3.18 \pm 0.15) \times 10^{-5}$ [31] this implies that CP violation is three orders of magnitude larger in the leptonic sector assuming $\delta \neq \{0, \pi\}$.

2.3 Nature of Neutrinos

The observation of neutrino oscillations proves neutrinos to be massive particles, in contrast to the SM prediction. As neutral fermions, neutrinos can either acquire a Dirac mass term by coupling them to a scalar field developing a non-zero VEV or carry a Majorana mass term if neutrinos are their own antiparticles. The only known experiment to test whether neutrinos are Dirac or Majorana particles is the observation of neutrinoless double beta decay[5] ($0\nu2\beta$): $(A, Z) \to (A, Z \pm 2) + 2e^{\mp}$. In this decay two neutrons decay into two protons and two electrons, violating lepton number by two units, which is only possible if neutrinos are Majorana. The Feynman diagram of the process is depicted in Fig. 2.2.

The difficulty of experimentally distinguishing between the Dirac or Majorana nature of neutrinos is often referred to as the *Practical Dirac-Majorana Confusion Theorem* [36].

[5] Or similar lepton number violating nuclear processes like double electron capture $2e^- + (A, Z) \to (A, Z - 2)$ (0νECEC) and positron emitting electron capture $e^- + (A, Z) \to (A,\ Z - 2) + e^+$ ($0\nu\beta^+$EC).

Experiments involving ultra-relativistic neutrinos ($p_\nu \gg m_\nu$) are not sensitive to the nature of the neutrino as neutrino neutral weak currents take the same form in the limit of a vanishing neutrino mass. Looking for lepton number violation in $0\nu2\beta$ that automatically points to the Majorana nature of neutrinos circumvents this theorem.

In general, while Dirac spinors contain two Weyl spinors with different chirality $\psi_D = \psi_L + \psi_R$, Majorana spinors contain a Weyl spinor and its CP conjugate $\psi_M = \psi_L + \psi_L^c$ (or $\psi_M = \psi_R + \psi_R^c$ for the right-handed field). Where charge conjugation is defined as $\psi^c = C\overline{\psi}^T$ with the charge conjugation operator $C = i\gamma^2$, satisfying $C^T = -C$ and $C^\dagger C = \mathbb{1}$. Therefore, Majorana spinors fulfill the condition that $\psi_M^c = e^{i\varphi}\psi_M$, with the Majorana phase φ. In the Lagrangian, a Majorana mass term takes the form[6]

$$\mathcal{L}_M = -\frac{1}{2}\overline{\psi_L^c} M \psi_L - \frac{1}{2}\overline{\psi_L} M \psi_L^c, \tag{2.17}$$

violating lepton number by two units. From this it can be shown that a Majorana mass matrix is a complex symmetric matrix by virtue of C being an antisymmetric operator and the anticommutativity of the fermion fields. Thus, by rearranging

$$\overline{\psi_L^c} M \psi_L = \left(\overline{\psi_L^c} M \psi_L\right)^T = -\psi_L^T (C^{-1})^T M^T \psi_L = \overline{\psi_L^c} M^T \psi_L, \tag{2.18}$$

and using $\overline{\psi_L^c} = -\psi_L^T C^{-1}$, it must hold that $M = M^T$. Therefore, only one unitary matrix U_M is required to diagonalize the Majorana mass matrix: $M = U_M^* D_M U_M^\dagger$. D_M denotes the diagonal matrix. Further, note that $\psi_R^c = (\psi_R)^c = (\psi^c)_L$. In addition to a Majorana mass term for the left-handed fields, there could also be a Majorana mass term for the right-handed fields, as well as a Dirac mass term in the Lagrangian:

$$\mathcal{L}_{D+M} = -\overline{\psi_L} M_D \psi_R - \frac{1}{2}\overline{\psi_L^c} M_L \psi_L - \frac{1}{2}\overline{\psi_R^c} M_N \psi_R + \text{h.c.}, \tag{2.19}$$

where only the Dirac mass term is invariant under global transformations $\psi_L \to e^{i\alpha}\psi_L$, $\psi_R \to e^{i\alpha}\psi_R$, resembling the conservation of lepton number L. As the SM predicts neutrinos to be massless particles, the SM conserves lepton number $L = L_e + L_\mu + L_\tau$ as an accidental (global) symmetry, resulting form the gauge symmetries and field content, to all orders in perturbation theory[7].

A Majorana mass term is only allowed for neutral fermions, as otherwise the conservation of electric charge (a local gauge symmetry) would be violated. A hint towards Dirac neutrinos would be the observation of electrically charged neutrinos. An upper bound on the neutrino charge Q_ν can be set from observing the correlation (or lack thereof) between the arrival time and the neutrino energy from supernova neutrinos. From the observation of supernova neutrinos of SN 1987A an upper bound for the neutrino charge was determined: $Q_\nu < 2 \times 10^{-15}\, e$ [37].

2.4 Number of Neutrinos

The number of active neutrinos N_ν can be determined from precision measurements of $Z \to f\overline{f}$ decays (where f denotes a fermion species), since the Z boson is mediating weak

[6] This is only a general consideration. Explicitly adding a Majorana mass term for the left-handed neutrinos $\overline{\nu_L^c} M_L \nu_L$ to the SM is not possible due to the $SU(2)_L \times U(1)_Y$ gauge symmetry.

[7] In general, the quantum numbers B and L are both anomalous in the SM, *i.e.* broken by quantum effects. Only the combination $(B-L)$ is anomaly-free. At high energies and temperatures the SM allows for non-perturbative transitions that break B, L, $(B+L)$, but respect $(B-L)$, the so-called sphaleron process.

interactions between all Standard Model fermions. By measuring the total Z decay width and the visible Z decay width from decays into quarks and charged leptons, the invisible Z decay width is obtained by subtracting the total from the visible width. The invisible width is from Z decaying into the active neutrino species. The result of Z decay measurements favors three active neutrinos with high accuracy $N_\nu = 2.984 \pm 0.008$ [31]. If additional neutrinos exist, they must be either sterile (*i.e.* not participating in weak interactions) or much heavier ($m_\nu > m_Z/2$).

Long-baseline neutrino oscillations experiments with solar ($L \simeq 10^8\,\mathrm{km}, E \lesssim 15\,\mathrm{MeV}$), atmospheric ($20 < L < 10^4\,\mathrm{km}, E \simeq 1\,\mathrm{GeV}$), reactor ($L \simeq 0.01-10^2\,\mathrm{km}, E \simeq 3\,\mathrm{MeV}$) and accelerator ($L \gtrsim 500\,\mathrm{km}, E \simeq 1\,\mathrm{GeV}$) neutrinos are in line with the three neutrino picture [38]. Short-baseline experiments (with distance-neutrino energy ratios $L/E \sim 1\,\mathrm{km/GeV}$) like LSND and MiniBooNE show data in tension with the three neutrino framework. This is referred to as *short-baseline anomaly.* Explaining the short-baseline (SBL) data would require mixing with at least one additional sterile neutrino added to the three active neutrinos with a mass squared difference of $\Delta m^2_{41} \sim \mathcal{O}(1)\,\mathrm{eV}^2$ [39], so-called (3+1) neutrino models. It must be noted that SBL results are not necessarily conclusive since there is a strong tension between experiments measuring the appearance and disappearance of $(\overline{\nu_e})$ and $(\overline{\nu_\mu})$. This appearance-disappearance-tension is reinforced as current 2018 MiniBooNE results are consistent with previous ν_e appearance experiments like LSND [40]. As an additional fourth, sterile neutrino would influence the atmospheric flux of ν_μ neutrinos compared to the standard scenario of three active neutrinos, the IceCube neutrino telescope is able to set stringent bounds on Δm^2_{41} and the mixing. Current IceCube data excludes the allowed region from the global best fit of Δm^2_{41} from appearance experiments such as LSND and MiniBooNE for the global fest fit value of $|U_{e4}|^2$ at 99 % CL [41].

Big Bang Nucleosynthesis (BBN) in standard ΛCDM cosmology predicts an effective number of neutrino species of $N_{\mathrm{eff}}^{\mathrm{SM}} = 3.046$, which includes three neutrinos plus extra relativistic degrees of freedom (from neutrino heating through $e^- e^+$ annihilations when the neutrinos were not yet fully decoupled) [42]. If another relativistic species is added *e.g.* in form of an additional neutrino, the radiation energy density increases. This leads to a delay of the epoch of radiation-matter equality, changing the height of the first baryonic acoustic oscillation peak of the Cosmic Microwave Background (CMB) angular power spectrum. Current 2018 CMB data from the *Planck* satellite constrains the effective number of neutrinos to be $N_{\mathrm{eff}} = 2.99^{+0.34}_{-0.33}$ (at 95 % CL) and is thus fully consistent with the Standard Model prediction of three light neutrinos [43]. This result strongly disfavors the existence of a thermalized eV-scale sterile neutrino, contributing about $\Delta N_{\mathrm{eff}} \simeq 1$ to N_{eff}, as required to explain short-baseline anomalies via mixing between the active neutrinos and one sterile neutrino. The required active-sterile mixing angle to alleviate the short-baseline tension would lead to thermalization in the early Universe between the active and the sterile species, such that $T_\nu = T_{\mathrm{sterile}}$ leading to a contribution of $\Delta N_{\mathrm{eff}} = 1$. There is still the possibility of light sterile neutrinos not in thermal equilibrium with the active species to evade N_{eff} constraints by invoking new physics, *e.g.* through the introduction of non-standard interactions (NSIs) beyond the weak force, suppressing the equilibration of light sterile neutrinos [44].

2.5 The Neutrino Mass Scale

Through measurements of the Kurie plot endpoint region of the e^- spectrum from tritium β-decay ${}^3\mathrm{H} \rightarrow {}^3\mathrm{He}^+ + e^- + \overline{\nu_e}$ [45, 46], model-independent upper limits on the neutrino

mass scale can be set by measuring the effective electron neutrino mass[8] m_β, given by the incoherent sum

$$m_\beta^2 = \sum_{i=1}^{3} |U_{ei}|^2 m_i^2, \tag{2.20}$$

where U is the PMNS matrix. Current results by the KATRIN experiment measuring the β-spectrum close to the endpoint energy at $E_0 = 18.57\,\text{keV}$ (the maximal energy of the emitted e^- if the $\overline{\nu_e}$ would be massless) report an upper limit on the absolute neutrino mass scale of $m_\beta < 1.1\,\text{eV}$ at 90 % CL [47]. This current upper limit set by KATRIN is expected to further improve through advanced sensitivity down to 0.2 eV at 90 % CL after 5 years. A corollary experiment to KATRIN with the goal of lowering the sensitivity beyond 0.2 eV with an improved electron spectroscopy technique by using cyclotron radiation is *Project 8* [48]. Another model-independent way to potentially measure the ν_e mass with sub-eV precision is electron capture (EC) in ^{163}Ho ($^{163}\text{Ho} + e^- \rightarrow {}^{163}\text{Dy}$), where the EC decay rate depends on the electron neutrino mass. The influence of the ν_e-mass on EC decay rate is largest for small nuclear Q-values, and as the EC decay of ^{163}Ho has the lowest known Q-value, it is the best candidate for this measurement [49].

Bounds on the neutrino mass sum $\sum_i (m_\nu)_i$ can also be derived from cosmological data as massive neutrinos leave footprints on the CMB and on the large-scale structure (LSS) of the Universe [50]. Combining both CMB and LSS data, the current 2018 *Planck* results present an upper limit of $\sum_i (m_\nu)_i < 0.12\,\text{eV}$ (at 95 % CL) [43] assuming a degenerate neutrino mass spectrum. 2018 *Planck* data finds for the normal hierarchy $\sum_i (m_\nu)_i < 0.146\,\text{eV}$ and inverted hierarchy $\sum_i (m_\nu)_i < 0.172\,\text{eV}$ both at 95 % CL [51]. However, the upper bounds depend on the specific cosmological model and the selection of data sets.

Neutrinoless double beta decay ($0\nu2\beta$) is not only a smoking gun for the Majorana nature of neutrinos but is also able to provide an upper bound on the effective Majorana mass $\langle m_{\beta\beta} \rangle$, if neutrinos are Majorana particles (for a review, see [52]). As the $0\nu2\beta$ is a second-order weak decay, the rate is proportional to the fourth power of the Fermi constant G_F^4, as well as the light neutrino masses, which strongly suppresses the decay. The derivation of the upper bound on the effective Majorana mass is not model-independent and carries theoretical uncertainties from the calculation of the nuclear matrix element M_{nuc}, relating the decay rate $\Gamma_{\beta\beta}$ with the effective mass: $\Gamma_{\beta\beta} \propto |M_{\text{nuc}}|^2 \langle m_{\beta\beta} \rangle^2$. Current 2017 results from the GERDA experiment searching for $0\nu\beta\beta$ in $^{76}\text{Ge} \rightarrow {}^{76}\text{Se} + 2e^-$ report a lower bound on the half-life of $T_{1/2} > 5.3 \times 10^{25}$ yrs which translates to an upper bound for the effective mass of $\langle m_{\beta\beta} \rangle < 0.15 - 0.33\,\text{eV}$ (depending on the matrix element), both at 90 % CL [53]. While the KamLAND-Zen experiment searches for $0\nu\beta\beta$ in ^{136}Xe to an excited state of ^{136}Ba, reporting in 2016 a lower bound of $T_{1/2} > 1.07 \times 10^{26}$ yrs on the half-life and a corresponding upper bound on the effective mass of $\langle m_{\beta\beta} \rangle < 0.064 - 0.165\,\text{eV}$ (again, depending on the matrix element), both also at 90 % CL [54]. The effective Majorana mass is related to the matrix elements of the PMNS matrix $U_{\text{PMNS}} = U$ from neutrino oscillations and the mass eigenstates m_i through

$$\langle m_{\beta\beta} \rangle = \left| \sum_{i=1}^{3} U_{ei}^2 m_i \right|. \tag{2.21}$$

[8] Measured is not a neutrino mass eigenstate, since the emitted electron neutrino ν_e is a flavor eigenstate. As m_β depends on all mass eigenstates weighted with the PMNS matrix elements $|U_{ei}|^2$, it constraints the absolute neutrino mass scale.

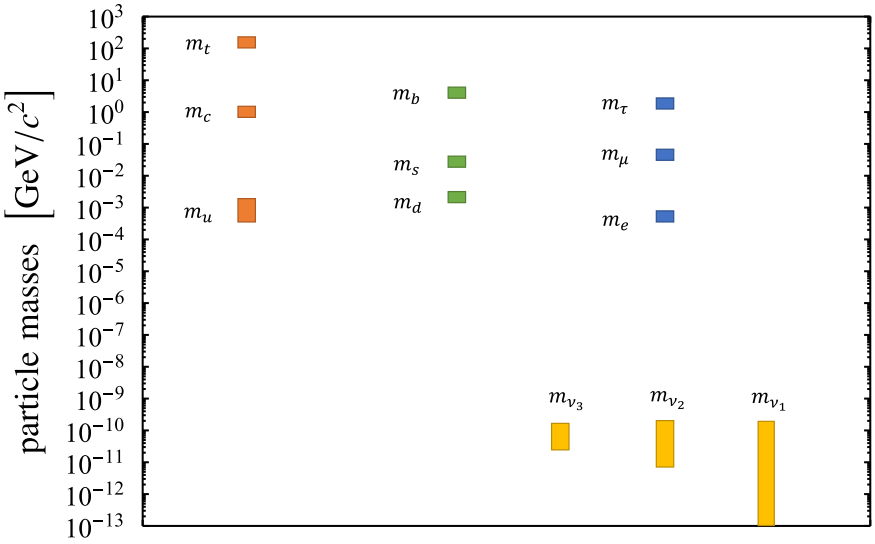

Figure 2.3: Mass spectrum of the Standard Model fermions.

From this expression we see that $\langle m_{\beta\beta} \rangle$ depends on the six independent observables form neutrino oscillations, the two unknown Majorana phases, the mass hierarchy (either NO or IO) as well as the absolute neutrino spectrum.

2.6 Comparison to the Quark Sector

Experimental evidence presented in the previous sections shows that the neutrino sector is quite distinct from the quark sector and the charged lepton sector in the Standard Model. The most striking differences compared to the quark sector are:

- The largest active neutrino mass is in the $m_\nu \simeq \mathcal{O}(0.1)\,\mathrm{eV}$ range, while the masses of the quarks range from a few MeV up to the GeV scale. If neutrinos get their masses after electroweak symmetry breaking via Yukawa interaction with the Higgs, the magnitude of the coupling would be $y_\nu \simeq 10^{-12}$. Compared to the top-quark coupling $y_t \simeq 1$ or even compared to the smallest Yukawa coupling in the SM, the electron coupling $y_e \simeq 3 \times 10^{-6}$, the value is several orders of magnitude smaller (for the SM fermion masses see [31]). The SM fermion mass spectrum is depicted in Fig. 2.3.

- From the mass squared differences the following mass hierarchy in the neutrino sector is found:

$$\begin{aligned} \left.\frac{m_{\text{largest}}}{m_{\text{2nd largest}}}\right|_{\text{NO}} &\simeq \sqrt{\frac{\Delta m^2_{31}}{\Delta m^2_{21}}} \simeq 6, \\ \left.\frac{m_{\text{largest}}}{m_{\text{2nd largest}}}\right|_{\text{IO}} &\simeq \sqrt{\frac{\Delta m^2_{13}}{\Delta m^2_{23}}} \simeq 1, \end{aligned} \tag{2.22}$$

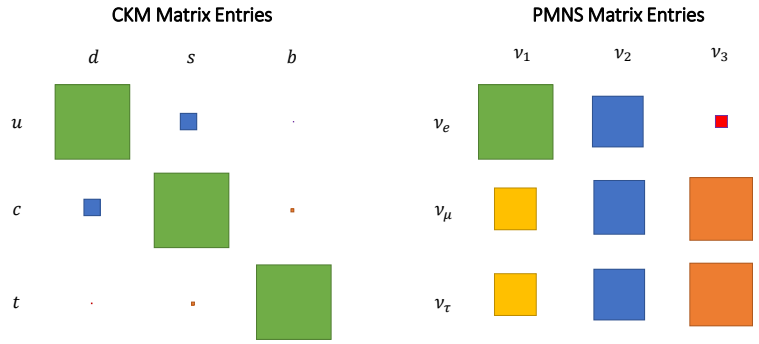

Figure 2.4: Illustration of the structure and relative sizes of the CKM and PMNS matrix elements. While the CKM matrix shows a hierarchical structure, the PMNS entries have comparable sizes. Colors indicate similar-sized elements within the respective matrices.

which is strikingly milder compared to the mass ratios in the SM fermion sector

$$\begin{aligned} \frac{m_\tau}{m_\mu} &\simeq 17, & \frac{m_\mu}{m_e} &\simeq 207, & \frac{m_t}{m_c} &\simeq 136, \\ \frac{m_b}{m_s} &\simeq 44, & \frac{m_c}{m_u} &\simeq 554, & \frac{m_s}{m_d} &\simeq 20, \end{aligned} \tag{2.23}$$

depicting a completely different pattern of mass ratios with a strong normal hierarchy.

- Compared to the quark sector, the mixing in the lepton sector is also quite different. While the CKM (Cabibbo-Kobayashi-Maskawa) matrix entries show a clearly hierarchical structure, *e.g.* $|V_{ub}| \ll |V_{cb}| \ll |V_{us}|$, the PMNS matrix entries seem anarchical. In Fig. 2.4 the relative sizes of the CKM and PMNS matrix entries are illustrated. The mixing angles in the PMNS matrix show almost maximal mixing ($\sim 45°$) with the exception of the θ_{13} angle ($\theta_{23} \simeq 48.3°, \theta_{12} \simeq 33.82°, \theta_{13} \simeq 8.61°$), where in the quark-sector all of the mixing angles are small in size ($\vartheta_{23} \simeq 2.4°, \vartheta_{12} \simeq 13°, \vartheta_{13} \simeq 0.2°$) [31].

Ideally, any neutrino mass model should therefore provide an answer to the following questions:

- Why are the neutrino masses much smaller than the other fermion masses in the SM?
- Why is the mass hierarchy of the neutrinos much milder than in the rest of the fermionic sector?
- Why are the mixing angles in the leptonic sector much larger than in the quark sector?

To provide possible answers to these questions will be the goal of the subsequent chapters.

Chapter 3

The Seesaw Mechanism

Considering Standard Model fields only, Majorana masses for the active neutrinos can be introduced by allowing for a non-renormalizable dimension-5 operator, which is also known as the Weinberg operator [55]:

$$\mathcal{O}_{\text{dim}-5} = \frac{c_{\alpha\beta}}{\Lambda}\left(\overline{L_\alpha}\widetilde{\Phi}\right)\left(\widetilde{\Phi}^T L_\beta^c\right) + \text{h.c.}, \tag{3.1}$$

where $c_{\alpha\beta}$ are the dimensionless Wilson coefficients and Λ is some unknown new physics scale. The effective mass scale of the neutrinos via Eq. (3.1) after EWSB will be $\mathcal{O}(v^2/\Lambda)$, with the Higgs VEV $v \simeq 246\,\text{GeV}$. To reproduce the observed neutrino mass scale of $\mathcal{O}(0.1)\,\text{eV}$, the suppressing mediator scale Λ must be of the order $\mathcal{O}\left(10^{14}\right)$ GeV, assuming $c_{\alpha\beta} \sim \mathcal{O}(1)$. The resulting mass term for the light neutrinos will be of Majorana nature.

The Weinberg operator leading to massive Majorana particles can arise from different high-energy completions, of which three canonical types of the seesaw mechanisms can be distinguished

- Type-I Seesaw: Introduces at least two neutral singlet fermions [19–22],
- Type-II Seesaw: Uses a newly introduced $SU(2)_L$ triplet scalar [56–58],
- Type-III Seesaw: At least two new $SU(2)_L$ triplet fermions are added [59],

where combinations of these mechanisms are also possible, *e.g.* left-right symmetric models have type-I and type-II as sources for neutrino masses, or $SU(5)$ GUT models can accommodate type-I and type-III [60, 61].

Before obtaining the Weinberg operator from an UV completion by integrating out the heavy right-handed neutrino fields, the basics of the type-I seesaw mechanism are reviewed.

3.1 Vanilla Type-I Seesaw

By extending the Standard Model Lagrangian in Eq. (2.1) with n_g right-handed singlet neutrinos N_i $(i = 1, ..., n_g)$, the following renormalizable terms are allowed under the SM gauge group:

$$\mathcal{L}_N \simeq \frac{1}{2}\overline{N_i}\not{\partial}N_i - \left(Y_{\alpha i}\overline{L_\alpha}\widetilde{\Phi}N_i + \frac{1}{2}M_{ij}\overline{N_i^c}N_j + \text{h.c.}\right), \tag{3.2}$$

with $\widetilde{\Phi} = i\sigma_2\Phi^*$, $\alpha = e, \mu, \tau$ and Y denotes the $3 \times n_g$ neutrino Yukawa coupling matrix and M is the complex symmetric $n_g \times n_g$ Majorana mass matrix for the right-handed neutrinos. The charge conjugated right-handed neutrino fields are denoted by $N_i^c = i\gamma^2 N_i$. Since the introduced right-handed neutrinos are singlets under the Standard Model gauge group $U(1)_Y \times SU(2)_L \times SU(3)_c \sim (0, \underline{\mathbf{1}}, \underline{\mathbf{1}})$, the covariant derivative in the kinetic term coincides with the partial derivative $D_\mu = \partial_\mu$. The neutrino Yukawa leads to an additional Dirac mass term for the neutrinos after the electroweak breaking of symmetry, such that

$$\mathcal{L}_N \simeq \frac{1}{2}\overline{N_i}\not{\partial} N_i - \left((M_D)_{\alpha i}\, \overline{\nu_\alpha} N_i + \frac{1}{2} M_{ij} \overline{N_i^c} N_j + \text{h.c.} \right), \tag{3.3}$$

where the Dirac mass matrix is defined as $M_D = \langle\Phi\rangle Y = vY/\sqrt{2}$, with the Higgs vacuum expectation value $v \simeq 246\,\text{GeV}$. The non-kinetic part of the Lagrangian can be written in vector form introducing the general $(3 + n_g) \times (3 + n_g)$ Majorana mass matrix $\mathfrak{M}_\nu$:

$$\mathcal{L}_N \simeq -\frac{1}{2} \begin{pmatrix} \overline{\nu} & \overline{N^c} \end{pmatrix} \mathfrak{M}_\nu \begin{pmatrix} \nu^c \\ N \end{pmatrix} + \text{h.c.} = \frac{1}{2} \begin{pmatrix} \overline{\nu} & \overline{N^c} \end{pmatrix} \begin{pmatrix} \mathbb{O} & M_D \\ M_D^T & M \end{pmatrix} \begin{pmatrix} \nu^c \\ N \end{pmatrix} + \text{h.c.} \tag{3.4}$$

The $(3 + n_g) \times (3 + n_g)$ neutrino mass matrix $\mathfrak{M}_\nu$ is symmetric and can therefore be block-diagonalized by an unitary transformation of the following form

$$\widehat{\mathfrak{M}}_\nu = \mathcal{U}^T \mathfrak{M}_\nu \mathcal{U} = \begin{pmatrix} U^* D_D U^\dagger & \mathbb{O} \\ \mathbb{O}^T & U_M^* D_M U_M^\dagger \end{pmatrix}, \tag{3.5}$$

where the matrices D_D and D_M indicate the diagonal matrices of M_D and M, respectively. $\mathbb{O}$ is the 3×3 null matrix, where all entries are equal to zero.

In order to gain a better understanding of the mass spectrum, let's assume for a moment that there is only one generation of each type of neutrino (left- and right-handed). In this case, $\mathfrak{M}_\nu$ becomes a 2×2 matrix which is easy to handle since M_D and M are just numbers. The two eigenvalues of the neutrino mass matrix $\hat{m}_1$ and $\hat{m}_2$ are then simply,

$$\hat{m}_{1,2} = \frac{M}{2} \pm \frac{1}{2}\sqrt{M^2 + 4M_D^2}. \tag{3.6}$$

Assuming we only have a Dirac mass term in our Lagrangian, then $M = 0$ and our neutrino mass spectrum becomes: $\hat{m}_1 = M_D$ and $\hat{m}_2 = -M_D$. In this case our neutrinos will be purely of Dirac nature. We can extend this scenario by allowing a tiny Majorana mass for the right-handed neutrino only, such that $M \ll M_D$. This leads to an almost degenerate mass spectrum of the form

$$\hat{m}_{1,2} = \pm M_D + \frac{M}{2} + \mathcal{O}(M^2). \tag{3.7}$$

The result are so-called *pseudo-Dirac* neutrinos [62], where the previous Dirac case is recovered in the limit $M \to 0$. The neutrinos behave like a pair of Dirac neutrinos, but cannot be combined to a standard Dirac pair due to the tiny, but finite mass splitting of $M/2$. The overall neutrino mass scale in the pseudo-Dirac scenario is given by M_D, while the order of the mass splitting between the pairs is M. The non-zero Majorana mass term makes the pseudo-Dirac pair indeed Majorana neutrinos. Another instance to consider is the case where the Majorana mass term dominates over the Dirac mass term, such that $M_D \ll M$. From this set-up the following mass spectrum is obtained:

$$\hat{m}_1 \simeq M, \qquad \hat{m}_2 \simeq -\frac{M_D^2}{M}. \tag{3.8}$$

This scenario is the well-known type-I seesaw mechanism, first described in [19]. Through the heaviness of the right-handed neutrino M, the left-handed neutrino obtains a tiny Majorana mass: $-M_D^2/M$. Thereby, the seesaw mechanism explains the smallness of the left-handed neutrino masses through the heaviness of the singlet right-handed neutrino masses. The relation in Eq. (3.8) is easily generalized to three or more generations, in general it reads

$$\mathcal{M}_\nu \simeq -M_D M^{-1} M_D^T = -\frac{v^2}{2} Y M^{-1} Y^T = U_\nu^* D_\mathcal{M} U_\nu^\dagger. \tag{3.9}$$

The seesaw relation also generates mixing between the different neutrino flavors. The unitary matrix $\mathcal{U}$ diagonalizing $\mathfrak{M}_\nu$ in Eq. (3.5) can be written as the matrix exponential of a skew-Hermitian matrix (*i.e.* a matrix with the property: $H^\dagger = -H$):

$$\mathcal{U} = \exp\begin{pmatrix} \mathbb{O} & R \\ -R^\dagger & \mathbb{O} \end{pmatrix} = \begin{pmatrix} \mathbb{1} - \frac{1}{2} R R^\dagger & R \\ -R^\dagger & \mathbb{1} - \frac{1}{2} R^\dagger R \end{pmatrix} + \mathcal{O}\left(R^3\right), \tag{3.10}$$

where R is a complex 3×3 matrix and $\mathbb{1}$ is the 3×3 identity matrix assuming three generations of right-handed neutrinos, $n_g = 3$. The Taylor expansion in the second equality needs R to be small. Using the approximated diagonalization matrix and only keeping the leading order, the following relations are obtained:

$$\begin{aligned} -M_D R^\dagger - R^* M_D^T + R^* M R^\dagger &\simeq U^* D_D U^\dagger, \\ M_D - R^* M &\simeq \mathbb{O}, \\ R^T M_D + M_D^T R + M &\simeq U_M^* D_M U_M^\dagger. \end{aligned} \tag{3.11}$$

The matrix R is indeed small if the following condition is fulfilled

$$\mathbb{1} \gg (M_D M^{-1})^*. \tag{3.12}$$

Therefore, $R^* \simeq M_D M^{-1}$. From Eq. (3.4) we can also find the mixing between active neutrinos ν_L and sterile right-handed neutrinos ν_R:

$$-\mathcal{L}_N \supset \frac{1}{2} \begin{pmatrix} \overline{\nu} & \overline{N^c} \end{pmatrix} \mathcal{U}^* \widehat{\mathfrak{M}}_\nu \mathcal{U}^\dagger \begin{pmatrix} \nu^c \\ N \end{pmatrix} + \text{h.c.} = \frac{1}{2} \begin{pmatrix} \overline{\nu_L} & \overline{\nu_R^c} \end{pmatrix} \widehat{\mathfrak{M}}_\nu \begin{pmatrix} \nu_L^c \\ \nu_R \end{pmatrix} + \text{h.c.}, \tag{3.13}$$

$$\mathcal{U} \begin{pmatrix} \nu_L^c \\ \nu_R \end{pmatrix} = \begin{pmatrix} \nu^c \\ N \end{pmatrix}, \tag{3.14}$$

where the active-sterile mixing is proportional to the size of matrix R, in detail:

$$\nu = \left(\mathbb{1} - \frac{1}{2} R R^\dagger\right) \nu_L + R N^c. \tag{3.15}$$

The introduction of sterile right-handed neutrinos N leads to active-sterile mixing and to the loss of unitarity of the U_ν matrix in Eq. (3.9), while the unitary PMNS mixing matrix reads

$$U_{\text{PMNS}} = U_e^\dagger \left(\mathbb{1} - \frac{1}{2} R R^\dagger\right) U_\nu = U_e^\dagger \left(\mathbb{1} + \eta\right) U_\nu, \tag{3.16}$$

with U_e diagonalizing the charged lepton mass matrix, such that $U_e^\dagger M_e M_e^\dagger U_e = \text{diag}(m_e^2, m_\mu^2, m_\tau^2)$. The amount of unitarity violation in the U_ν mixing matrix is measured by the parameter

$\eta = -RR^\dagger/2$. As long as η is small, we can use the approximation $U_{\text{PMNS}} \simeq U_e^\dagger U_\nu$. Both, active-sterile mixing and deviation from unitarity of the U_ν matrix are phenomenological implications from the introduction of right-handed neutrinos.

The deviation from unitarity in Eq. (3.16) of U_ν induces lepton flavor violating (LFV) processes in the charged lepton sector, which are suppressed by the seesaw scale. LFV in charged leptons is therefore one of the predictions of the seesaw mechanism. One of the experimentally best constraint decays in this regard is the upper limit for the branching ratio $BR(\mu^+ \to e^+\gamma) < 4.2 \times 10^{-13}$ at 90% CL [63] from the MEG experiment.

The interactions between the neutrinos (ν, N) and the vector bosons $(W^\pm, Z^0)$ are included in the charged current (CC) and neutral current (NC) weak interaction components of the Lagrangian containing the leptonic fields. In detail, we have for the left-handed neutrinos

$$\begin{aligned}
-\mathcal{L}_\nu^{\text{CC}} &= \frac{e}{\sqrt{2}\sin\theta_W} \overline{\begin{pmatrix} e_L & \mu_L & \tau_L \end{pmatrix}} \gamma_\mu U_{\text{PMNS}} \begin{pmatrix} \nu_1 \\ \nu_2 \\ \nu_3 \end{pmatrix} W^\mu + \text{h.c.} \\
&= \frac{e}{\sqrt{2}\sin\theta_W} \overline{\begin{pmatrix} e_L & \mu_L & \tau_L \end{pmatrix}} \gamma_\mu U_e^\dagger (\mathbb{1} + \eta) U_\nu \begin{pmatrix} \nu_1 \\ \nu_2 \\ \nu_3 \end{pmatrix} W^\mu + \text{h.c.}, \qquad (3.17) \\
-\mathcal{L}_\nu^{\text{NC}} &= \frac{e}{2\sin\theta_W\cos\theta_W} \overline{\begin{pmatrix} \nu_e & \nu_\mu & \nu_\tau \end{pmatrix}} \gamma_\mu \begin{pmatrix} \nu_e \\ \nu_\mu \\ \nu_\tau \end{pmatrix} Z^\mu + \text{h.c.} \\
&= \frac{e}{2\sin\theta_W\cos\theta_W} \overline{\begin{pmatrix} \nu_1 & \nu_2 & \nu_3 \end{pmatrix}} \gamma_\mu U_{\text{PMNS}}^\dagger U_{\text{PMNS}} \begin{pmatrix} \nu_1 \\ \nu_2 \\ \nu_3 \end{pmatrix} Z^\mu + \text{h.c.} \\
&\simeq \frac{e}{2\sin\theta_W\cos\theta_W} \overline{\begin{pmatrix} \nu_1 & \nu_2 & \nu_3 \end{pmatrix}} \gamma_\mu U_\nu^\dagger \left(\mathbb{1} + \eta + \eta^\dagger\right) U_\nu \begin{pmatrix} \nu_1 \\ \nu_2 \\ \nu_3 \end{pmatrix} Z^\mu + \text{h.c.}, \qquad (3.18)
\end{aligned}$$

where θ_W denotes the Weinberg angle, such that $e = g_2 \sin\theta_W$ with the $SU(2)_L$ gauge boson coupling g_2, W^μ and Z^μ are the W-boson and Z-boson fields respectively. In the last line we see the non-unitarity of the U_ν mixing matrix showing up, neglecting terms of order $\mathcal{O}(\eta^2)$. The additional term η capturing the unitarity violation therefore shows up in decay widths of W and Z decays. Due to the active-sterile mixing there are also weak CC and NC interactions between the right-handed neutrinos and the W and Z vector bosons:

$$\begin{aligned}
-\mathcal{L}_N^{\text{CC}} &\simeq \frac{e}{\sqrt{2}\sin\theta_W} \overline{\begin{pmatrix} e_L & \mu_L & \tau_L \end{pmatrix}} \gamma_\mu R U_M \frac{(\mathbb{1} - \gamma_5)}{2} \begin{pmatrix} N_1 \\ N_2 \\ N_3 \end{pmatrix} W^\mu + \text{h.c.}, \qquad (3.19) \\
-\mathcal{L}_N^{\text{NC}} &\simeq \frac{e}{2\sin\theta_W\cos\theta_W} \overline{\begin{pmatrix} \nu_e & \nu_\mu & \nu_\tau \end{pmatrix}} \gamma_\mu R U_M \begin{pmatrix} N_1 \\ N_2 \\ N_3 \end{pmatrix} Z^\mu + \text{h.c.}, \qquad (3.20)
\end{aligned}$$

with the diagonalizing matrix U_M as in Eq. (3.5). The matrix RU_M can be seen as the mixing matrix between the light and the heavy neutrino states.

3.2 Integrating Out Heavy Right-Handed Neutrinos

If the eigenvalues of Majorana mass matrix M_i are far above the electroweak scale, the right-handed neutrinos N_i cannot be observed experimentally. The right-handed neutrinos still have an effect on the low-energy physics after they have been integrated out through effective operators. In case of the type-I seesaw, the renormalizable ultraviolet completion at Λ leading to Eq. (3.1) at low-energy scales $\mu \ll \Lambda$, is obtained by adding n_g right-handed neutrinos, N_{R_i} with $i = 1, ..., n_g$, to the Standard Model field content:

$$\mathcal{L}_N \simeq \overline{N_{R_i}} i\partial\!\!\!/ N_{R_i} - \left(Y_{\alpha i} \overline{L_\alpha} \widetilde{\Phi} N_{R_i} + \frac{1}{2} M_{ij} \overline{N^c_{R_i}} N_{R_j} + \text{h.c.} \right). \tag{3.21}$$

The Majorana mass matrix is a symmetric complex $n_g \times n_g$ matrix with n_g complex eigenvalues, $M_i = |M_i| e^{i\varphi_i} = \chi_i |M_i|$, where φ_i denotes the Majorana phase. For convenience it is possible to work in the basis in which the Majorana mass matrix M is real and diagonal. Then the mass eigenstates of the right-handed neutrinos are henceforth denoted by N_i, fulfilling the Majorana property $N_i = N_i^c$, such that

$$N_i = \sqrt{\chi_i} N_{R_i} + \sqrt{\chi_i^*} N^c_{R_i}. \tag{3.22}$$

The part of the Lagrangian containing all right-handed neutrino fields becomes

$$\mathcal{L}_N = \frac{1}{2} \overline{N_i} i\partial\!\!\!/ N_i - \frac{1}{2} \left(Y_{\alpha i} \overline{L_\alpha} \widetilde{\Phi} \sqrt{\chi_i^*} N_i + Y^*_{\alpha i} \overline{L^c_\alpha} \widetilde{\Phi}^* \sqrt{\chi_i} N_i + \overline{N_i} M_i N_i + \text{h.c.} \right). \tag{3.23}$$

Below the energy scale of the heavy right-handed neutrinos Λ, an effective Lagrangian can be constructed by integrating-out the heavy degrees of freedom. The heavy Majorana neutrino fields still give corrections to the effective theory, but are suppressed by powers of the scale Λ,

$$\mathcal{L}_{\text{eff}} = \mathcal{L}_{SM} + \frac{1}{\Lambda} \mathcal{L}_{\text{dim}-5} + \frac{1}{\Lambda^2} \mathcal{L}_{\text{dim}-6} + \cdots, \tag{3.24}$$

where each $\mathcal{L}_{\text{dim}-k}$ contains operators of the dimension k. Following [64], the effective Lagrangian $\mathcal{L}_{\text{eff}}$ is obtained by integrating-out the Majorana neutrino fields

$$e^{iS_{\text{eff}}} = \exp\left(i \int d^4x \mathcal{L}_{\text{eff}}(x) \right) \equiv \int \mathcal{D}N \mathcal{D}\overline{N} e^{iS} = e^{iS_{SM}} \int \mathcal{D}N \mathcal{D}\overline{N} e^{iS_N}, \tag{3.25}$$

using the equations of motion and setting $N = \text{const.}$, since the right-handed neutrinos have almost no kinetic energy below the scale Λ,

$$\begin{aligned} \left. \frac{\partial \mathcal{L}_N}{\partial \overline{N}_i(x)} \right|_{N_i = \text{const.}} &= \frac{1}{2} \left(i\partial\!\!\!/ - M_i \right) N_i - \frac{1}{2} \left(\sqrt{\chi_i} Y^*_{i\alpha} \widetilde{\Phi}^\dagger L_\alpha + \sqrt{\chi_i^*} Y_{i\alpha} \widetilde{\Phi}^T L^c_\alpha \right) \Big|_{N_i = \text{const.}} = 0, \\ \left. \frac{\partial \mathcal{L}_N}{\partial N_i(x)} \right|_{N_i = \text{const.}} &= \frac{1}{2} \overline{N}_i \left(i \overleftarrow{\partial\!\!\!/} - M_i \right) - \frac{1}{2} \left(Y_{\alpha i} \overline{L_\alpha} \widetilde{\Phi} \sqrt{\chi_i^*} + Y^*_{\alpha i} \overline{L^c_\alpha} \widetilde{\Phi}^* \sqrt{\chi_i} \right) \Big|_{N_i = \text{const.}} = 0, \end{aligned} \tag{3.26}$$

and inserting them back into the Lagrangian $\mathcal{L}_N[N_0]$. The effective theory becomes:

$$\mathcal{L}_{\text{eff}} = \mathcal{L}_{SM} + \mathcal{L}_N[N_0], \tag{3.27}$$

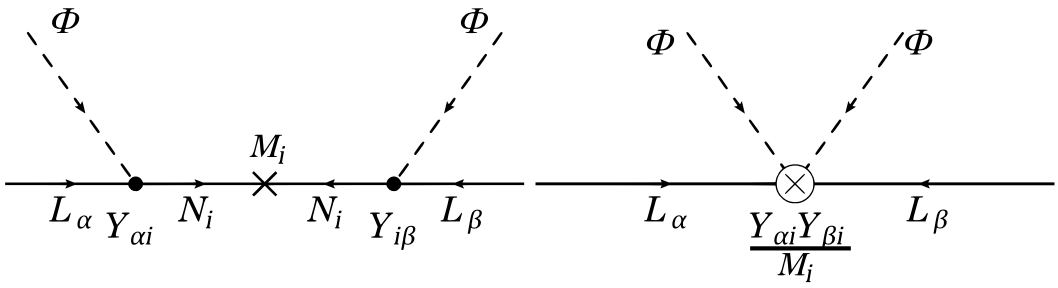

Figure 3.1: Feynman diagrams for the high-scale realization of the type-I seesaw mechanism (left) and the effective dimension-5 operator for neutrino masses after the heavy right-handed neutrinos N_i have been integrated out (right).

with

$$\mathcal{L}_N[N_0] \simeq -\frac{1}{2}\left(\sqrt{\chi_i}Y^*_{i\alpha}\widetilde{\Phi}^\dagger L_\alpha + \sqrt{\chi^*_i}Y_{i\alpha}\widetilde{\Phi}^T L^c_\alpha\right)\frac{\delta_{ij}}{i\not{\partial} - M}\left(Y_{\beta j}\overline{L_\beta}\widetilde{\Phi}\sqrt{\chi^*_j} + Y^*_{\beta j}\overline{L^c_\beta}\widetilde{\Phi}^*\sqrt{\chi_j}\right). \tag{3.28}$$

The propagator of the right-handed neutrinos can be evolved for large M into the following power series,

$$\frac{1}{i\not{\partial} - M} = -\frac{1}{M} - \frac{i\not{\partial}}{M^2} - \cdots \tag{3.29}$$

Neglecting the dimension-6 and higher-order contributions, the effective dimension-5 contribution becomes

$$\begin{aligned}\mathcal{L}_N[N_0] &= -\frac{1}{2}\left(Y\frac{\chi}{M}Y^T\right)_{\alpha\beta}\left(\overline{L_\alpha}\widetilde{\Phi}\right)\left(\widetilde{\Phi}^T L^c_\beta\right) + \text{h.c.},\\ &= -\frac{1}{2}\kappa_{\alpha\beta}\left(\overline{L_\alpha}\widetilde{\Phi}\right)\left(\widetilde{\Phi}^T L^c_\beta\right) + \text{h.c.},\end{aligned} \tag{3.30}$$

where χ is the $n_g \times n_g$ diagonal Majorana phase matrix. The high-scale phases χ from the heavy Majorana mass matrix are handed down to the low-scale Majorana mass matrix of the active neutrinos. By integrating-out the heavy fields, the Feynman diagram for the type-I seesaw in the left of Fig. 3.1 becomes an effective vertex $\kappa_{\alpha\beta}$ in the right-hand side of the figure. After ESWB, the Majorana mass term $\overline{\nu^c_\alpha}\,(\mathcal{M}_\nu)_{\alpha\beta}\,\nu_\beta$ of the active neutrinos takes the form

$$(\mathcal{M}_\nu)_{\alpha\beta} = -\frac{v^2}{2}\left(Y\frac{\chi}{M}Y^T\right)_{\alpha\beta} = -\frac{v^2}{2}\kappa_{\alpha\beta}, \tag{3.31}$$

which is the same result as previously obtained in Eq. (3.9).

3.3 Parameter Counting

In order to have a benchmark on the vanilla type-I seesaw in terms of the necessary parameters, the number of physical parameters is determined. For the basic type-I seesaw

scenario, the SM is extended to include right-handed neutrino fields. The corresponding leptonic sector of the theory reads:

$$\mathcal{L}_{\text{lep}} = \overline{L} i \not{D} L + \overline{e_R} i \not{D} e_R + \overline{N} i \not{\partial} N - \left(\overline{L} Y_e \Phi e_R + \overline{L} Y \widetilde{\Phi} N + \frac{1}{2} \overline{N^c} M N + \text{h.c.} \right) , \tag{3.32}$$

which is invariant under $U(3)_N \times U(3)_L \times U(3)_e$ global transformations for vanishing neutrino, charged-lepton Yukawa couplings and Majorana mass matrix $Y = Y_e = M = 0$. Three RHN species are assumed for this analysis. Using the rule presented in [65], the number of physical parameters can be counted with

$$\#\text{ total parameters} - \#\text{ broken generators} = \#\text{ physical parameters.} \tag{3.33}$$

Where the number of moduli in a general complex 3×3 matrix like Y is equal to 9 and the number of moduli in a general symmetric and complex matrix equals to 6, making the number of total parameters 24. The number of phases equals the number of moduli. For non-vanishing, general Yukawa couplings and Majorana mass matrix, the global $U(3)_N \times U(3)_L \times U(3)_e$ symmetry is broken down to nothing. The number of real generators of a $U(n)$ matrix equals $n(n-1)/2$, which makes nine generators in case of a $U(3)^3$ global symmetry. The number of physical parameters thus equals

$$(9+9+6)\text{ parameters in total} - 9\text{ broken real parameters} = 15\text{ physical parameters.} \tag{3.34}$$

The number of phases in a general $U(n)$ matrix is equal to $n(n+1)/2$, which makes 18 in total for $U(3)^3$. Similarly, the number of physical phases is equal to

$$(9+9+6)\text{ phases in total} - 18\text{ broken phase parameters} = 6\text{ physical phases.} \tag{3.35}$$

In total, the standard seesaw scenario has 21 physical parameters in the leptonic sector at the high-energy scale: the 9 eigenvalues of the Y_e, Y and M matrices, as well as 6 angles and 6 phases. At low energies the number of observable parameters is 12 $(\theta_{13}, \theta_{23}, \theta_{12}, \delta, \alpha, \beta, m_1, m_2, m_3, m_e, m_\mu, m_\tau)$. Or if the charged-lepton sector is excluded, the number for of high-scale parameters is 18, while the low-scale theory consists of 9 physical parameters. One way to constrain the high-energy theory with the available low-energy experimental information is to use the parametrization suggested in [66] for the neutrino Yukawa

$$Y = i \frac{\sqrt{2}}{v} U_\nu^* \sqrt{D_\mathcal{M}} \Omega \sqrt{D_M} U_M^\dagger, \tag{3.36}$$

where U_M is the unitary matrix diagonalizing the RHN mass matrix as in Eq. (3.5) and U_ν is unitary matrix diagonalizing the active neutrino mass matrix, given in Eq. (3.9), while Ω is a complex, orthogonal matrix, such that $\Omega^T \Omega = \mathbb{1}$. The difference of 9 parameters between the high- and low-energy physics, due to the decoupling of the heavy neutrino degrees of freedom, is captured in D_M and Ω.

After discussing the basics of the seesaw mechanism, the next chapter studies quantum effects on the RHN masses, before investigating their impact on the low-scale phenomenology through the seesaw.

Chapter 4

Two-Loop Quantum Effects on Seesaw Parameters

In this chapter, a minimal extension of the SM, adding right-handed singlet neutrinos is considered. It will be shown that in this generic extension two-loop quantum effects can have a significant impact on the right-handed neutrino parameters. While the corrections to the Yukawa couplings are small as expected from two-loop quantum effects, the corrections to the Majorana mass matrix can be comparable to or even dominate the tree-level contribution [2, 67]. The reason for this striking difference is that the Majorana mass term introduces violation of total lepton number (by two units). Since the Majorana mass matrix is in general not protected by any symmetry, large quantum corrections from above the electroweak scale are possible. After introducing the model, the relevant quantum effects from the renormalization group equations (RGEs) are investigated.

4.1 Two-Loop Renormalization Group Equations for Right-Handed Neutrinos

The Standard Model in Eq. (2.1) is expanded to include n_g right-handed neutrinos, N_i with $i = 1, ..., n_g$, neutral under the SM gauge group. The most general, renormalizable extension to the SM involving the newly introduced right-handed neutrino fields reads:

$$\mathcal{L}_N = \frac{1}{2}\overline{N_i} i\not{\partial} N_i - \left(Y_{\alpha i} \overline{L_\alpha} \widetilde{\Phi} N_i + \frac{1}{2} M_{ij} \overline{N_i^c} N_j + \text{h.c.} \right) , \tag{4.1}$$

where L_α with $\alpha = e, \mu, \tau$ denotes the lepton doublets and $\widetilde{\Phi} = i\sigma_2 \Phi^*$ is the charge conjugated Standard Model Higgs field, Y is the $3 \times n_g$ neutrino Yukawa coupling matrix and M is the $n_g \times n_g$ complex symmetric Majorana mass matrix with eigenvalues M_i.

As long as $M = 0$ and $Y = 0$, the Lagrangian in Eq. (4.1) is invariant under global $U(3)_L$ transformations with $L \to \mathcal{V}L$ as well as global $U(n_g)_N$ transformations of the form $N \to \mathcal{W}N$, where $\mathcal{V}$ and $\mathcal{W}$ are unitary 3×3 and $n_g \times n_g$ matrices respectively. Assuming that $n_g = 3$ and letting Y be a general, non-vanishing 3×3 Yukawa coupling matrix, it is sufficient to have only one right-handed neutrino with a non-vanishing tree-level mass $M_3 \neq 0$ (while $M_1 = M_2 = 0$) to completely break the global $U(3)_L \times U(3)_N$ down to nothing [2]. This means there is no residual symmetry protecting the lighter right-handed neutrino masses M_1 and M_2 against radiative effects. The radiative masses are generated

through loop corrections and are proportional to the mass scale at which the lepton number breaking was introduced, M_3. If either Y or M_3 stay zero, the symmetry protecting M_1 and M_2 from quantum corrections would be restored. The same logic applies in the case of $n_g = 2$ or $n_g > 3$.

This reasoning is confirmed by explicitly calculating the corrections to the right-handed neutrino masses. As shown in [68, 69], the calculation at one-loop level only leads to corrections proportional to the tree-level masses, such that in the case of $n_g = 3$, N_1 and N_2 would stay massless for $M_1 = M_2 = 0$ at all scales, even if $M_3 \neq 0$. It is therefore necessary to consider higher-order contributions to capture the quantum effects leading to the rank-increasing corrections.

The evolution of the right-handed Majorana mass matrix M with the energy scale μ is described by its beta function. Considering corrections up to the two-loop level, the renormalization group equation for M is of the form:

$$\frac{dM}{d\log\mu} = \beta_M^{(1)} + \beta_M^{(2)}, \tag{4.2}$$

where $\beta_M^{(1)}$ and $\beta_M^{(2)}$ denote one- and two-loop beta functions respectively. The full one-loop beta function [68] and two-loop beta function [3] explicitly read

$$\begin{aligned}
16\pi^2\beta_M^{(1)} &= M(Y^\dagger Y) + (Y^\dagger Y)^T M, \\
(16\pi^2)^2\beta_M^{(2)} &= 4(Y^\dagger Y)^T M (Y^\dagger Y) - \frac{1}{4}\left[M(Y^\dagger Y)(Y^\dagger Y) + (Y^\dagger Y)^T (Y^\dagger Y)^T M\right] \\
&\quad + \left\{\frac{17}{8}g_1^2 + \frac{51}{8}g_2^2 - \frac{9}{2}\mathrm{Tr}(Y_u Y_u^\dagger) - \frac{3}{2}\mathrm{Tr}(Y^\dagger Y)\right\}\left[M(Y^\dagger Y) + (Y^\dagger Y)^T M\right].
\end{aligned} \tag{4.3}$$

The beta functions were calculated in the $\overline{\mathrm{MS}}$ renormalization scheme. g_1 and g_2 denote the gauge couplings of the $U(1)_Y$ and $SU(2)_L$ gauge groups respectively, while Y_u is the up-type Yukawa coupling. The other SM Yukawa couplings (Y_e, Y_d) are neglected. For completeness, the RGE for the neutrino Yukawa coupling matrix up to the two-loop order is given by

$$\frac{dY}{d\log\mu} = \beta_Y^{(1)} + \beta_Y^{(2)}, \tag{4.4}$$

where $\beta_Y^{(1)}$ and $\beta_Y^{(2)}$ denote the corresponding one- and two-loop beta functions. Taken from [70, 71] and reproduced with `SARAH` [72, 73], working in the $\overline{\mathrm{MS}}$ scheme, they explicitly take the form

$$\begin{aligned}
16\pi^2\beta_Y^{(1)} &= \left[3\,\mathrm{Tr}(Y_u Y_u^\dagger) + \mathrm{Tr}(Y^\dagger Y) - \frac{3}{4}g_1^2 - \frac{9}{4}g_2^2\right]Y + \frac{3}{2}YY^\dagger Y, \\
(16\pi^2)^2\beta_Y^{(2)} &= \left[\frac{93}{16}g_1^2 + \frac{135}{16}g_2^2 - \frac{27}{4}\mathrm{Tr}(Y_u Y_u^\dagger) - \frac{9}{4}\mathrm{Tr}(Y^\dagger Y) - 12\lambda\right]YY^\dagger Y \\
&\quad + \left[6\lambda^2 - \frac{27}{4}\,\mathrm{Tr}\big((Y_u Y_u^\dagger)^2\big) - \frac{9}{4}\,\mathrm{Tr}\big((Y^\dagger Y)^2\big) - \frac{9}{4}g_1^2 g_2^2 + \frac{35}{24}g_1^4 - \frac{23}{4}g_2^4\right. \\
&\quad \left. + \left(\frac{85}{24}g_1^2 + \frac{45}{8}g_2^2 + 20g_s^2\right)\mathrm{Tr}(Y_u Y_u^\dagger) + \left(\frac{5}{8}g_1^2 + \frac{15}{8}g_2^2\right)\mathrm{Tr}(Y^\dagger Y)\right]Y + \frac{3}{2}Y(Y^\dagger Y)^2,
\end{aligned} \tag{4.5}$$

where g_s is the gauge coupling of $SU(3)_c$ and λ is the quartic coupling in the Higgs potential in Eq. (2.5). Again, the charged lepton and down-type Yukawa couplings are neglected.

To simplify the RGEs given above, it is convenient to use the following shorthand quantities:

$$\begin{aligned} P &= \frac{1}{16\pi^2} Y^\dagger Y \,, \\ \mathcal{G} &= \frac{1}{16\pi^2}\Big(\frac{17}{8}g_1^2 + \frac{51}{8}g_2^2 - \frac{9}{2}\mathrm{Tr}(Y_u Y_u^\dagger)\Big) - \frac{3}{2}\mathrm{Tr}(P) \,, \\ Q &= (1+\mathcal{G})P - \frac{1}{4}P^2, \end{aligned} \tag{4.6}$$

which allow to rewrite the energy-scale evolution of the Majorana mass matrix as

$$\frac{dM}{d\log\mu} = MQ + Q^T M + 4P^T M P. \tag{4.7}$$

In order to study the properties of the RGE, it is useful to decompose the Majorana mass matrix such that $M = U_M^* D_M U_M^\dagger$, where U_M denotes an unitary and D_M a diagonal matrix which contains the real eigenvalues M_i on its main diagonal, with $i = 1, ..., n_g$. Defining the $n_g \times n_g$ quantities P and Q in the basis where M is diagonal, $\widehat{P} = U_M^\dagger P U_M$ and $\widehat{Q} = U_M^\dagger Q U_M$, the RGE becomes:

$$\begin{aligned} &\frac{dD_M}{d\log\mu} + U_M^T\frac{dU_M^*}{d\log\mu}D_M + D_M\frac{dU_M^\dagger}{d\log\mu}U_M = D_M\widehat{Q} + \widehat{Q}^T D_M + 4\widehat{P}^T D_M \widehat{P}, \\ &\frac{dM_i}{d\log\mu}\delta_{ij} + \left(U^T\frac{dU_M^*}{d\log\mu}\right)_{ij} M_i + \left(\frac{dU_M^\dagger}{d\log\mu}U_M\right)_{ij} M_i = 2\widehat{Q}_{ij}M_i + 4\sum_k M_k \widehat{P}_{ki}\widehat{P}_{kj}, \end{aligned} \tag{4.8}$$

where the diagonal components can be separated into a real and an imaginary part

$$\frac{dM_i}{d\log\mu} = 2M_i\widehat{Q}_{ii} + 4\sum_k M_k \mathrm{Re}\left(\widehat{P}_{ki}^2\right), \tag{4.9}$$

$$-2M_i\mathrm{Im}\left(T_{ii}\right) = 4\sum_k M_k \mathrm{Im}\left(\widehat{P}_{ki}^2\right), \tag{4.10}$$

and equivalently for the off-diagonal elements

$$(M_j - M_i)\mathrm{Re}\left(T_{ij}\right) = (M_i + M_j)\mathrm{Re}\left(\widehat{Q}_{ij}\right) + 4\sum_k M_k \mathrm{Re}\left(\widehat{P}_{ki}\widehat{P}_{kj}\right), \tag{4.11}$$

$$-(M_j + M_i)\mathrm{Im}\left(T_{ij}\right) = (M_i - M_j)\mathrm{Im}\left(\widehat{Q}_{ij}\right) + 4\sum_k M_k \mathrm{Im}\left(\widehat{P}_{ki}\widehat{P}_{kj}\right), \tag{4.12}$$

where T is skew-Hermitian (in order to preserve the unitarity nature of U_M in the scale evolution), and satisfies

$$\frac{dU_M}{d\log\mu} = U_M T, \tag{4.13}$$

The Hermitian matrices $\widehat{P}$ and $\widehat{Q}$ satisfy the property of real-valued diagonal entries, $\mathrm{Im}(\widehat{P}_{ii}) = 0$, $\mathrm{Im}(\widehat{Q}_{ii}) = 0$, which was used for recasting the RGE.

From splitting up the RGE, the following effects of the RG running by including two-loop contributions on the Majorana mass matrix can be observed:

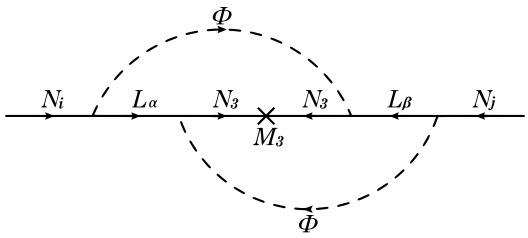

Figure 4.1: Two-loop overlapping Feynman diagram leading to potentially dominant corrections to right-handed neutrino masses, shown for the case of three right-handed neutrinos.

- From Eq. (4.9) it can be seen how the right-handed neutrinos get mass corrections proportional to the mass of heavier RHNs. Depending on how hierarchical the tree-level mass spectrum of the RHNs is, the corrections can be sizable or dominant and therefore heavily influence the phenomenology of the seesaw mechanism. The effect arises from the two-loop diagram shown in Fig. 4.1 and is absent in the one-loop treatment [2, 67].

- According to Eq. (4.10), the RG running drives the right-handed mixing matrix U_M into an infrared quasi-fixed point if the RHN tree-level mass M_i at the cut-off energy scale either vanishes or is dominated by quantum contributions to its physical mass, such that

$$\sum_{k\neq i} M_k \mathrm{Im}\left(\widehat{P}_{ki}^2\right) \simeq 0. \tag{4.14}$$

- Further infrared quasi-fixed points in the RG running for the right-handed mixing matrix U_M come from Eqs. (4.11) and (4.12). If two RHNs have degenerate tree-level masses or if their tree-level mass difference is dominated by the quantum contribution to their physical mass difference, a quasi-fixed point is assumed, such that

$$\sum_{k\neq i,j} M_k \widehat{P}_{ki}\widehat{P}_{kj} \simeq 0, \tag{4.15}$$

  for degenerate vanishing masses $M_i = M_j = 0$ and $M_k \neq 0$ or

$$M_i \mathrm{Re}\left(\widehat{Q}_{ij}\right) + 2\sum_k M_k \mathrm{Re}\left(\widehat{P}_{ki}\widehat{P}_{kj}\right) \simeq 0, \tag{4.16}$$

  if the masses are degenerate but non-vanishing $M_i = M_j \neq 0$.

The quasi-fixed point of U_M in the RG evolution below the cut-off of the theory can be explicitly calculated using Eq. (4.13) in the three right-handed neutrino case for $M_1, M_2 \ll M_3$ in leading orders of $\mathcal{O}(P)$, assuming real parameters:

$$U_M(\mu) \simeq \frac{1}{\sqrt{P_{31}^2 + P_{32}^2}} \begin{pmatrix} P_{32} & P_{31} & 0 \\ -P_{31} & P_{32} & 0 \\ 0 & 0 & \sqrt{P_{31}^2 + P_{32}^2} \end{pmatrix}. \tag{4.17}$$

The useful $\widehat{P}$-matrix is the P-matrix in the basis where the Majorana mass matrix is diagonal. Below the cut-off scale, the RG running rotates the P-matrix, such that its elements for the three right-handed neutrino case read

$$\widehat{P}(\mu) \simeq \begin{pmatrix} \frac{P_{22}P_{31}^2+P_{11}P_{32}^2-2P_{12}P_{31}P_{32}}{P_{31}^2+P_{32}^2} & \frac{P_{12}(P_{31}^2+P_{32}^2)+P_{31}P_{32}(P_{11}-P_{22})}{P_{31}^2+P_{32}^2} & 0 \\ \frac{P_{12}(P_{31}^2+P_{32}^2)+P_{31}P_{32}(P_{11}-P_{22})}{P_{31}^2+P_{32}^2} & \frac{P_{22}P_{32}^2+P_{11}P_{31}^2+2P_{12}P_{31}P_{32}}{P_{31}^2+P_{32}^2} & \sqrt{P_{31}^2+P_{32}^2} \\ 0 & \sqrt{P_{31}^2+P_{32}^2} & P_{33} \end{pmatrix}, \quad (4.18)$$

assuming real-valued parameters and a hierarchical neutrino spectrum at the cut-off.

4.2 Iteratively Solving the Majorana Mass Matrix RGE

In the following, the general solution for the RGE of the Majorana mass matrix is derived. The RGE for the Majorana mass matrix for the right-handed neutrinos takes the following general form:

$$\frac{dM(t)}{dt} = \beta_M[M(t)], \quad (4.19)$$

introducing the convenient scale parameter $t \equiv \log(\mu/\Lambda)$, where Λ is the high-scale cut-off and $\beta_M = \beta_M^{(1)} + \beta_M^{(2)}$ is the beta function up to the two-loop level from Eq. (4.3). The formal solution to the RGE is then just

$$M(t) = M_0 + \int_0^t \beta_M[M(t')]dt', \quad (4.20)$$

using as boundary condition the tree-level Majorana mass matrix of the right-handed neutrinos $M(t=0) \equiv M_0$ at the cut-off. Through the method of Picard iteration, an analytical solution to the RGE can derived. The iterative steps are defined in the following way

$$M^{(0)}(t) = M_0, \qquad \text{for} \qquad n = 0, \quad (4.21)$$

$$M^{(n)}(t) = M_0 + \int_0^t \beta_M[M^{(n-1)}(t')]dt' \qquad \text{for} \qquad n > 0. \quad (4.22)$$

The first three non-trivial orders in the iteration explicitly read

$$M^{(1)}(t) = M_0 + \int_0^t \beta_M[M^{(0)}(t')]dt' = M_0 + \beta_M[M_0]t, \quad (4.23)$$

$$\begin{aligned} M^{(2)}(t) &= M_0 + \int_0^t \beta_M[M^{(1)}(t')]dt' \\ &= M_0 + \beta_M[M_0]t + \frac{1}{2}(\beta_M \circ \beta_M)[M_0]t^2, \\ M^{(3)}(t) &= M_0 + \int_0^t \beta_M[M^{(2)}(t')]dt' \\ &= M_0 + \beta_M[M_0]t + \frac{1}{2}(\beta_M \circ \beta_M)[M_0]t^2 + \frac{1}{6}(\beta_M \circ \beta_M \circ \beta_M)[M_0]t^3, \end{aligned} \quad (4.24)$$

with the notation for a function composition $(f \circ g)(x) = f(g(x))$, with which the solution for the n-th order iteration can be expressed as a power series

$$M^{(n)}(t) = \sum_{k=0}^{n} \frac{1}{k!}\beta_M^k[M_0]t^k, \quad (4.25)$$

defining the Picard sequence for a n-fold composed function $\beta_M^n := \underbrace{\beta_M \circ \beta_M \circ \cdots \circ \beta_M}_{n-\text{times}}$ with $\beta_M^0 = M$. The beta function of the Majorana mass matrix in Eq. (4.2) is in general of the structure:

$$\beta_M = \sum_{n,m} a_{nm} \left(P^T\right)^n M P^m, \tag{4.26}$$

with the coefficients $a_{nm} = a_{mn}$ which contain scalar functions in flavor space depending on gauge couplings and traces of Yukawa couplings. After four iteration steps of the beta function in Eq. (4.25) and keeping terms up to the order $\mathcal{O}(P^4)$, the approximate solution to the RGE becomes:

$$\begin{aligned}
M(t) \simeq\ & M + a_{10} t \Big(MP + P^T M\Big) \\
& + \frac{t}{2}\Big[a_{10}^2 t + 2a_{20}\Big]\Big(MPP + P^T P^T M\Big) \\
& + t\Big[a_{11} + a_{10}^2 t\Big] P^T M P \\
& + \frac{t}{6}\Big[6a_{30} + 6a_{10}a_{20}t + a_{10}^3 t^2\Big]\Big(MPPP + P^T P^T P^T M\Big) \\
& + \frac{t}{2}\Big[2a_{21} + 2a_{10}(a_{11} + a_{20})t + a_{10}^3 t^2\Big]\Big(P^T MPP + P^T P^T MP\Big) \\
& + \frac{t}{24}\Big[24a_{40} + (12a_{20}^2 + 24a_{10}a_{30})t + 12a_{10}^2 a_{20} t^2 + a_{10}^4 t^3\Big]\Big(MPPPP + P^T P^T P^T P^T M\Big) \\
& + \frac{t}{6}\Big[6a_{31} + 6\Big(a_{10}(a_{21} + a_{30}) + a_{11}a_{20}\Big)t + 3a_{10}^2(a_{11} + 2a_{20})t^2 + a_{10}^4 t^3\Big] \\
& \times \Big(P^T MPPP + P^T P^T P^T MP\Big) \\
& + \frac{t}{4}\Big[4a_{22} + 2(a_{11}^2 + 2a_{20}^2 + 4a_{10}a_{21})t + 4a_{10}^2(a_{11} + a_{20})t^2 + a_{10}^4 t^3\Big] P^T P^T MPP.
\end{aligned} \tag{4.27}$$

Here, some coefficients can readily be identified with the two-loop RGE in Eq. (4.7) and Eq. (4.6), such that

$$\begin{aligned}
a_{00} &= 0, \\
a_{10} &= 1 + \mathcal{G} + \cdots, \\
a_{20} &= -\frac{1}{4} + \cdots, \\
a_{11} &= 4 + \cdots.
\end{aligned} \tag{4.28}$$

Higher-order contributions, suppressed by loop factors and corresponding to the generic $(P^T)^n M P^m$ structure are indicated by the dots. From the form of Eq. (4.27), the necessary order to radiatively generate RHN masses can be read off. If M is rank-2 at the cut-off scale, then terms up to the order $\mathcal{O}(P^2)$ are enough to increase the rank up to rank-3. If M at the cut-off is rank-1, $\mathcal{O}(P^2)$ terms increase the rank by one, and considering terms up to the order $\mathcal{O}(P^4)$, will increase the rank by two (assuming generic neutrino Yukawa couplings).

Chapter 5

Phenomenological Implications of Two-Loop Quantum Effects

After discussing the quantum corrections for the right-handed neutrino masses in the renormalization group running, the model is investigated phenomenologically in the following. Before considering the SM extended with three neutrinos, corresponding to the typical three generation structure of the SM, a simplified scenario with only two right-handed neutrinos is investigated, similar to the toy model discussed in [2]. This chapter follows closely the publication [3].

5.1 Two Right-Handed Neutrino Model

Starting with the Lagrangian in Eq. (4.1) with $n_g = 2$ right-handed neutrinos, it is convenient to work in the basis where the Majorana mass matrix M for the RHNs is real and diagonal at the cut-off scale Λ, such that

$$M(\mu)\Big|_{\mu=\Lambda} = \begin{pmatrix} M_1 & 0 \\ 0 & M_2 \end{pmatrix}, \tag{5.1}$$

with the eigenvalues M_1 and M_2 ordered in this way: $M_2 > M_1$. We keep only terms up to the order $\mathcal{O}(P^2)$ in Eq. (4.27), since the leading-order effects are the most interesting. The Majorana mass matrix $M(\Lambda)$ at the scale $\mu < \Lambda$ becomes through the RG running

$$M(t) \simeq M + t\Big(MP + P^T M\Big) - \frac{t}{4}(1-2t)\Big(MPP + P^T P^T M\Big) + t(4+t)P^T MP\,, \tag{5.2}$$

using again the convenient scale parameter $t \equiv \log(\mu/\Lambda)$ as above. In order to focus on the leading-order effects, terms proportional to an additional loop suppression at order $\mathcal{O}(P^2)$, like $\mathcal{G}$, are neglected.

After diagonalizing the matrix in Eq. (5.2), the eigenvalues at the scale μ read:

$$D_M(\mu) = U_M^T M U_M = \begin{pmatrix} M_1 - 4M_2 P_{21}^2 \log(\Lambda/\mu) & 0 \\ 0 & M_2 \end{pmatrix}, \tag{5.3}$$

where the right-handed mixing matrix $U_M(\mu) \simeq \mathbb{1}$, which does not significantly change in the running for $\mu < \Lambda$ in the two RHN scenario, as can be seen from Eq. (4.9). Below the

energy scale of the heavy RHN $\mu \simeq M_2$, the theory is described by an effective Lagrangian (see Sec. 3.2), obtained from integrating-out N_2:

$$\mathcal{L}_{\text{eff}} \simeq -\frac{1}{2}\frac{Y_{\alpha 2}Y_{\beta 2}}{M_{22}}\left(\overline{L_\alpha}\widetilde{\Phi}\right)\left(\widetilde{\Phi}^T L_\beta^c\right) - \mathbb{Y}_{\alpha 1}\overline{L_\alpha}\widetilde{\Phi}N_1 - \frac{1}{2}\mathbb{M}_{11}\overline{N_1^c}N_1 + \text{h.c.}, \tag{5.4}$$

where all parameters are evaluated at the scale $\mu \simeq M_2$ and the Yukawa coupling and mass matrix are redefined accordingly by the quantities

$$\begin{aligned}\mathbb{Y}_{\alpha 1} &= Y_{\alpha 1} - \frac{M_{12}Y_{\alpha 2}}{M_{22}}\,,\\ \mathbb{M}_{11} &= M_{11} - \frac{M_{12}M_{21}}{M_{22}}\,,\end{aligned} \tag{5.5}$$

which leads to the same result for the physical mass for N_1 as above, namely

$$M_1^{\text{phys}} \simeq \mathbb{M}_{11}\Big|_{\mu=M_2} \simeq M_1 - 4M_2P_{21}^2\log\left(\frac{\Lambda}{M_2}\right). \tag{5.6}$$

After integrating out N_1 at the scale of its physical mass, the Weinberg operator is obtained:

$$\mathcal{L}_{\text{eff}} \simeq -\frac{1}{2}\left(\frac{Y_{\alpha 2}Y_{\beta 2}}{M_{22}}\Big|_{\mu=M_2} + \frac{\mathbb{Y}_{\alpha 1}\mathbb{Y}_{\beta 1}}{\mathbb{M}_{11}}\Big|_{\mu=M_1}\right)\left(\overline{L_\alpha}\widetilde{\Phi}\right)\left(\widetilde{\Phi}^T L_\beta^c\right) + \text{h.c.}, \tag{5.7}$$

which is evolved down to the electroweak scale before calculating the active neutrino masses. The RG running of the Weinberg operator is discussed in [74, 75]. For the qualitative discussion, the effects from the running between the M_1^{phys} and the EW scale are neglected and the neutrino mass parameters can be calculated directly. After EWSB, the Majorana mass term for the active neutrinos becomes (*cf.* Eq. (3.1)):

$$\mathcal{M}_\nu \simeq -\frac{v^2}{2}\left(YM^{-1}Y^T\right)\Big|_{\mu=M_2}. \tag{5.8}$$

The impact of including the two-loop corrections can significantly alter the phenomenology. For the lighter RHN mass, the radiative correction in Eq. (5.6) is proportional to the heavy RHN mass M_2. This effects stems from the P^TMP term in the RGE in Eq. (4.7) which reappears in the approximate solution for the mass matrix in Eq. (5.2). Depending on the parameters of the high-scale theory, the quantum corrections to M_1 may give significant or dominant contributions and must be considered in these instances.

Two-loop effects have a dominant impact on the right-handed neutrino mass spectrum in the limit $M_1 = 0$ or more generally $M_1 \ll 4M_2P_{21}^2\log(\Lambda/M_2)$, when the tree-level contribution M_1 is completely washed-out. The latter is a generic feature if the RHN mass spectrum at the cut-off is very hierarchical (M is approximately a rank-1 matrix). This scenario is studied in the following. For the simplified scenario with only one lepton doublet L_1 (as discussed in [2]), the active neutrino masses are

$$\begin{aligned}m_\nu &\simeq \left(\frac{Y_{12}^2}{M_2}\Big|_{\mu=M_2} + \frac{Y_{11}^2}{M_1}\Big|_{\mu=M_1}\right)\frac{v^2}{2},\\ &\simeq \left(Y_{12}^2 - \frac{(16\pi^2)^2}{4Y_{12}^2\log(\Lambda/M_2)}\right)\frac{v^2}{2M_2},\end{aligned} \tag{5.9}$$

where it was used that $\mathbb{Y}_{11} \simeq Y_{11}$ which comes from the fact that $M_{12}/M_{22}Y_{12} \sim Y_{11}Y_{12}^2/(16\pi^2) \ll Y_{11}$. The result is insensitive to Y_{11}, since the contribution cancels out due to the dependence of the radiative mass on Y_{11} as well as to the tree-level mass of N_1 as it is completely washed-out. In detail,

$$m_\nu \simeq 0.05\,\text{eV} \left(\frac{Y_{12}}{0.6}\right)^{-2} \left(\frac{M_2}{1.2\times 10^{19}\,\text{GeV}}\right)^{-1}, \tag{5.10}$$

taking M_2 close to the cut-off, $\log(\Lambda/M_2) \simeq 1$ (the Planck scale is chosen as a natural cut-off to the theory). For a hierarchical mass spectrum in the RHN matrix and a Planck scale-sized M_2, the ballpark of the experimentally observed values for an active neutrino mass is reproduced for a Yukawa coupling of order $Y_{12} \simeq \mathcal{O}(1)$. Also note the parameter reduction, as the final result is insensitive to Y_{11} and the exact value of the M_1 tree-level mass. Furthermore, no new mass scale was introduced by setting the lepton number violating scale M_2 close to the Planck mass $M_P \simeq 1.2\times 10^{19}\,\text{GeV}$.

For the SM scenario with three lepton doublets, the left-handed neutrino masses can be calculated from the neutrino mass matrix $\mathcal{M}_\nu$ in Eq. (5.8) with the help of tensor invariants. Due to three active neutrino masses in the theory, the first three tensor invariants need to be considered. They can be constructed by using the recursive Faddeev–LeVerrier algorithm. Explicitly, they take the form

$$\begin{aligned}
I_1 &= \text{Tr}\left[\mathcal{M}_\nu\right] = (16\pi^2)\text{Tr}\left[M^{-1}P\right]\frac{v^2}{2},\\
I_2 &= \frac{1}{2}\left(\text{Tr}\left[\mathcal{M}_\nu\right]^2 - \text{Tr}\left[\mathcal{M}_\nu^2\right]\right) = \frac{(16\pi^2)^2}{2}\left(\text{Tr}\left[M^{-1}P\right]^2 - \text{Tr}\left[M^{-1}PM^{-1}P\right]\right)\frac{v^4}{4},\\
I_3 &= \frac{1}{6}\Big(\text{Tr}\left[\mathcal{M}_\nu\right]^3 - 3\,\text{Tr}\left[\mathcal{M}_\nu\right]\text{Tr}\left[\mathcal{M}_\nu^2\right] + 2\,\text{Tr}\left[\mathcal{M}_\nu^3\right]\Big) = \frac{(16\pi^2)^3}{6}\Big(\text{Tr}\left[M^{-1}P\right]^3\\
&\quad - 3\,\text{Tr}\left[M^{-1}P\right]\text{Tr}\left[M^{-1}PM^{-1}P\right] + 2\,\text{Tr}\left[M^{-1}PM^{-1}PM^{-1}P\right]\Big)\frac{v^6}{8},
\end{aligned} \tag{5.11}$$

where $\mathcal{M}_\nu$ is assumed to be a real matrix. For two RHNs and three left-handed doublets, the invariants become

$$\begin{aligned}
I_1 &= m_1 + m_2 + m_3 \simeq (16\pi^2)\frac{v^2}{2}\frac{P_{11}}{M_1},\\
I_2 &= m_1m_2 + m_1m_3 + m_2m_3 \simeq (16\pi^2)^2\frac{v^4}{4}\frac{P_{11}P_{22} - P_{12}^2}{M_1M_2},\\
I_3 &= m_1m_2m_3 = 0.
\end{aligned} \tag{5.12}$$

Here, I_3 is exactly zero for 2RHNs, since $m_1 = 0$ (neglecting two-loop quantum corrections to m_1 between M_1 and the EW scale, which only give tiny contributions proportional to the other light neutrinos [76–79]). For the non-vanishing invariants only the leading orders in the loop-suppressed P matrix elements are kept. For a general complex $\mathcal{M}_\nu$, the Hermitian matrix $\mathcal{M}_\nu^\dagger\mathcal{M}_\nu$ is constructed to calculate the tensor invariants, such that $I_1 = \text{Tr}[\mathcal{M}_\nu^\dagger\mathcal{M}_\nu] = m_2^2 + m_3^2$, $I_2 = m_2^2m_3^2$ (for $m_1 = 0$), and so on. Assuming a hierarchy in the active neutrino

mass spectrum, the light neutrino masses are

$$m_3 \simeq I_1 \simeq (16\pi^2)\frac{v^2}{2}\frac{P_{11}}{M_1}\Big|_{\mu=M_2},$$
$$m_2 \simeq \frac{I_2}{I_1} \simeq (16\pi^2)\frac{v^2}{2M_2}\left(\frac{P_{11}P_{22}-P_{12}^2}{P_{11}}\right)\Big|_{\mu=M_2}. \tag{5.13}$$

Formally, the $3 \times n_g$ neutrino Yukawa matrix Y in Eq. (4.1) can be parametrized in terms of its singular value decomposition (SVD), such that

$$Y = U_L D_Y U_R^\dagger, \text{ with } D_Y = \text{diag}(y_1, ..., y_{n_g}), \tag{5.14}$$

where U_L is a 3×3 and U_R a $n_g \times n_g$ unitary matrix, while D_Y is a $3 \times n_g$ rectangular diagonal matrix with basis-independent, real parameters $0 \leq y_1 \leq ... \leq y_{n_g}$ on its main diagonal. With this parametrization, the P-matrix defined in Eq. (4.6) becomes for two RHNs: $P = \frac{1}{16\pi^2} U_R \text{diag}(y_1^2, y_2^2) U_R^\dagger$. The active neutrino mass eigenstates thus read

$$m_3 \simeq \frac{(16\pi^2)^2(y_1^2U_{11}^2 + y_2^2U_{21}^2)v^2}{8M_2(y_2^2-y_1^2)^2U_{11}^2U_{12}^2\log(M_2/\Lambda)},$$
$$m_2 \simeq \frac{y_1^2y_2^2v^2}{2M_2(y_1^2U_{11}^2 + y_2^2U_{21}^2)}, \tag{5.15}$$

where the U_{ij} $(i, j = 1, 2)$ denote the elements of U_R, making the active neutrino masses only dependent on the high-scale mass M_2, the Yukawa eigenvalues and the right-handed mixing angles in U_R (Ref. [80] discusses the role of U_R in the low-energy phenomenology of neutrino masses). As shown for the one left-handed doublet case in Eq. (5.10), the mass m_3 will be in the ballpark of experimental values for M_2 close to the Planck scale and y_2 of the order $\mathcal{O}(1)$ and generic right-handed mixing angles in U_R. Although this scenario predicts the correct neutrino mass scale with generic assumptions and two RHNs, the hierarchy between the active neutrino masses tends to be larger than the observed mild hierarchy (see Eq. (2.22)). The neutrino mass hierarchy has the following lower bound in the two RHNs scenario:

$$\left|\frac{m_3}{m_2}\right| \gtrsim \frac{(16\pi^2)^2}{(y_2^2-y_1^2)^2\log(M_2/\Lambda)}. \tag{5.16}$$

In order to stay within the experimental upper limit $|m_3/m_2| \lesssim 6$, the Yukawa couplings need to be larger than allowed by perturbativity constraints, assuming $\log(M_2/\Lambda) \simeq 1$, as above.

A numerical scan plot in Fig. 5.1 shows the heaviest active neutrino mass m_3 vs. the active neutrino mass hierarchy, assuming a massive RHN with the reduced Planck mass $M_2 = M_P/\sqrt{8\pi}$ and $M_1 = 0$ at $\Lambda = M_P$. The eigenvalues of the neutrino Yukawa are scanned within the range $10^{-2} \leq y_2 < y_1 \leq \sqrt{4\pi}$ and the right-handed mixing angles in U_R take on random values between 0 and 2π. The experimentally observed neutrino mass scale $m_3 = \mathcal{O}(0.05)$ eV can be reproduced within the parameter range of the scan, but the mass hierarchy is too large.

5.2 Three Right-Handed Neutrino Model

In this section, the SM extended with $n_g = 3$ right-handed neutrinos is considered, with the neutrino Lagrangian given in Eq. (4.1). Again, the basis is chosen in which the Majorana

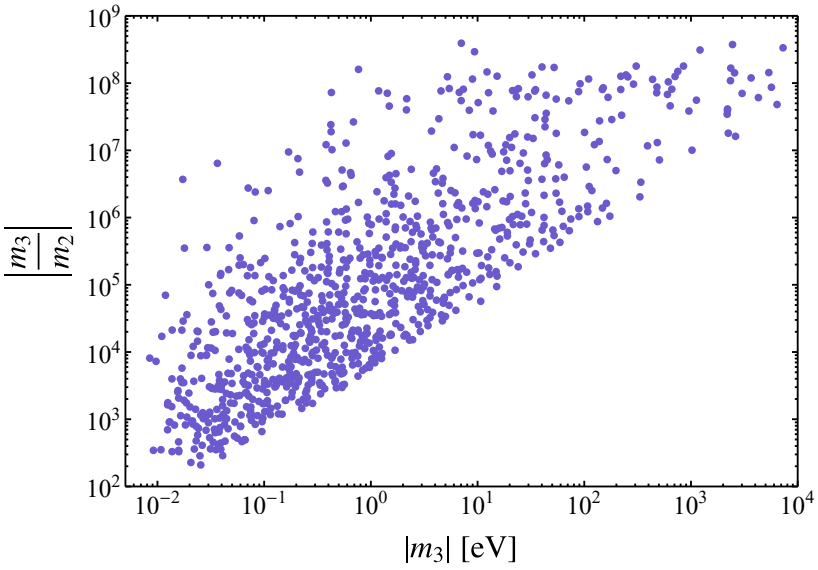

Figure 5.1: Scan plot showing the heaviest active neutrino mass $|m_3|$ vs. the mass hierarchy $|m_3/m_2|$ in a minimal model with only two RHN and three lepton doublets. For the numerical scan the initial conditions are $M_2 = M_P/\sqrt{8\pi}$, $M_1 = 0$ at the cut-off scale $\Lambda = M_P$, while the neutrino Yukawa eigenvalues are randomly scanned between $10^{-2} \leq y_2 < y_1 \leq \sqrt{4\pi}$, and the right-handed mixing angles in U_R take on random values within 0 and 2π.

mass matrix for the right-handed neutrinos M is real and diagonal at the cut-off

$$M(\mu)\Big|_{\mu=\Lambda} = \begin{pmatrix} M_1 & 0 & 0 \\ 0 & M_2 & 0 \\ 0 & 0 & M_3 \end{pmatrix}, \tag{5.17}$$

where a hierarchical mass spectrum $M_1 \ll M_2 \ll M_3$ is assumed in order to investigate the influence of two-loop quantum effects. While M_3 will receive small radiative corrections, the tree-level masses M_1 and M_2 can receive sizable or dominant corrections. The radiative corrections to M_3 come in leading-order from one-loop effects, explicitly

$$M_3\Big|_{\mu=M_3} \simeq M_3 + 2M_3 P_{33} \log\left(\frac{M_3}{\Lambda}\right). \tag{5.18}$$

Below the scale Λ, the RG evolution correctly describes the energy-scale behavior of the Majorana mass matrix, which is approximately given by Eq. (4.27), capturing the relevant two-loop effects. At energies $\mu < M_3$ it is possible to integrate-out the heavy N_3 and describe the full theory with an effective field theory instead:

$$\mathcal{L}_{\text{eff}} \simeq -\frac{1}{2}\frac{Y_{\alpha 3}Y_{\beta 3}}{M_{33}}\left(\overline{L_\alpha}\widetilde{\Phi}\right)\left(\widetilde{\Phi}^T L_\beta^c\right) - \mathbb{Y}_{\alpha i}\overline{L_\alpha}\widetilde{\Phi}N_i - \frac{1}{2}\mathbb{M}_{ij}\overline{N_i^c}N_j + \text{h.c.}, \tag{5.19}$$

where analogous to Eq. (5.5) the double struck quantities define the neutrino Yukawa and Majorana mass matrix in the effective theory

$$\begin{aligned} \mathbb{Y}_{\alpha i} &= \left(Y_{\alpha i} - \frac{M_{i3}Y_{\alpha 3}}{M_{33}}\right), \\ \mathbb{M}_{ij} &= \left(M_{ij} - \frac{M_{i3}M_{j3}}{M_{33}}\right), \end{aligned} \tag{5.20}$$

with $i, j = 1, 2$ and couplings evaluated at the scale $\mu = M_3$. The first term in Eq. (5.19) is the Weinberg operator which gives a negligible contribution to the lightest active neutrino mass, $m_1 \lesssim 10^{-6}$ eV (for a Planck scale-sized M_3). Therefore, it is possible to study the two-loop effects on the low-scale neutrino parameters with sufficient precision using the following approximation for the effective Lagrangian:

$$\mathcal{L}_{\text{eff}} \simeq -\mathbb{Y}_{\alpha i}\overline{L_\alpha}\widetilde{\Phi}N_i - \frac{1}{2}\mathbb{M}_{ij}\overline{N_i^c}N_j + \text{h.c.} \tag{5.21}$$

Similar to the technique in Eq. (5.11) used to calculate the mass eigenvalues, the right-handed mass eigenstates can be obtained from using the tensor invariants, where all parameters are assumed to be real and evaluated at $\mu = M_3$,

$$\begin{aligned} I_1 &= \text{Tr}\,[\mathbb{M}] = M_1(t) + M_2(t) \simeq M_1 + M_2 + 4M_2P_{21}^2 t + 4M_3(P_{31}^2 + P_{32}^2)t, \\ I_2 &= \det\,[\mathbb{M}] = M_1(t)M_2(t) \simeq M_1M_2 + 4\left(M_1^2P_{21}^2 + M_2^2P_{21}^2\right)t + 4M_3\left(M_1P_{32}^2 + M_2P_{31}^2\right)t \\ &\quad + 32M_3^2[P_{21}\left(P_{31}^2 - P_{32}^2\right) - \left(P_{11} - P_{22}\right)P_{31}P_{32}]^2t^3, \end{aligned} \tag{5.22}$$

using the scale parameter $t \equiv \log(\mu/\Lambda)$. We keep the leading-orders in the P-matrix (but still consider terms up to $\mathcal{O}(P^4)$ in the Picard expansion in Eq. (4.27), to capture all terms at two-loop level). For the general complex case, the Hermitian quantity $\mathbb{M}^\dagger\mathbb{M}$ is considered instead of $\mathbb{M}$ in the invariants above. Generically, for a hierarchical mass spectrum in the right-handed neutrinos, the following approximation holds

$$\begin{aligned} M_2\Big|_{\mu=M_3} &\simeq I_1, \\ M_1\Big|_{\mu=M_3} &\simeq \frac{I_2}{I_1}. \end{aligned} \tag{5.23}$$

Depending on the exact high-scale parameters for the tree-level masses and the neutrino Yukawa coupling, different terms in Eq. (5.22) are dominant and thus lead to different right-handed masses and accordingly to a different low-energy phenomenology for the active neutrinos. In general, the following three distinct scenarios can be identified:

i) All right-handed neutrino masses are well dominated by their tree-level masses – quantum effects lead only to small corrections.

ii) At least one of the RHN tree-level masses is washed-out by quantum effects, while the other receives corrections.

iii) Both RHN tree-level masses, M_1 and M_2, are washed-out by dominant radiative corrections.

The most interesting scenarios involving two-loop effects are clearly *ii*) and *iii*), where the predictions can significantly deviate from tree-level and even one-loop calculations and introduce new qualitative features to the phenomenology. Another attractive feature of tree-level masses dominated by quantum corrections is the enhanced predictivity of the model due to a lower number of free high-scale parameters. Case *i*) is the well-studied scenario corresponding to a type-I seesaw model with minor radiative corrections to the heavy RHN masses which do not lead to new qualitative features in the low-scale parameters.

In the discussion of the following subsections, the scenarios *ii*) and *iii*) are investigated in detail.

5.2.1 One Right-Handed Neutrino Mass Dominated by Quantum Effects

For the case, where at least one RHN tree-level mass is washed-out by radiative contributions, either the lightest or next-to-lightest tree-level mass is dominated. In order to obtain explicit expressions for the right-handed masses, the Eqs. (5.22) and (5.23) are used, such that

$$\begin{aligned} M_i\Big|_{\mu=M_3} &\simeq 4M_3\left(P_{31}^2+P_{32}^2\right)\log\left(\frac{M_3}{\Lambda}\right), \\ M_j\Big|_{\mu=M_3} &\simeq \frac{M_1P_{32}^2+M_2P_{31}^2}{P_{31}^2+P_{32}^2}, \end{aligned} \tag{5.24}$$

both evaluated at the scale $\mu = M_3$ and assuming that neutrino masses which stem from the Dirac term are negligible. This is generically the case for lepton number breaking far above the EW scale and generic neutrino Yukawa couplings. As either the lightest or next-to-lightest RHN mass is dominated, depending on the exact high-scale parameters, it is *a priori* unspecified which mass is heavier, therefore keeping the labeling general ($i = 1$, $j = 2$ or $j = 1$, $i = 2$ is both possible). For the general complex case, the mass formulas read accordingly,

$$\begin{aligned} M_i\Big|_{\mu=M_3} &\simeq 4M_3\left(|P_{31}|^2+|P_{32}|^2\right)\log\left(\frac{M_3}{\Lambda}\right), \\ M_j\Big|_{\mu=M_3} &\simeq \frac{M_1|P_{32}|^2+M_2|P_{31}|^2}{|P_{31}|^2+|P_{32}|^2}. \end{aligned} \tag{5.25}$$

Instead of using the invariants, the mass formulas in Eq. (5.24) can also be obtained from diagonalizing $\mathbb{M} \simeq U_{\mathbb{M}}\mathrm{diag}(M_i, M_j)U_{\mathbb{M}}^T$ in Eq. (5.20) with the unitary 2×2 matrix $U_{\mathbb{M}}$, which reads in detail

$$U_{\mathbb{M}}\Big|_{\mu=M_3} \simeq \frac{1}{\sqrt{P_{31}^2+P_{32}^2}}\begin{pmatrix} P_{32} & P_{31} \\ -P_{31} & P_{32}\end{pmatrix}, \tag{5.26}$$

and has sizable entries in general (also see Eq. (4.17)). Due to the RG running, the unitary mixing matrix moves into a quasi-fixed point below the cut-off scale, inducing a sizable mixing for the initially diagonal mass matrix. The mixing induced by the energy-scale evolution leads to the linear combination of tree-level masses M_1 and M_2 in the expression for $M_j|_{\mu=M_3}$.

The lightest active neutrino will be $m_1 \lesssim 10^{-6}\,\mathrm{eV}$ for M_3 close to the Planck scale (or at least be of a negligible size for $M_1, M_2 \ll M_3$ compared to the other active neutrino masses). Therefore, it makes sense to study the two-loop effects on the low-scale parameters within the framework of the two RHN effective Lagrangian in Eq. (5.21). After integrating-out the two RHNs, the Majorana mass for the active neutrinos is obtained:

$$\mathcal{M}_\nu \simeq -\frac{v^2}{2}\left(\mathbb{Y}\mathbb{M}^{-1}\mathbb{Y}^T\right). \tag{5.27}$$

Following the same scheme as in Eq. (5.11), the eigenvalues can be calculated with the

following tensor invariants:

$$
\begin{aligned}
I_1 &= \mathrm{Tr}\left[\mathcal{M}_\nu\right] = (16\pi^2)\mathrm{Tr}\left[\mathbb{M}^{-1}\mathbb{P}\right]\frac{v^2}{2}, \\
I_2 &= \frac{1}{2}\left(\mathrm{Tr}\left[\mathcal{M}_\nu\right]^2 - \mathrm{Tr}\left[\mathcal{M}_\nu^2\right]\right) = \frac{(16\pi^2)^2}{2}\left(\mathrm{Tr}\left[\mathbb{M}^{-1}\mathbb{P}\right]^2 - \mathrm{Tr}\left[\mathbb{M}^{-1}\mathbb{P}\mathbb{M}^{-1}\mathbb{P}\right]\right)\frac{v^4}{4}, \\
I_3 &= \frac{1}{6}\Big(\mathrm{Tr}\left[\mathcal{M}_\nu\right]^3 - 3\,\mathrm{Tr}\left[\mathcal{M}_\nu\right]\mathrm{Tr}\left[\mathcal{M}_\nu^2\right] + 2\,\mathrm{Tr}\left[\mathcal{M}_\nu^3\right]\Big) = \frac{(16\pi^2)^3}{6}\Big(\mathrm{Tr}\left[\mathbb{M}^{-1}\mathbb{P}\right]^3 \\
&\quad - 3\,\mathrm{Tr}\left[\mathbb{M}^{-1}\mathbb{P}\right]\mathrm{Tr}\left[\mathbb{M}^{-1}\mathbb{P}\mathbb{M}^{-1}\mathbb{P}\right] + 2\,\mathrm{Tr}\left[\mathbb{M}^{-1}\mathbb{P}\mathbb{M}^{-1}\mathbb{P}\mathbb{M}^{-1}\mathbb{P}\right]\Big)\frac{v^6}{8},
\end{aligned}
\tag{5.28}
$$

defining $\mathbb{P} \equiv \frac{1}{16\pi^2}\mathbb{Y}^T\mathbb{Y}$. In the used two RHN approximation, the third invariant exactly vanishes $I_3 = 0$ which implies $m_1 = 0$, and

$$
\begin{aligned}
I_1 &= m_2 + m_3 \simeq \frac{16\pi^2 v^2}{2M_j|_{\mu=M_3}}\frac{P_{22}P_{31}^2 + P_{11}P_{32}^2 - 2P_{31}P_{32}P_{21}}{P_{31}^2 + P_{32}^2}\,, \\
I_2 &= m_2 m_3 \simeq \frac{\left(16\pi^2\right)^2 v^4}{4M_i|_{\mu=M_3}M_j|_{\mu=M_3}}\left(P_{11}P_{22} - P_{21}^2\right).
\end{aligned}
\tag{5.29}
$$

Assuming a hierarchy between the active neutrino masses, the mass spectrum becomes

$$
\begin{aligned}
m_\alpha &\simeq I_1 = \frac{16\pi^2 v^2}{2M_j|_{\mu=M_3}}\frac{P_{22}P_{31}^2 + P_{11}P_{32}^2 - 2P_{31}P_{32}P_{21}}{P_{31}^2 + P_{32}^2}\,, \\
m_\beta &\simeq \frac{I_2}{I_1} = \frac{16\pi^2 v^2}{2M_i|_{\mu=M_3}}\frac{\left(P_{31}^2 + P_{32}^2\right)\left(P_{11}P_{22} - P_{21}^2\right)}{P_{22}P_{31}^2 + P_{11}P_{32}^2 - 2P_{31}P_{32}P_{21}},
\end{aligned}
\tag{5.30}
$$

and accordingly for the general complex case

$$
\begin{aligned}
m_\alpha &\simeq I_1 = \frac{16\pi^2 v^2}{2M_j|_{\mu=M_3}}\frac{P_{22}|P_{31}|^2 + P_{11}|P_{32}|^2 - 2\,\mathrm{Re}\left(P_{31}P_{32}P_{21}\right)}{|P_{31}|^2 + |P_{32}|^2}\,, \\
m_\beta &\simeq \frac{I_2}{I_1} = \frac{16\pi^2 v^2}{2M_i|_{\mu=M_3}}\frac{\left(|P_{31}|^2 + |P_{32}|^2\right)\left(P_{11}P_{22} - |P_{21}|^2\right)}{P_{22}|P_{31}|^2 + P_{11}|P_{32}|^2 - 2\,\mathrm{Re}\left(P_{31}P_{32}P_{21}\right)}.
\end{aligned}
\tag{5.31}
$$

Depending on the high-scale parameters, either m_α or m_β is the heavier active neutrino mass. Thus, the labeling of the states is *a priori* unspecified (either $\alpha = 2$, $\beta = 3$ or $\alpha = 3$, $\beta = 2$ are possible).

By using the parametrization from Eq. (5.14) for the neutrino Yukawa coupling, such that $P = \frac{1}{16\pi^2}U_R\mathrm{diag}(y_1^2, y_2^2, y_3^2)U_R^\dagger$, the light neutrino masses can be approximated with

$$
\begin{aligned}
m_\alpha &\simeq \begin{cases} \frac{y_2^2 v^2}{2M_2}\frac{U_{13}^2}{U_{31}^2}, & \text{for } \frac{P_{31}^2}{P_{32}^2} \gg \sqrt{\frac{M_1}{M_2}} \\ \frac{y_2^2 v^2}{2M_1}\frac{U_{13}^2}{U_{32}^2}, & \text{for } \frac{P_{31}^2}{P_{32}^2} \ll \sqrt{\frac{M_1}{M_2}} \end{cases}\,, \\
m_\beta &\simeq \frac{(16\pi^2)^2 v^2}{8M_3 y_3^2 U_{33}^2 \log(M_3/\Lambda)},
\end{aligned}
\tag{5.32}
$$

where the parameters are evaluated at the energy scale $\mu = M_3$. Note that $(P_{31}/P_{32})^2 \gg \sqrt{M_1/M_2}$ is generically expected for a hierarchical RHN mass spectrum at the cut-off with

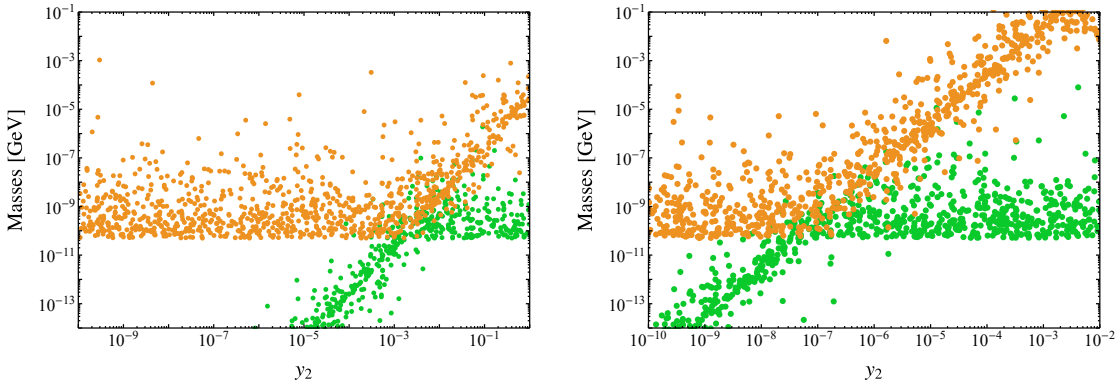

Figure 5.2: Random scan plot for the light neutrino masses $|m_3|$ (orange) and $|m_2|$ (green) vs. the neutrino Yukawa eigenvalue y_2, assuming $y_3 = 1$, $y_1 = 0$, $M_1 = 0$, $M_3 = M_P/\sqrt{8\pi}$, $M_2 = 10^9$ GeV (left plot) or $M_2 = 1$ GeV (right plot) at the scale $\Lambda = M_P$. The right-handed mixing angles in U_R take on random values within 0 and 2π.

$M_1 \ll M_2$. For a special choice of parameters it still can be possible that $M_j|_{\mu=M_3}$ is dominated by the tree-level mass M_1. Considering the generic scenario with explicit numbers,

$$\begin{aligned} m_\alpha &\simeq 0.03\,\text{eV}\ \left(\frac{y_2}{10^{-3}}\right)^{-2}\left(\frac{U_{31}}{U_{13}}\right)^{-2}\left(\frac{M_2}{1\times 10^9\,\text{GeV}}\right)^{-1}, \\ m_\beta &\simeq 0.05\,\text{eV}\ \left(\frac{y_3}{1}\right)^{-2}\left(\frac{U_{33}}{0.6}\right)^{-2}\left(\frac{M_3}{1.2\times 10^{19}\,\text{GeV}}\right)^{-1}, \end{aligned} \tag{5.33}$$

taking M_3 close to the theory cut-off, such that $\log(\Lambda/M_3) \simeq 1$. The analytical results are tested by a numerical scan in Fig. 5.2, showing the expected active neutrino masses m_3 (orange) and m_2 (green) vs. the neutrino Yukawa eigenvalue y_2, while $y_3 = 1$ and $y_1 = 0$. The right-handed mixing angles in U_R take on random values between 0 and 2π. The RHN masses are $M_3 = M_P/\sqrt{8\pi}$, $M_1 = 0$, and $M_2 = 10^9$ GeV (left plot) or $M_2 = 1$ GeV (right plot) at $\Lambda = M_P$. One of the neutrino masses is in the ballpark of the observed values for $y_3 \simeq \mathcal{O}(1)$ and $M_3 = M_P$ for generic mixing angles. The second neutrino mass shows considerable sensitivity to the values of M_2 and y_2. For the considered scenarios, $y_2 \sim 10^{-2}$ is necessary if $M_2 \sim 10^9$ GeV and in case of $M_2 \sim 1$ GeV, $y_2 \sim 10^{-7}$ is required to reproduce the observations from oscillation experiments.

For the case shown in the left plot of Fig. 5.2, the whole physical neutrino mass spectrum is depicted in Fig. 5.3. The fully radiative RHN mass is generically at the seesaw scale $\sim 10^{14}$ GeV, while the second RHN mass can significantly deviate from its tree-level mass of $M_2 = 10^9$ GeV due to mixing effects induced by the RG running. The lightest active neutrino mass m_1 lies outside the range of the plot and is $\mathcal{O}(10^{-6})$ eV.

5.2.2 Two Right-Handed Neutrino Masses Dominated by Quantum Effects

Generically, for a hierarchical RHN mass spectrum at the cut-off $M_1 \ll M_2 \ll M_3$, both RHN tree-level masses M_1 and M_2 are washed-out, meaning the quantum corrections proportional to the heavy M_3 dominate. In this scenario, the RHN mass matrix at Λ is well-approximated by a rank-1 matrix. In order to obtain the eigenvalues below the scale $\mu = M_3$, one can either use the tensor invariants in Eqs. (5.22) and (5.23) or right away diagonalize

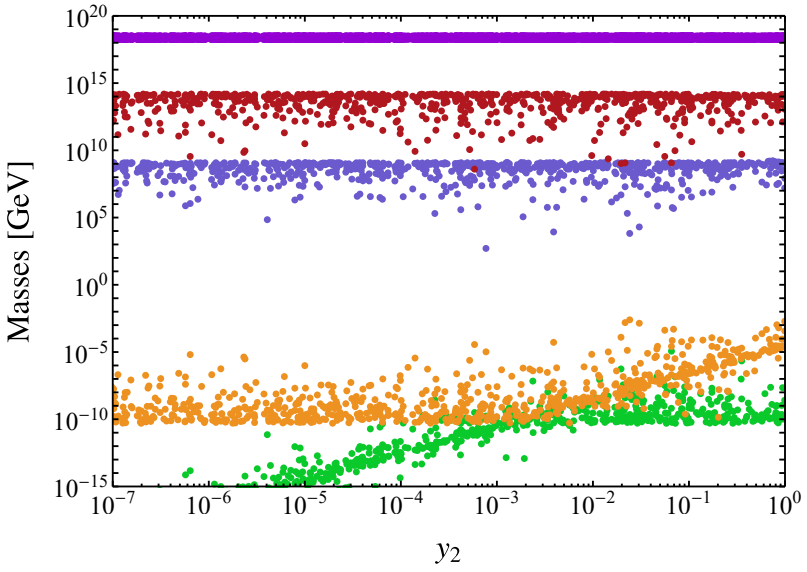

Figure 5.3: Spectrum of physical neutrino masses in dependence of the neutrino Yukawa eigenvalue y_2, taking $y_3 = 1$, $y_1 = 0$, $M_3 = M_P/\sqrt{8\pi}$, $M_1 = 0$, and $M_2 = 10^9$ GeV at the cut-off energy scale $\Lambda = M_P$. The right-handed mixing angles in U_R are scanned between 0 and 2π. m_1 lies outside the range of the plot.

$\mathbb{M} \simeq U_{\mathbb{M}} \mathrm{diag}(M_1, M_2) U_{\mathbb{M}}^T$, where the matrix $U_{\mathbb{M}}(\mu = M_3)$ is still the same as in Eq. (5.26). The masses explicitly read,

$$
\begin{aligned}
M_2\Big|_{\mu=M_3} &\simeq 4M_3 \left(P_{31}^2 + P_{32}^2\right) \log\left(\frac{M_3}{\Lambda}\right) \,, \\
M_1\Big|_{\mu=M_3} &\simeq 8M_3 \frac{\left(P_{21}\left(P_{31}^2 - P_{32}^2\right) - \left(P_{11} - P_{22}\right) P_{31} P_{32}\right)^2}{P_{31}^2 + P_{32}^2} \log^2\left(\frac{M_3}{\Lambda}\right) \,,
\end{aligned}
\tag{5.34}
$$

and correspondingly for the complex case,

$$
\begin{aligned}
M_2\Big|_{\mu=M_3} &\simeq 4M_3 \left(|P_{31}|^2 + |P_{32}|^2\right) \log\left(\frac{M_3}{\Lambda}\right) \,, \\
M_1\Big|_{\mu=M_3} &\simeq 8M_3 \frac{\left|P_{21}\left(P_{31}^2 - P_{32}^2\right) - \left(P_{11} - P_{22}\right) P_{31} P_{32}\right|^2}{|P_{31}|^2 + |P_{32}|^2} \log^2\left(\frac{M_3}{\Lambda}\right) \,.
\end{aligned}
\tag{5.35}
$$

Interestingly, one purely radiative mass arises at order $\mathcal{O}(P^2)$ and has the same structure as in Eq. (5.24), while the other is generated at order $\mathcal{O}(P^4)$, effectively looking like a four-loop contribution, but can be traced back to the $P^T M P$ term in the two-loop RGE in Eq. (4.7). From general symmetry considerations this term is expected since no protective symmetry is forbidding these radiative contributions assuming a generic Yukawa structure. The radiative effects change the rank of the Majorana mass matrix in the running from effectively rank-1 up to the full rank. One might ask, if M_1 is created at $\mathcal{O}(P^4)$, are there other contributions beyond the two-loop order in the RGE which might have an impact? So far, only terms with $n+m \leq 2$ in the beta function in Eq. (4.26) were considered. Extending this to higher-order terms up to $\mathcal{O}(P^4)$ in the beta function, the expression in Eq. (4.27) was found, which leads after diagonalizing to the lightest radiative mass

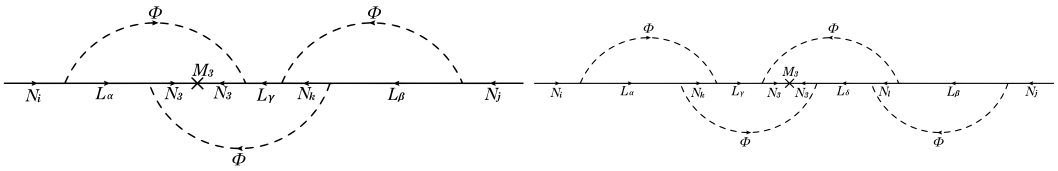

Figure 5.4: Feynman diagrams beyond the two-loop order contributing rank-increasing terms to the RGE of the Majorana mass matrix, leading to an at most $\mathcal{O}(1)$ correction to the two-loop result.

$$M_1\Big|_{\mu=M_3} \simeq 8M_3 \frac{\left(P_{21}\left(P_{31}^2 - P_{32}^2\right) - \left(P_{11} - P_{22}\right)P_{31}P_{32}\right)^2}{P_{31}^2 + P_{32}^2} \times \left[\log^2\left(\frac{M_3}{\Lambda}\right) + \frac{4a_{22} - a_{21}^2}{32}\log\left(\frac{M_3}{\Lambda}\right)\right]. \tag{5.36}$$

From here it can be seen that the higher-order terms only lead to a correction to Eq. (5.34) which is expected to be at most $\mathcal{O}(1)$ for M_3 close to the cut-off scale, such that $\log(\Lambda/M_3) \simeq 1$. The factors a_{21} and a_{22} stem from three- and four-loop diagrams respectively and can be seen in Fig. 5.4. As the corrections do not lead to any new qualitative features not already captured in the two-loop effects and are expected to be minor, they are neglected in the further discussion.

Employing the decomposition of the neutrino Yukawa as in Eq. (5.14), making $P = \frac{1}{16\pi^2}U_R\mathrm{diag}(y_1^2, y_2^2, y_3^2)U_R^\dagger$, the radiative right-handed neutrino masses become

$$\begin{aligned} M_2\Big|_{\mu=M_3} &\simeq \frac{4}{(16\pi^2)^2}M_3 y_3^4 U_{33}^2\left(U_{31}^2 + U_{32}^2\right)\log\left(\frac{M_3}{\Lambda}\right), \\ M_1\Big|_{\mu=M_3} &\simeq \frac{8}{(16\pi^2)^4}M_3 y_2^4 y_3^4 \frac{U_{13}^2 U_{23}^2}{\left(U_{31}^2 + U_{32}^2\right)}\log^2\left(\frac{M_3}{\Lambda}\right), \end{aligned} \tag{5.37}$$

using the simplifying assumption of a hierarchical neutrino Yukawa spectrum $y_1 \ll y_2 \ll y_3$. From these formulas it can be seen how it is necessary to have at least a rank-2 neutrino Yukawa in the three RHN case to generate two non-vanishing masses via two-loop effects.

For a mass of M_3 well above the EW scale, the heavier RH radiative mass $M_2|_{\mu=M_3}$ will be much larger than the Dirac neutrino masses, and thus be identical to the mass eigenstate of N_2 – assuming generic neutrino Yukawa couplings. Due to the effective four-loop suppression $1/(16\pi^2)^4$ and a potentially tiny y_2^4, the lighter radiative mass $M_1|_{\mu=M_3}$ may be small enough to expect a sizable mixing between the physical state N_1 and the active neutrino states. This instance must be considered when investigating the low-energy phenomenology of the active neutrino parameters. After integrating out the heavy N_3 and working in the basis where the effective right-handed neutrino mass matrix $\mathbb{M}$ is diagonal by rotating the fields $N' = U_{\mathbb{M}}^T N$, the effective Lagrangian reads

$$\mathcal{L}_{\text{eff}} \simeq -\mathbb{Y}'_{\alpha i}\overline{L_\alpha}\widetilde{\Phi}N'_i - \frac{1}{2}M_i\overline{N_i'^c}N'_i + \text{h.c.}, \tag{5.38}$$

with $i, j = 1, 2$ and $\mathbb{Y}' = \mathbb{Y}U_{\mathbb{M}}$. After integrating out N'_2 at the corresponding scale $\mu = M_2$, the theory is described by

$$\mathcal{L}_{\text{eff}} \simeq -\frac{1}{2}\frac{\mathbb{Y}'_{\alpha 2}\mathbb{Y}'_{\beta 2}}{M_2}\left(\overline{L_\alpha}\widetilde{\Phi}\right)\left(\widetilde{\Phi}^T L_\beta^c\right) - \mathbb{Y}'_{\alpha 1}\overline{L_\alpha}\widetilde{\Phi}N'_1 - \frac{1}{2}M_1\overline{N_1'^c}N'_1 + \text{h.c.} \tag{5.39}$$

Below the electroweak symmetry breaking scale, this effective Lagrangian gives rise to a 4×4 neutrino mass matrix, in detail:

$$\mathcal{M}_\nu \simeq \begin{pmatrix} -\frac{v^2}{2}\frac{\mathbb{Y}'_{\alpha 2}\mathbb{Y}'_{\beta 2}}{M_2} & \frac{v}{\sqrt{2}}\mathbb{Y}'_{\alpha 1} \\ \frac{v}{\sqrt{2}}(\mathbb{Y}'_{\alpha 1})^T & M_1 \end{pmatrix}. \tag{5.40}$$

To get the masses of the four neutrinos, the neutrino mass matrix can be decomposed into four rank-1 quantities in the following way:

$$\mathcal{M}_\nu \simeq \mathfrak{m}_1 \vec{u}_1 \otimes \vec{u}_1^T + \mathfrak{m}_2 \vec{u}_2 \otimes \vec{u}_2^T + \mathfrak{m}_3 \left(\vec{u}_3 \otimes \vec{u}_3^T - \vec{u}_4 \otimes \vec{u}_4^T\right), \tag{5.41}$$

where the rank-1 matrices are tensor products of the normalized (but not necessarily orthonormal) $\vec{u}_i$ vectors

$$\vec{u}_1 = \frac{1}{\sqrt{\mathbb{P}'_{22}}}\begin{pmatrix} \mathbb{Y}'_{12} \\ \mathbb{Y}'_{22} \\ \mathbb{Y}'_{32} \\ 0 \end{pmatrix}, \qquad \vec{u}_2 = \begin{pmatrix} 0 \\ 0 \\ 0 \\ 1 \end{pmatrix}, \qquad \vec{u}_{3,4} = \frac{1}{\sqrt{2\mathbb{P}'_{11}}}\begin{pmatrix} \mathbb{Y}'_{11} \\ \mathbb{Y}'_{21} \\ \mathbb{Y}'_{31} \\ \pm\sqrt{\mathbb{P}'_{11}}, \end{pmatrix}, \tag{5.42}$$

and with the three mass parameters $\mathfrak{m}_i$ which are defined to be positive,

$$\mathfrak{m}_1 = -\frac{v^2}{2}\frac{\mathbb{P}'_{22}}{M_2}, \qquad \mathfrak{m}_2 = M_1, \qquad \mathfrak{m}_3 = \frac{v}{\sqrt{2}}\sqrt{\mathbb{P}'_{11}}, \tag{5.43}$$

introducing the 2×2 matrix $\mathbb{P}' = \mathbb{Y}'^\dagger \mathbb{Y}' = U_\mathbb{M}^\dagger \mathbb{Y}^\dagger \mathbb{Y} U_\mathbb{M}$, with $\mathbb{Y}$ and $U_\mathbb{M}$ as in Eqs. (5.20) and (5.26). The individual $\mathbb{P}$-matrix elements can be written explicitly (also see Eq. (4.18)),

$$\begin{aligned} \mathbb{P}'_{11} &\simeq (16\pi^2)\frac{P_{22}P_{31}^2 + P_{11}P_{32}^2 - 2P_{12}P_{31}P_{32}}{P_{31}^2 + P_{32}^2}, \\ \mathbb{P}'_{22} &\simeq (16\pi^2)\frac{P_{22}P_{32}^2 + P_{11}P_{31}^2 + 2P_{12}P_{31}P_{32}}{P_{31}^2 + P_{32}^2}, \\ \mathbb{P}'_{12} &\simeq (16\pi^2)\frac{P_{12}\left(P_{31}^2 + P_{32}^2\right) + P_{31}P_{32}(P_{11} - P_{22})}{P_{31}^2 + P_{32}^2}, \end{aligned} \tag{5.44}$$

and for the general complex case they are

$$\begin{aligned} \mathbb{P}'_{11} &\simeq (16\pi^2)\frac{P_{22}|P_{31}|^2 + P_{11}|P_{32}|^2 - 2\,\mathrm{Re}\,(P_{12}^* P_{31}P_{32})}{|P_{31}|^2 + |P_{32}|^2}, \\ \mathbb{P}'_{22} &\simeq (16\pi^2)\frac{P_{22}|P_{32}|^2 + P_{11}|P_{31}|^2 + 2\,\mathrm{Re}\,(P_{12}^* P_{31}P_{32})}{|P_{31}|^2 + |P_{32}|^2}. \\ \mathbb{P}'_{12} &\simeq (16\pi^2)\frac{\left|P_{12}^*(P_{31}^2 + P_{32}^2) + P_{31}P_{32}(P_{11} - P_{22})\right|}{|P_{31}|^2 + |P_{32}|^2}. \end{aligned} \tag{5.45}$$

Continuing with real-valued parameters, the spectral decomposition of the neutrino Yukawa reads $P = \frac{1}{16\pi^2} U_R \mathrm{diag}(y_1^2, y_2^2, y_3^2) U_R^\dagger$, for which the $\mathbb{P}$ matrix elements simplify to

$$\begin{aligned} \mathbb{P}'_{11} &\simeq \frac{U_{13}^2}{U_{31}^2 + U_{32}^2} y_2^2, \\ \mathbb{P}'_{22} &\simeq (U_{31}^2 + U_{32}^2) y_3^2, \\ \mathbb{P}'_{12} &\simeq \frac{2U_{31}^3 U_{32}}{U_{31}^2 + U_{32}^2} y_3^2. \end{aligned} \tag{5.46}$$

In the two RHNs approximation (neglecting effects of the heavy N_3 on the low-energy parameters as in the previous section), the mass matrix $\mathcal{M}_\nu$ in Eq. (5.41) is rank-3, such that $\det(\mathcal{M}_\nu) = 0$, leading to a lightest active neutrino that is exactly massless $m_1 = 0$.

The characteristic equation for $\mathcal{M}_\nu$ is cubic and the solution for the non-vanishing neutrino masses (m_2, m_3, and the sterile neutrino mass m_s) is complicated and does not give a feel for the dependence on the high-scale physics. It is therefore much more convenient and insightful to use degenerate perturbation theory by assuming that one of the three mass scales $\mathfrak{m}_i$ dominates over the remaining two. In this way, it is possible to derive analytical expressions for the light neutrino masses which clearly show the dependence on the high-scale parameters.

5.2.3 Degenerate Perturbation Theory

In this section, it is outlined how the light neutrino mass eigenstates can be calculated analytically by using degenerate perturbation theory up to the second order. The neutrino mass matrix in Eq. (5.41) can be cast as

$$\mathcal{M}_\nu = \mathcal{M}_\nu^{(0)} + \delta\mathcal{M}_\nu^{(1)}, \tag{5.47}$$

where $\delta\mathcal{M}_\nu^{(1)}$ is treated as containing perturbation corrections to $\mathcal{M}_\nu^{(0)}$. The small perturbation parameters are two of the three mass scales ($\mathfrak{m}_1, \mathfrak{m}_2, \mathfrak{m}_3$), where one of the mass scales is assumed to be dominating the other two. This generically leads to a 3-fold degenerate vanishing eigenvalue of the "unperturbed" 4×4 neutrino mass matrix $\mathcal{M}_\nu^{(0)}$ if either

a) $\mathfrak{m}_2 \gg \mathfrak{m}_1, \mathfrak{m}_3$ or

b) $\mathfrak{m}_1 \gg \mathfrak{m}_2, \mathfrak{m}_3$ and

to a 2-fold degenerate vanishing eigenvalue for

c) $\mathfrak{m}_3 \gg \mathfrak{m}_1, \mathfrak{m}_2$.

According to degenerate perturbation theory, $\delta\mathcal{M}_\nu^{(1)}$ should be diagonalized in the degenerate subspace. Concretely, for the case $\mathfrak{m}_2 \gg \mathfrak{m}_1, \mathfrak{m}_3$, $\mathcal{M}_\nu^{(0)}$ has one non-vanishing mass eigenstate $\widehat{m}_1^{(0)} = \mathfrak{m}_2$ with the corresponding eigenket $\{|1\rangle\}$ and three vanishing, 3-fold degenerate mass eigenstates $\widehat{m}_2^{(0)}, \widehat{m}_3^{(0)}, \widehat{m}_4^{(0)} = 0$. The latter have the corresponding orthonormal eigenkets $\{|2\rangle, |3\rangle, |4\rangle\}$ spanning the degenerate subspace. The projection operator onto the degenerate subspace of $\mathcal{M}_\nu^{(0)}$ is defined as

$$\mathfrak{P} = \mathbb{1} - \sum_{k \notin D} |k\rangle\langle k|, \tag{5.48}$$

where the index k runs over all states which are not in the degenerate subspace of $\mathcal{M}_\nu^{(0)}$. The perturbation is then projected onto the degenerate subspace:

$$\delta\widehat{\mathcal{M}}_\nu^{(1)} = \mathfrak{P}\delta\mathcal{M}_\nu^{(1)}\mathfrak{P}. \tag{5.49}$$

The eigenvalues of $\delta\widehat{\mathcal{M}}_\nu^{(1)}$ do not lift the degeneracy yet, but lead to another non-vanishing mass eigenstate $\mathfrak{m}_1$. To fully lift the degeneracy, second-order corrections to the mass eigenstates must be considered, which can be obtained by diagonalizing the 3×3 matrix

$$\delta M_{pq}^{(2)} = \sum_{k \notin D} \frac{\langle p|\delta\mathcal{M}_\nu^{(1)}|k\rangle\langle k|\delta\mathcal{M}_\nu^{(1)}|q\rangle}{\widehat{m}_p^{(0)} - \widehat{m}_k^{(0)}}, \tag{5.50}$$

where k runs over all states in the non-degenerate subspace and the indices $p, q \neq k$ correspond to the eigenstates in the degenerate subspace. The equation above takes the following form for the concrete example

$$\delta M^{(2)}_{pq} = -\frac{\langle p|\delta\mathcal{M}^{(1)}_\nu|1\rangle\langle 1|\delta\mathcal{M}^{(1)}_\nu|q\rangle}{\mathfrak{m}_2}, \tag{5.51}$$

with $p, q = 2, 3, 4$ and yields the non-vanishing eigenvalue $-\mathfrak{m}_3^2/\mathfrak{m}_2$, which fully lifts the degeneracy. For the case $\mathfrak{m}_1 \gg \mathfrak{m}_2, \mathfrak{m}_3$, the analytical expressions for the mass eigenstates can be obtained through the same procedure. Only for $\mathfrak{m}_3 \gg \mathfrak{m}_1, \mathfrak{m}_2$, first-order degenerate perturbation theory is sufficient to calculate all non-vanishing mass eigenstates.

5.2.4 Active Neutrino Masses

By applying degenerate perturbation theory for the three cases defined above, we find:

a) $\mathfrak{m}_2 \gg \mathfrak{m}_1, \mathfrak{m}_3$ where the three non-vanishing eigenvalues are,

$$\begin{aligned} m_s &\simeq \mathfrak{m}_2 = M_1, \\ m_3 &\simeq -\frac{\mathfrak{m}_3^2}{\mathfrak{m}_2} = -\frac{v^2}{2}\frac{\mathbb{P}'_{11}}{M_1}, \\ m_2 &\simeq \mathfrak{m}_1 = -\frac{v^2}{2}\frac{\mathbb{P}'_{22}}{M_2}. \end{aligned} \tag{5.52}$$

The lightest right-handed neutrino mass M_1 is the mass eigenstate of the sterile neutrino in the spectrum, while the other two masses are small and suppressed via the seesaw mechanism. Expressing the neutrino masses in terms of the high-energy parameters, they read[1]:

$$\begin{aligned} m_s &\simeq 8M_3\frac{y_2^4 y_3^4}{(16\pi^2)^4}\frac{U_{13}^2U_{23}^2}{U_{31}^2+U_{32}^2}\log^2\left(\frac{M_3}{\Lambda}\right), \\ m_3 &\simeq -\frac{(16\pi^2)^4 v^2}{16M_3 y_2^2 y_3^4 U_{23}^2\log^2(M_3/\Lambda)}, \\ m_2 &\simeq -\frac{(16\pi^2)^2 v^2}{8M_3 y_3^2 U_{33}^2\log(M_3/\Lambda)}. \end{aligned} \tag{5.53}$$

Using explicit numbers, similar to Eq. (5.33), the neutrino mass eigenstate m_2 reads

$$|m_2| \simeq 0.05\,\text{eV}\,\left(\frac{y_3}{1}\right)^{-2}\left(\frac{U_{33}}{0.6}\right)^{-2}\left(\frac{M_3}{1.2\times 10^{19}\,\text{GeV}}\right)^{-1}, \tag{5.54}$$

which reproduces the observed neutrino mass scale from neutrino oscillation experiments (where the assumption $\log(\Lambda/M_3) \simeq 1$ is used again). Considering the mass hierarchy between m_3 and m_2,

$$\left|\frac{m_3}{m_2}\right| \simeq \frac{(16\pi^2)^2}{2y_2^2U_{23}^2\log(\Lambda/M_3)}, \tag{5.55}$$

[1] In the shown calculations some neutrino masses have a negative sign, even if the mass matrix in Eq. (5.41) is positive semi-definite. A negative mass eigenvalue means that the neutrino has a positive physical mass (therefore absolute values of the masses are used), but a negative CP parity. By redefining the matrix diagonalizing $\mathcal{M}_\nu$, the eigenvalues can always be made positive.

it is always too large compared to the observed mild hierarchy, even if values of y_2 close to the perturbativity limit are chosen due to the two-loop factor in the numerator.

b) $\mathfrak{m}_1 \gg \mathfrak{m}_2, \mathfrak{m}_3$ leads to the following non-vanishing eigenvalues after using degenerate perturbation theory up to the second order,

$$\begin{aligned} m_\alpha &\simeq \mathfrak{m}_1 = -\frac{v^2}{2}\frac{\mathbb{P}'_{22}}{M_2}, \\ m_{s,\beta} &\simeq \frac{1}{2}\left(\mathfrak{m}_2 \pm \sqrt{\mathfrak{m}_2^2 + 4\mathfrak{m}_3^2 - 4\frac{v^2}{2}\frac{\mathbb{P}'^2_{12}}{\mathbb{P}'_{22}}}\right), \end{aligned} \tag{5.56}$$

where an *a priori* labeling of the mass states is not possible without making assumptions on the high-scale parameters. The sterile neutrino with mass m_s forms a pseudo-Dirac pair with the active neutrino with mass m_β. Inserting Eqs. (5.43) and (5.46), one finds that $\mathfrak{m}_3 \sim y_2 v/\sqrt{2}$. Thus, to reproduce the correct neutrino mass scale, the typical Yukawa size for Dirac neutrinos is needed, namely $y_2 \sim 10^{-12}$. This choice implies $\mathfrak{m}_3 \gg \mathfrak{m}_2 = M_1$. Expressing the masses in terms of the cut-off parameters,

$$\begin{aligned} m_\alpha &\simeq -\frac{(16\pi^2)^2 v^2}{8 M_3 y_3^2 U_{33}^2 \log\left(M_3/\Lambda\right)}, \\ m_{s,\beta} &\simeq \pm y_2 \frac{v}{\sqrt{2}}\sqrt{\frac{U_{13}^2}{U_{31}^2 + U_{32}^2}}, \end{aligned} \tag{5.57}$$

where the mass m_α is given by Eq. (5.54) and therefore typically lies in the correct ballpark. The mass hierarchy between m_α and pseudo-Dirac pair reads:

$$\left|\frac{m_\alpha}{m_\beta}\right| = \frac{\sqrt{2} M_3 y_2 y_3^2}{64\pi^4 v} U_{33}^2 \sqrt{\frac{U_{13}^2}{U_{31}^2 + U_{32}^2}} \log\left(\frac{\Lambda}{M_3}\right), \tag{5.58}$$

which can take values smaller or larger than one, but most importantly, can reproduce the observed mild hierarchy for appropriate parameters. For the final case,

c) $\mathfrak{m}_3 \gg \mathfrak{m}_1, \mathfrak{m}_2$, the mass matrix $\mathcal{M}_\nu$ has the non-vanishing eigenvalues:

$$\begin{aligned} m_{\alpha,s} &\simeq \pm \mathfrak{m}_3 = \pm \frac{v}{\sqrt{2}}\sqrt{\mathbb{P}'_{11}}, \\ m_\beta &\simeq \frac{v^2}{2}\frac{\mathbb{P}'_{11}\mathbb{P}'_{22} - \mathbb{P}'^2_{12}}{\mathbb{P}'_{22}}\frac{\mathfrak{m}_1}{\mathfrak{m}_3^2}, \end{aligned} \tag{5.59}$$

leaving the labeling of states unspecified at this point, as the concrete mass ordering is not determined *a priori*. One of the active neutrinos forms again a pseudo-Dirac pair together with the sterile neutrino state, with the following tiny mass splitting:

$$\delta m_{s-\beta} \simeq -\frac{v^2}{M_2}\frac{\mathbb{P}'^2_{12}}{\mathbb{P}'_{11}}. \tag{5.60}$$

Rewriting the neutrino mass formulas in terms of the high-energy parameters, they become:

$$\begin{aligned} m_{\alpha,s} &\simeq \pm y_2 \frac{v}{\sqrt{2}}\sqrt{\frac{U_{13}^2}{U_{31}^2 + U_{32}^2}}, \\ m_\beta &\simeq -\frac{(16\pi^2)^2 v^2}{8 M_3 y_3^2 U_{33}^2 \log\left(M_3/\Lambda\right)}, \end{aligned} \tag{5.61}$$

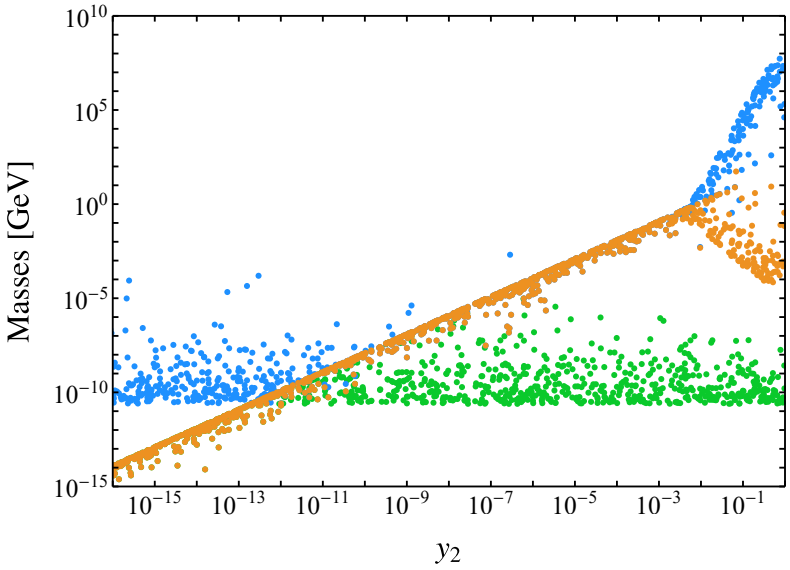

Figure 5.5: Random scan plot showing the light (active and sterile) neutrino masses $|m_3|$ (orange), $|m_2|$ (green) and $|m_s|$ (blue) vs. the neutrino Yukawa eigenvalue y_2. At the cut-off scale $\Lambda = M_P$, the following parameters are assumed: $y_3 = 1$, $y_1 = 0$, $M_3 = M_P/\sqrt{8\pi}$ and $M_1 = M_2 = 0$. The mixing angles in U_R take on random values within 0 and 2π.

which is identical to the result obtained in the previous case *b*). Therefore, reproducing the correct neutrino mass scale as well as the observed neutrino mass hierarchy is possible for the appropriate high-energy parameters.

A numerical analysis for the discussed scenarios is shown in Fig. 5.5. The scan plot is obtained from diagonalization of the 6×6 neutrino mass matrix (see Eq. (3.4)) after numerically solving the two-loop RGE and shows the mass spectrum of the light neutrinos (active and sterile), m_2, m_3 and m_s, depending on the neutrino Yukawa eigenvalue y_2. The values at the cut-off scale $\Lambda = M_P$ are $y_1 = 0$, $y_3 = 1$, $M_3 = M_P/\sqrt{8\pi}$ and $M_1 = M_2 = 0$. The right-handed mixing angles in U_R take on random values between 0 and 2π. Not considered in the mass spectrum are the much heavier RHNs N_3 and N_2 as well as the lightest active neutrino mass m_1 which is of order $\mathcal{O}(10^{-6})$ eV. The three scenarios analyzed above correspond to the following regimes in the scan plot: *a*) $y_2 \gtrsim 10^{-2}$, *b*) $y_2 \lesssim 10^{-12}$, and *c*) $10^{-12} \lesssim y_2 \lesssim 10^{-3}$. Case *a*) corresponds to the seesaw scenario where both, the atmospheric and solar neutrino mass are Majorana, but the atmospheric mass scale is predicted to be far larger than the observed values. Within the parameter space of $y_2 \sim 10^{-13} - 10^{-11}$, encompassing the region between cases *b*) and *c*), the observed neutrino mass hierarchy as well as the correct mass scales can be reproduced. For these two cases either the atmospheric or the solar neutrino mass scale is of pseudo-Dirac type, while the other is purely Majorana. Note that in the full parameter space of y_2, one light neutrino is always in the ballpark of the experimentally observed mass scale, by only making mild assumptions on the cut-off parameters at $\Lambda = M_P$, namely $M_3 \simeq \mathcal{O}(M_P)$ and $y_3 \sim \mathcal{O}(1)$.

5.3 Neutrinoless Double Beta Decay

In the relevant parameter space $y_2 \sim 10^{-13} - 10^{-9}$ with $y_3 \sim \mathcal{O}(1)$, which can reproduce the observed data from neutrino oscillation experiments, the 4×4 neutrino mass matrix in Eq. (5.40) is diagonalized by $\mathcal{U}$. In the limit of vanishing y_1 compared to y_2, this matrix is well approximated by

$$\mathcal{U} \simeq \begin{pmatrix} W_{11} & W_{13} & W_{12}/\sqrt{2} & W_{12}/\sqrt{2} \\ W_{21} & W_{23} & W_{22}/\sqrt{2} & W_{22}/\sqrt{2} \\ W_{31} & W_{33} & W_{32}/\sqrt{2} & W_{32}/\sqrt{2} \\ 0 & 0 & 1/\sqrt{2} & 1/\sqrt{2} \end{pmatrix}, \tag{5.62}$$

for the ordering of neutrino masses $|m_s| \simeq |m_3| > m_2 > m_1 = 0$, and

$$\mathcal{U} \simeq \begin{pmatrix} W_{11} & W_{12}/\sqrt{2} & W_{12}/\sqrt{2} & W_{13} \\ W_{21} & W_{22}/\sqrt{2} & W_{22}/\sqrt{2} & W_{23} \\ W_{31} & W_{32}/\sqrt{2} & W_{32}/\sqrt{2} & W_{33} \\ 0 & 1/\sqrt{2} & 1/\sqrt{2} & 0 \end{pmatrix}, \tag{5.63}$$

for the mass ordering $m_3 > |m_s| \simeq |m_2| > m_1 = 0$. Here, the W_{ij} are the elements of the unitary 3×3 matrix U_L, when the neutrino Yukawa coupling at the cut-off is parametrized as in Eq. (5.14), namely $Y = U_L D_Y U_R^\dagger$. The effective electron neutrino Majorana mass, relevant in neutrinoless doublet beta decay (see Sec. 2.5), is then calculated as

$$\langle m_{\beta\beta} \rangle = \left| m_1 \mathcal{U}_{e1}^2 + m_2 \mathcal{U}_{e2}^2 + m_3 \mathcal{U}_{e3}^2 + m_s \mathcal{U}_{es}^2 \right|. \tag{5.64}$$

In the case where the atmospheric mass scale is pseudo-Dirac with $m_s \simeq -m_3$, the effective mass becomes

$$\langle m_{\beta\beta} \rangle = \left| m_2 \mathcal{U}_{e2}^2 + m_s \left(\mathcal{U}_{es}^2 - \mathcal{U}_{e3}^2 \right) \right| = \left| m_2 \mathcal{U}_{e2}^2 \right| = \left| m_2 W_{13}^2 \right|, \tag{5.65}$$

neglecting the tiny mass splitting in Eq. (5.60) between the pseudo-Dirac states, leading to a cancellation due to opposite CP parity of the nearly degenerate states. When the atmospheric mass scale is Majorana and the solar mass scale is pseudo-Dirac with $m_s \simeq -m_2$ the corresponding expression reads

$$\langle m_{\beta\beta} \rangle = \left| m_2 \left(\mathcal{U}_{es}^2 - \mathcal{U}_{e2}^2 \right) + m_3 \mathcal{U}_{e3}^2 \right| = \left| m_3 \mathcal{U}_{e3}^2 \right| = \left| m_3 W_{13}^2 \right|, \tag{5.66}$$

again neglecting the tiny mass splitting. In both cases, only the Majorana mass scale of the purely Majorana neutrino gives a considerable contribution to $\langle m_{\beta\beta} \rangle$ which takes the form

$$m_{2,3} \simeq -\frac{(16\pi^2)^2 v^2}{8 M_3 y_3^2 U_{33}^2 \log\left(M_3/\Lambda\right)} \tag{5.67}$$

in terms of the cut-off parameters (*cf.* Eqs. (5.57) and (5.61)). Putting in concrete numbers,

$$\langle m_{\beta\beta} \rangle \simeq 5 \times 10^{-4}\,\text{eV} \left(\frac{|W_{13}^2|}{0.01} \right) \left(\frac{y_3}{1} \right)^{-2} \left(\frac{U_{33}}{0.6} \right)^{-2} \left(\frac{M_3}{1.2 \times 10^{19}\,\text{GeV}} \right)^{-1}, \tag{5.68}$$

where U_{33} is an element of the unitary matrix U_R. The overall scale of $\langle m_{\beta\beta} \rangle$ strongly depends on the overall size of the matrix element W_{13}. The pseudo-Dirac state can be

regarded as a pure Dirac particle, if the tiny mass splitting is neglected, such that $\nu'_\alpha = [(\nu_\alpha + \nu^c_\alpha) + i(\nu_s + \nu^c_s)]/\sqrt{2}$, where $\alpha = 2$ or 3. In this limit $\mathcal{U}$ can be written as an unitary 3×3 matrix, U_ν:

$$U_\nu \simeq \begin{pmatrix} W_{11} & W_{12} & W_{13} \\ W_{21} & W_{22} & W_{23} \\ W_{31} & W_{32} & W_{33} \end{pmatrix}, \tag{5.69}$$

for the case in which the solar mass scale is pseudo-Dirac. So far, the mixing from the charged lepton sector was neglected (*e.g.* by assuming a CKM-like structure $U_e \simeq \mathbb{1}$), but which is necessary to calculate the leptonic mixing matrix $U_{\text{PMNS}} = U_e^\dagger U_\nu$. The relevant matrix element $|W^2_{13}|$ for $\langle m_{\beta\beta} \rangle$ is still perturbed by an influence from the charged lepton sector, such that it is replaced by $|U^2_{13}|$ from the PMNS matrix in the equations above. As no constraints are put on the Yukawa structures from imposing flavor symmetries, it is not possible to make predictions on the leptonic mixing. Assuming generic mixing angles in the lepton sector, which are neither small nor large, an "anarchic" structure is expected, in qualitative agreement with the observations from neutrino oscillation experiments (see Eq. (2.13)). Note that the resulting active and sterile neutrino masses are completely independent from the left-handed mixing matrix U_L in Eq. (5.14).

5.4 Parameter Counting

For the analyzed scenarios presented in Sec. 5.2.1 and Sec. 5.2.2, in which radiative effects are used to generate one and two right-handed neutrino masses respectively, the number of physical parameters is reduced compared to the standard seesaw scenario (see Sec. 3.3). Consider the leptonic part of the Lagrangian (with family indices suppressed),

$$\mathcal{L}_{\text{lep}} = \overline{L} i \not{D} L + \overline{e_R} i \not{D} e_R + \overline{N} i \not{\partial} N - \left(\overline{L} Y_e \Phi e_R + \overline{L} Y \widetilde{\Phi} N + \frac{1}{2} \overline{N^c} M N + \text{h.c.} \right), \tag{5.70}$$

invariant under $U(3)_N \times U(3)_L \times U(3)_e$ global transformations for vanishing Yukawa couplings and Majorana mass matrix, $Y = Y_e = M = 0$. By using the rule presented in [65], the number of physical parameters of the model can be determined.

5.4.1 Quantum Effects Washing Out One Right-Handed Neutrino Mass

When radiative effects dominate at least one RHN mass, as in Sec. 5.2.1, it is enough to consider the Lagrangian in Eq. (5.70), in which both, Y and M are effectively rank-2 for $n_g = 3$ at the cut-off, to reproduce the observed neutrino data (see Eq. (5.33)). For this, the symmetric 3×3 Majorana mass matrix can be decomposed in the following way

$$M = U^*_M \begin{pmatrix} 0 & 0 & 0 \\ 0 & M_2 & 0 \\ 0 & 0 & M_3 \end{pmatrix} U^\dagger_M, \tag{5.71}$$

where U_M is a 3×3 unitary matrix, which can be parametrized by three angles and three phases and M_i are in general complex mass eigenstates. The number of moduli and phases is therefore 5. Similarly, a general complex 3×3 rank-2 Yukawa matrix can be decomposed

via the bi-unitary transformation,

$$Y = U_L \begin{pmatrix} 0 & 0 & 0 \\ 0 & y_2 & 0 \\ 0 & 0 & y_3 \end{pmatrix} U_R^\dagger, \tag{5.72}$$

where U_L and U_R are both 3×3 unitary matrices which can be parametrized by three angles and three phases. The total number of moduli and phases is therefore 8. No assumptions on the charged lepton Yukawa Y_e are made. In this scenario the $U(3)_N \times U(3)_L \times U(3)_e$ symmetry is broken down to a residual $U(1)_{\nu_1}$, leaving the lightest active neutrino massless. (Neglecting the impact of quantum effects from the charged lepton sector.) Breaking $U(3)^3 \to U(1)$ adds up to 9 broken real parameters and 17 broken phases. The physical moduli and phases thus amount to

$$\begin{aligned} &(9+8+5) \text{ parameters in total} - 9 \text{ broken real parameters} = 13 \text{ physical parameters}, \\ &(9+8+5) \text{ phases in total} - 17 \text{ broken phase parameters} = 5 \text{ physical phases}. \end{aligned} \tag{5.73}$$

The 18 physical parameters correspond to four eigenvalues (M_2, M_3, y_2, y_3), three angles and two phases from the neutral lepton sector, and three eigenvalues (y_e, y_μ, y_τ), three angles and three phases from the charged lepton sector.

5.4.2 Quantum Effects Washing Out Two Right-Handed Neutrino Masses

When two right-handed neutrinos get significant quantum corrections, as in Sec. 5.2.2, the Majorana mass matrix effectively only needs to be a complex, symmetric rank-1 matrix, while the neutral lepton Yukawa coupling is still needs to be a complex rank-2 matrix. In this minimal scenario is parameter space in which the observed neutrino parameters can be reproduced, see Eqs. (5.57) and (5.61). Again, no assumptions on the structure of the charged lepton Yukawa coupling are made. It is possible to parametrize a complex symmetric rank-1 matrix as the tensor product of a vector with itself

$$M = \begin{pmatrix} a \\ b \\ c \end{pmatrix} \begin{pmatrix} a & b & c \end{pmatrix} = \begin{pmatrix} a^2 & ab & ac \\ ab & b^2 & bc \\ ac & bc & c^2 \end{pmatrix}, \tag{5.74}$$

which amounts to 3 moduli and 3 phases in general. In this scenario the lightest active neutrino also stays massless, leaving an unbroken $U(1)_{\nu_1}$ global symmetry (neglecting the impact of quantum effects from the charged lepton sector). The number of physical parameters equals

$$\begin{aligned} &(9+8+3) \text{ parameters in total} - 9 \text{ broken real parameters} = 11 \text{ physical parameters}, \\ &(9+8+3) \text{ phases in total} - 17 \text{ broken phase parameters} = 3 \text{ physical phases}. \end{aligned} \tag{5.75}$$

The 14 physical parameters can be identified with three eigenvalues (M_3, y_2, y_3) and two angles from the neutral lepton sector, and three eigenvalues (y_e, y_μ, y_τ), three angles and three phases coming from the charged lepton sector. This is a significant reduction compared to the vanilla seesaw scenario with 21 physical parameters.

In Table 5.1 the residual groups for different scenarios involving three right-handed neutrinos are summarized.

		rank $[Y_\nu]$		
		1	2	3
rank $[M]$	1	$U(1)_N \times U(2)_{\nu_1}$	$U(1)_{\nu_1}$	nothing
	2	$U(2)_{\nu_1}$	$U(1)_{\nu_1}$	nothing
	3	$U(2)_{\nu_1}$	$U(1)_{\nu_1}$	nothing

Table 5.1: Residual groups after the breaking of the $U(3)_L \times U(3)_N$ flavor group by a non-vanishing neutral lepton sector, assuming a generic rank-k Y_ν coupling (with $k = 1, 2, 3$). (Neglecting effects from the other SM fermion sectors.)

5.5 Motivations for Planck-Scale Lepton Number Violation

So far, the assumption of a hierarchical RHN Majorana mass matrix at the Planck scale was motivated by purely phenomenological arguments. A two-loop suppressed Planck-scale RHN mass leads to a light neutrino mass in the ballpark of experimentally observed values through the seesaw mechanism after EWSB [2]

$$m_\nu \simeq (16\pi^2)^2 \frac{v^2}{M_P} \simeq \mathcal{O}(0.1)\,\text{eV}, \tag{5.76}$$

assuming an order $\mathcal{O}(1)$ neutrino Yukawa coupling, where $M_P \simeq 1.2 \times 10^{19}\,\text{GeV}$ and the Higgs VEV has the value $v \simeq 246\,\text{GeV}$. Note that the neutrino mass in Eq. (5.76) depends only on two fundamental scales, the electroweak symmetry breaking scale (the Higgs VEV) and the Planck mass M_P. Without taking advantage of two-loop effects, the resulting neutrino mass would be of order $\mathcal{O}(10^{-6})\,\text{eV}$, making intermediary scales necessary to explain the neutrino oscillation parameters [81].

It has been put forward that the structure of a light neutrino mass matrix induced by gravity would be "democratic" where the dimensionless coefficients in Eq. (3.1), suppressed by the scale of gravitational interactions $\Lambda \simeq M_P$, take the following form: $c_{\alpha\beta} = 1$. This is motivated by the flavor-blindness of gravitational interactions [82]. Analogous to this train of thought, this would mean for gravitationally induced right-handed neutrino masses

$$M(\Lambda) = \omega M_P \begin{pmatrix} 1 & 1 & 1 \\ 1 & 1 & 1 \\ 1 & 1 & 1 \end{pmatrix}, \tag{5.77}$$

assuming three generations of RHNs, where $\omega \simeq \mathcal{O}(1)$. A mass matrix of this structure is exactly rank-1 and has the corresponding eigenvalues $D_M = \text{diag}(0, 0, 3\omega M_P)$. Ref. [83] discusses deviations from this exactly "democratic" texture induced by topological fluctuations (*e.g.* wormholes) [84, 85]. Small corrections to the mass matrix in Eq. (5.77) lead to a very hierarchical mass spectrum for the right-handed neutrinos $M_1 \ll M_2 \ll M_3$, where the heaviest mass is close to the Planck scale, while the other two are non-vanishing but much lighter, as assumed on a phenomenological basis throughout this work.

In the Standard Model, neutrinos stay massless to all orders of perturbation theory as well as through non-perturbative effects. This is because the global $(B - L)$ symmetry is respected throughout the SM. The non-perturbative sphaleron process violates baryon number B and lepton number L, but not the combination $(B - L)$. The inclusion of gravity

in perturbation theory does not change this picture, as couplings to gravity also respect the $(B-L)$ symmetry [86]. But the picture changes if non-perturbative gravitational effects (like black holes and wormholes) are considered, which violate all global symmetries,[2] *e.g.* lepton number and $(B-L)$ [88–90]. The thought experiment is the following: any number of particles carrying lepton or baryon number can be thrown into a black hole, but when the black hole evaporates over time by emitting Hawking radiation, the leptons or baryons are not recovered. This renders the Planck scale as the natural choice for lepton number violating Majorana masses. Planck-scale RHN masses are disfavored by the standard seesaw scenario where the resulting active neutrino masses would be of the order of $\mathcal{O}(10^{-6})$ eV [91] and thus three orders of magnitude too small to explain the experimental observations, but are favored if two-loop effects analyzed in [1–4] are taken into account.

Another possibility to give a Planck-scale mass to the right-handed neutrinos is via a Yukawa interaction between a singlet scalar σ which obtains a sufficiently large vacuum expectation value [92, 93]. The additional complex scalar $\sigma = (\langle\sigma\rangle + R + iJ)/\sqrt{2}$ is neutral under the SM gauge group and carries a charge of $L = -2$. The corresponding Lagrangian containing the RHN fields reads (family indices suppressed):

$$\mathcal{L}_N = \overline{N} i\partial\!\!\!/ N - \left(\overline{L} Y \widetilde{\Phi} N + \frac{1}{2}\overline{N^c} Y_\sigma \sigma N + \text{h.c.}\right), \tag{5.78}$$

where Y is a general complex matrix and Y_σ can be taken as a real and symmetric matrix, without loss of generality. After spontaneous symmetry breaking of the $U(1)_{B-L}$ symmetry by the complex scalar field assuming its vacuum expectation value $\langle\sigma\rangle = v_\sigma$, the right-handed neutrinos N_i get the Majorana mass term $M = \langle\sigma\rangle Y_\sigma/\sqrt{2}$. If $U(1)_{B-L}$ is a global symmetry, its spontaneous breaking leads to a massless Nambu-Goldstone boson, the CP-odd Majoron J [92]. If cosmic inflation is driven by the field breaking the $U(1)_{B-L}$, then the vacuum expectation value $\langle\sigma\rangle$ must be trans-Planckian $v_\sigma \simeq \mathcal{O}(100 \times M_P)$ [94, 95]. After inflation, the σ field settles down at the minimum of the potential and breaks lepton number by two units, giving rise to massive RH neutrinos. Ref. [96] uses this set-up to explain inflation, the BAU, dark matter and neutrino masses. For a hierarchical Y_σ, where the largest eigenvalue is of order of the charged lepton Yukawa, a similar RHN mass spectrum as in Eq. (5.77) is obtained. In this way neutrino masses and inflation can be related.

Without any fundamental guiding principle, the assumptions made on the neutrino Yukawa coupling are generic. While the Majorana mass matrix is approximately democratic, which is reasonable in absence of any distinguishing principle, the neutrino Yukawa sector may be anarchic. One may invoke the so-called *flavor-blind principle* for Yukawas [97], introduced in order to explain fermion mixing patterns like the empirical Gatto-Sartori-Tonin relation. It states Yukawa interactions should be introduced in a way such that flavor-blindness is initially conserved and the global permutation symmetry $S_3^L \times S_3^R$ (separate invariance under the permutation of rows and columns) is initially retained. This maximal flavor symmetry is then successively and minimally broken in order to increase the rank and to retain a residual flavor symmetry, $S_2^L \times S_2^R$ and so on, until all generations become massive. This suggests a democratic ansatz also for the Yukawa sector.

Considering the SM Yukawa sector, the neutrino Yukawa coupling can have a rank larger than one and a sizable eigenvalue. In order to simplify the analytical treatment and as a proxy for a hierarchical Yukawa spectrum, rank-1 couplings are considered in this

[2] Discrete charges like Z_2, which will be used in chapter 7, may still be preserved by non-perturbative gravitational effects as was argued in [87].

work whenever possible. In fact, for the considered Planck-scale lepton number breaking scenarios, the largest neutrino Yukawa eigenvalue should be $\mathcal{O}(1)$ (*cf.* Eq. (5.76)). Looking for analogues in the SM, the bottom quark and τ-lepton couplings are of the same order $y_b \sim y_\tau$, thus one might assume that the largest neutrino Yukawa coupling is of the same order as the top quark coupling, $y_t \sim y_3$. At least one neutrino Yukawa coupling at the order of the top quark coupling is also generically expected within $SO(10)$ Grand Unifying Theories [98].

Chapter 6

Two-Loop Quantum Effects in the Seesaw Model Extended by a Second Higgs Doublet

So far, a minimally extended Standard Model by a number of right-handed neutrinos was considered. Within this extension, two-loop effects in the context of radiative generation of right-handed neutrino masses were studied. These quantum effects can have a crucial impact on the neutrino phenomenology if the RHN mass spectrum is hierarchical.

Under the conditions outlined in the previous chapter, a RHN tree-level mass can be completely washed out by radiative corrections and thus reduced the effective number of parameters required by the model. In the specific case of three right-handed neutrinos, the lightest RHN gets radiative contributions effectively at the four-loop level (see Eq. (5.34)). This suppression may be too large to reproduce the observed neutrino parameters for generic neutrino Yukawa couplings Y. With the addition of extra scalars, both right-handed neutrino masses can be generated at the two-loop level.

There are further theoretical motivations in favor of two-Higgs doublet models (2HDMs). Well-motivated theories with two Higgs doublets could explain flavor anomalies and the muon anomalous magnetic moment $g-2$ [99]. For successful electroweak baryogenesis several models involve two Higgses, where the extra doublet explicitly [100] or spontaneously [101] introduces additional sources of CP-violation in order to produce the observed baryon asymmetry of the universe (BAU). The scalar sector is the experimentally least constrained part of the Standard Model and an extension can address problems left open by the SM. The discussion of two-loop effects with extended scalar sectors in chapters 6 and 7 follows closely [4].

6.1 Scalar Potential

In this part, extensions of the Standard Model with three right-handed neutrinos and at least one additional complex $SU(2)_L$ doublet scalar, sharing the same quantum numbers as the SM Higgs doublet (with hypercharge $Y=1$), are investigated. The most general renormalizable scalar potential $V(\Phi_1,\Phi_2)$ that can be written down, invariant under the

SM gauge group, containing two Higgs doublets Φ_a (with $a = 1, 2$), is the following [102]:

$$V = \sum_{a,b} \mu_{ab}^2 \Phi_a^\dagger \Phi_b + \sum_{a,b,c,d} \lambda_{abcd} \left(\Phi_a^\dagger \Phi_b\right) \left(\Phi_c^\dagger \Phi_d\right), \tag{6.1}$$

where due to the Hermiticity of the potential $\mu_{ab}^2 = (\mu_{ba}^2)^*$ and $\lambda_{abcd} = \lambda_{badc}^*$. Written in a different notation, the scalar potential takes the form

$$\begin{aligned} V(\Phi_1, \Phi_2) = {} & \mu_{11}^2 \Phi_1^\dagger \Phi_1 + \mu_{22}^2 \Phi_2^\dagger \Phi_2 - \left(\mu_{12}^2 \Phi_1^\dagger \Phi_2 + \text{h.c.}\right) + \frac{1}{2}\lambda_1 \left(\Phi_1^\dagger \Phi_1\right)^2 \\ & + \frac{1}{2}\lambda_2 \left(\Phi_2^\dagger \Phi_2\right)^2 + \lambda_3 \left(\Phi_1^\dagger \Phi_1\right)\left(\Phi_2^\dagger \Phi_2\right) + \lambda_4 \left(\Phi_1^\dagger \Phi_2\right)\left(\Phi_2^\dagger \Phi_1\right) \\ & + \left[\frac{1}{2}\lambda_5 \left(\Phi_1^\dagger \Phi_2\right)^2 + \lambda_6 \left(\Phi_1^\dagger \Phi_1\right)\left(\Phi_1^\dagger \Phi_2\right) + \lambda_7 \left(\Phi_2^\dagger \Phi_2\right)\left(\Phi_1^\dagger \Phi_2\right) + \text{h.c.}\right]. \end{aligned} \tag{6.2}$$

The couplings $\mu_{12}^2, \lambda_5, \lambda_6$ and λ_7 can be complex in general, but if the potential should be invariant under CP transformations like $\Phi_i \to i\sigma_2 \Phi_i^*$, these parameters are required to be real. For the corresponding quartic couplings, one finds $\lambda_1 = 2\lambda_{1111}$, $\lambda_5 = 2\lambda_{1212} = 2\lambda_{2121}^*$, *etc.* With two complex scalar doublets, there are eight scalar fields in total and each doublet is given by

$$\Phi_a = \begin{pmatrix} \Phi_a^+ \\ \frac{1}{\sqrt{2}}\left(v_a + \phi_a + iA_a\right) \end{pmatrix}, \tag{6.3}$$

with $a = 1, 2$. The factor $\sqrt{2}$ is a convention for convenient normalization. After spontaneous symmetry breaking, both doublets acquire their VEVs v_i along the neutral direction

$$\langle \Phi_1 \rangle = \frac{1}{\sqrt{2}} \begin{pmatrix} 0 \\ v_1 \end{pmatrix}, \qquad \langle \Phi_2 \rangle = \frac{1}{\sqrt{2}} \begin{pmatrix} 0 \\ v_2 \end{pmatrix}, \tag{6.4}$$

with ground states chosen such that the vacuums are neither CP violating, nor $U(1)_{\text{em}}$ breaking,[1] to have the normal electroweak minimum.

The scalar potential in Eq. (6.2) needs to fulfill theoretical constraints in order to be viable. Perturbativity demands that all quartic couplings in the potential should be less than 4π. In connection to unitarity there are also perturbative unitarity limits on the couplings, demanding that tree-level scalar-scalar scattering is not unitarity violating. This is satisfied if all eigenvalues of the scalar-scalar S matrix are less than 8π [103]. Going forward without a detailed analysis of the perturbative unitarity, it is enough to demand that the λ_i are not too large and well within the perturbative limit. The bounded-from-below condition which means there is no direction in field space in which the scalar potential goes to minus infinity $V \to -\infty$, to have a stable global minimum in the potential, must also be fulfilled. The necessary conditions for the λ_i parameters, to have a stable vacuum bounded from below at tree-level are [104]

$$\begin{aligned} \lambda_1 \geq 0, \qquad & \lambda_3 \geq -\sqrt{\lambda_1 \lambda_2}, \\ \lambda_2 \geq 0, \qquad & \lambda_3 + \lambda_4 - |\lambda_5| \geq -\sqrt{\lambda_1 \lambda_2}, \\ 2|\lambda_6 + \lambda_7| < {} & \frac{1}{2}(\lambda_1 + \lambda_2) + \lambda_3 + \lambda_4 + \lambda_5. \end{aligned} \tag{6.5}$$

[1] Both non-zero VEVs are real-valued, thus no CP violation and all charged fields Φ_a^+ get a zero VEV, otherwise the breaking of $U(1)_{\text{em}}$ would lead to a massive photon.

These conditions become sufficient in the case of vanishing λ_6 and λ_7.

Without any additional symmetries associated with the newly introduced complex scalar, both Φ_1 and Φ_2 are indistinguishable from each other. Therefore, one can choose to work in a basis where only one of the scalars is getting a non-zero VEV, the so-called *Higgs basis* [102]. This can be done by performing the following rotation of the fields

$$\begin{pmatrix} \widehat{\Phi}_1 \\ \widehat{\Phi}_2 \end{pmatrix} = \begin{pmatrix} \cos\beta & \sin\beta \\ -\sin\beta & \cos\beta \end{pmatrix} \begin{pmatrix} \Phi_1 \\ \Phi_2 \end{pmatrix}, \tag{6.6}$$

such that $\sqrt{2}\langle\widehat{\Phi}_1\rangle = v = \sqrt{v_1^2 + v_2^2}$ and $\sqrt{2}\langle\widehat{\Phi}_2\rangle = 0$, with $v \simeq 246\,\text{GeV}$. The rotation angle is defined as

$$\tan\beta = \frac{v_2}{v_1}, \tag{6.7}$$

a parameter that we will use later on when discussing the phenomenology of the model.

6.2 Two-Loop RGEs for Extended Scalar Sectors

The leading quantum effects on the RHN mass matrix M the in RG evolution are now studied. The RHN-Lagrangian for the two-Higgs doublet model extended by n_g right-handed neutrinos N_i $(i = 1, ..., n_g)$ reads:

$$\mathcal{L}_N = \frac{1}{2}\overline{N_i} i\partial\!\!\!/ N_i - \left(Y^{(a)}_{\alpha i}\overline{L_\alpha} N_i \widetilde{\Phi}_a + \frac{1}{2} M_{ij}\overline{N_i^c} N_j + \text{h.c.} \right), \tag{6.8}$$

with the complex scalar doublets Φ_a $(a = 1, 2)$, as discussed in the previous section, their charge conjugate $\widetilde{\Phi}_a = i\sigma_2\Phi_a^*$, and L_α $(\alpha = e, \mu, \tau)$ denotes the lepton doublets. The scalar potential can be seen in Eq. (6.2).

Similarly to Eq. (4.2) for the one-Higgs doublet case, the renormalization group equations up to two-loop order for the Majorana mass matrix M take the following general form:

$$\frac{dM}{d\log\mu} = \beta_M^{(1)} + \beta_M^{(2)}, \tag{6.9}$$

with the one- and two-loop beta functions, $\beta_M^{(1)}$ and $\beta_M^{(2)}$. They read in detail:

$$\begin{aligned}
\beta_M^{(1)} &= \sum_a \left[P^{(aa)T} M + M P^{(aa)} \right], \\
\beta_M^{(2)} &= \sum_{a,b} \Bigg\{ 4 P^{(ba)T} M P^{(ab)} + \left(\frac{17}{8} g_1^2 + \frac{51}{8} g_2^2 \right) \left[P^{(aa)T} M + M P^{(aa)} \right] \\
&\quad - \left(\frac{9}{2} \frac{\text{Tr}\left(Y_u^{(a)} Y_u^{(b)\dagger} \right)}{16\pi^2} + \frac{3}{2} \text{Tr}\left(P^{(ab)} \right) \right) \left[P^{(ba)T} M + M P^{(ba)} \right] \\
&\quad - \frac{1}{4} \left[P^{(ab)T} P^{(ba)T} M + M P^{(ab)} P^{(ba)} \right] \Bigg\},
\end{aligned} \tag{6.10}$$

where for convenience the following shorthand quantities are defined:

$$
\begin{aligned}
P^{(ab)} &= \frac{1}{16\pi^2} Y^{(a)\dagger} Y^{(b)}, \\
Q^{(ab)} &= (1+\mathcal{G})\, P^{(ab)} \delta_{ab} - \frac{1}{4} P^{(ab)} P^{(ba)} - \left(\frac{9}{2} \frac{\mathrm{Tr}\left(Y_u^{(a)} Y_u^{(b)\dagger} \right)}{16\pi^2} + \frac{3}{2} \mathrm{Tr}\left(P^{(ba)} \right) \right) P^{(ab)}, \\
\mathcal{G} &= \frac{1}{16\pi^2} \left(\frac{17}{8} g_1^2 + \frac{51}{8} g_2^2 \right),
\end{aligned} \tag{6.11}
$$

and the $U(1)_Y$ and $SU(2)_L$ gauge couplings couplings are denoted by g_1 and g_2 respectively. $Y_u^{(a)}$ is the up-type Yukawa coupling to each of the doublets. The charged lepton and down-type Yukawa couplings to both doublets are neglected. The RGE was calculated working in the $\overline{\mathrm{MS}}$ renormalization scheme and using the shorthand quantities it be cast as:

$$
\frac{dM}{d\log\mu} = \sum_{a,b} \left(M Q^{(ab)} + Q^{(ab)T} M + 4 P^{(ba)T} M P^{(ab)} \right). \tag{6.12}
$$

Equivalently, the energy-scale evolution for the neutrino Yukawa in the 2HDM reads up to the two-loop level,

$$
\frac{dY^{(a)}}{d\log\mu} = \beta^{(1)}_{Y^{(a)}} + \beta^{(2)}_{Y^{(a)}}, \tag{6.13}
$$

with

$$
\begin{aligned}
16\pi^2 \beta^{(1)}_{Y^{(a)}} &= \left[3 \sum_b \mathrm{Tr}\left(Y_u^{(a)} Y_u^{(b)\dagger} \right) + \sum_b \mathrm{Tr}\left(Y^{(a)} Y^{(b)\dagger} \right) - \frac{3}{4} g_1^2 - \frac{9}{4} g_2^2 \right] Y^{(a)} \\
&\quad + \sum_b Y^{(b)} Y^{(b)\dagger} Y^{(a)} + \sum_b \frac{1}{2} Y^{(a)} Y^{(b)\dagger} Y^{(b)}, \\
(16\pi^2)^2 \beta^{(2)}_{Y^{(a)}} &= \left[6\lambda_1^2 + \lambda_3^2 + \lambda_4^2 + \lambda_3\lambda_4 + \frac{3}{2}\lambda_5^2 + \frac{13}{8} g_1^4 - \frac{21}{4} g_2^4 - \frac{9}{4} g_1^2 g_2^2 \right] Y^{(a)} - 12\lambda_a Y^{(a)} \widetilde{P}^{(aa)} \\
&\quad + \sum_b \Bigg[\sum_c \Bigg\{ \left(20 g_s^2 + \frac{85}{24} g_1^2 + \frac{45}{8} g_2^2 \right) \mathrm{Tr}\left(Y_u^{(b)} Y_u^{(c)\dagger} \right) + \left(\frac{5}{8} g_1^2 + \frac{45}{8} g_2^2 \right) \mathrm{Tr}\left(Y^{(b)} Y^{(c)\dagger} \right) \\
&\quad - \frac{27}{4} \mathrm{Tr}\left((Y_u^{(b)} Y_u^{(c)\dagger})^2 \right) - \frac{3}{4} \mathrm{Tr}\left((Y^{(b)} Y^{(c)\dagger})^2 \right) \Bigg\} \Bigg] Y^{(b)} - 6\lambda_5 \sum_b Y^{(b)} \widetilde{P}^{(ab)} (1 - \delta_{ab}) \\
&\quad + \frac{3}{2} Y^{(a)} \widetilde{P}^{(aa)2} + \left(\frac{31}{8} g_1^2 + \frac{45}{8} g_2^2 - \sum_c \left\{ \frac{9}{2} \mathrm{Tr}\left(Y_u^{(a)} Y_u^{(c)\dagger} \right) + \frac{3}{2} \mathrm{Tr}\left(Y^{(a)} Y^{(c)\dagger} \right) \right\} \right) \\
&\quad \times \sum_b \left(Y^{(b)} Y^{(b)\dagger} Y^{(a)} + \frac{1}{2} Y^{(a)} Y^{(b)\dagger} Y^{(a)} \right) - (2\lambda_3 + 4\lambda_4) \sum_b Y^{(a)} \widetilde{P}^{(bb)} (1 - \delta_{ab}) \\
&\quad + \frac{1}{4} \sum_b \Big(7 Y^{(a)} \widetilde{P}^{(ba)} \widetilde{P}^{(ab)} - Y^{(a)} \widetilde{P}^{(ab)} \widetilde{P}^{(ba)} - Y^{(a)} \widetilde{P}^{(bb)} \widetilde{P}^{(aa)} - Y^{(b)} \widetilde{P}^{(bb)2} \\
&\quad - Y^{(b)} \widetilde{P}^{(bb)} \widetilde{P}^{(ba)} + 8 Y^{(b)} \widetilde{P}^{(ba)} \widetilde{P}^{(bb)} + 7 Y^{(b)} \widetilde{P}^{(aa)} \widetilde{P}^{(ba)} \Big) (1 - \delta_{ab}).
\end{aligned} \tag{6.14}
$$

Here, g_s denotes the $SU(3)_c$ gauge coupling and the λ_i are the quartic couplings in the scalar potential in Eq. (6.2), and $\widetilde{P} = Y^{(a)\dagger} Y^{(b)}$. At two-loop level the quartic couplings enter into the Yukawa beta function. The RGEs for the neutrino Yukawa were obtained using `SARAH` [72, 73], working in the $\overline{\mathrm{MS}}$ scheme.

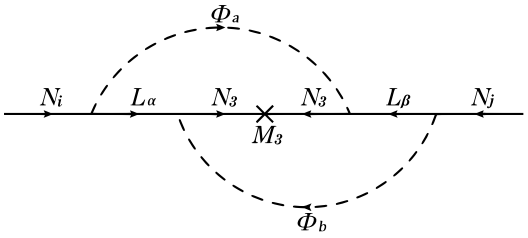

Figure 6.1: Leading two-loop diagram to generate right-handed neutrino masses.

6.3 Effects on Right-Handed Neutrinos

The main impact of two-loop quantum effects can be understood by assuming three RHNs and a Majorana mass matrix showing strong a hierarchical spectrum at the cut-off energy scale of the theory,

$$M(\mu)\Big|_{\mu=\Lambda} = \begin{pmatrix} M_1 & 0 & 0 \\ 0 & M_2 & 0 \\ 0 & 0 & M_3 \end{pmatrix}, \tag{6.15}$$

where the basis was chosen in which the mass matrix is real and diagonal, such that $U_M(\Lambda) = \mathbb{1}$. Due to the hierarchical spectrum $M_1, M_2 \ll M_3$, the mass matrix well approximates a rank-1 matrix.

Solving the RGE for the RHN mass matrix in Eq. (6.12) with the method shown in Sec. 4.2, the solution at the scale $\mu < \Lambda$, only keeping terms up to the order $\mathcal{O}\left(P^{(ab)2}\right)$, can be cast as

$$\begin{aligned} M(\mu) \simeq & \left[1 + \sum_a \left(P^{(aa)}t + \frac{1}{2}P^{(aa)2}t^2\right)\right]^T M \left[1 + \sum_b \left(P^{(bb)}t + \frac{1}{2}P^{(bb)2}t^2\right)\right] \\ & + 4\sum_{a,b} P^{(ba)T} M P^{(ab)} t + \mathcal{O}\left(P^{(ab)3}\right). \end{aligned} \tag{6.16}$$

Here, terms beyond $\mathcal{O}\left(P^{(ab)}\right)$ in $Q^{(ab)}$ (see Eq. (6.11)) were neglected which only lead to small corrections to the non-vanishing tree-level masses in $M(\Lambda)$. Again, the convenient scale parameter $t = \log(\mu/\Lambda)$ is used. The main one-loop correction to the tree-level mass M_3 at $M_3 < \Lambda$ from the first line in Eq. (6.16) reads,

$$M_3(\mu)\Big|_{\mu=M_3} \simeq M_3 + 2M_3\left(P_{33}^{(11)} + P_{33}^{(22)}\right)\log\left(\frac{M_3}{\Lambda}\right). \tag{6.17}$$

But much more interesting are the contributions proportional to M_3 to the small tree-level masses M_1 and M_2 coming from the second line in Eq. (6.16). Even in the exact rank-1 case ($M_1 = M_2 = 0$), the mass matrix will become rank-3 for generic neutrino Yukawa couplings due to the $P^{(ba)T}MP^{(ab)}$ term, coming from the two-loop diagram depicted in Fig. 6.1. Through the energy-scale evolution, non-vanishing M_1 and M_2 are created at order $\mathcal{O}(P^{(ab)})$, while in the one doublet scenario in Sec. 5.2.2 $M(\Lambda)$ would be at most rank-2 at order $\mathcal{O}(P^2)$ and at most rank-3 at the order $\mathcal{O}(P^4)$ in perturbation theory. The addition of another Higgs doublet coupling to the RHNs via $Y^{(2)}$ provides more flavor symmetry

breaking parameters, leading to a full rank mass matrix at lower order in perturbation theory.

At the scale $\mu = M_3$, the heaviest right-handed neutrino can be integrated out. The theory is then correctly described by the effective Lagrangian,

$$\mathcal{L}_{\text{eff}} - \simeq \frac{1}{2}\frac{Y^{(a)}_{\alpha 3}Y^{(b)}_{\beta 3}}{M_{33}}\left(\overline{L_\alpha}\widetilde{\Phi}_a\right)\left(\widetilde{\Phi}^T_b L^c_\beta\right) - \mathbb{Y}^{(a)}_{\alpha i}\overline{L_\alpha}\widetilde{\Phi}_a N_i - \frac{1}{2}\mathbb{M}_{ij}\overline{N^c_i}N_j + \text{h.c.}, \tag{6.18}$$

where neutrino Yukawa coupling and RHN neutrino mass matrix of the effective theory

$$\begin{aligned}\mathbb{Y}^{(a)}_{\alpha i} &\simeq \left(Y^{(a)}_{\alpha i} - \frac{M_{i3}Y^{(a)}_{\alpha 3}}{M_{33}}\right)\Bigg|_{\mu=M_3},\\ \mathbb{M}_{ij} &\simeq \left(M_{ij} - \frac{M_{i3}M_{j3}}{M_{33}}\right)\Bigg|_{\mu=M_3},\end{aligned} \tag{6.19}$$

with $i,j = 1,2$ are defined (similar to Eq. (5.20)), and all parameters are evaluated at $\mu = M_3$.

By integrating out N_3, the dimension-5 operator arises in Eq. (6.18), leading to an active neutrino mass suppressed by M_3 (assuming M_3 is close to the Planck scale, the resulting neutrino mass will be $\gtrsim 10^{-6}$ eV and thus far too small to play a role in explaining neutrino oscillation experiments), which will be neglected in the following:

$$\mathcal{L}_{\text{eff}} \simeq -\mathbb{Y}^{(a)}_{\alpha i}\overline{L_\alpha}\widetilde{\Phi}_a N_i - \frac{1}{2}\mathbb{M}_{ij}\overline{N^c_i}N_j + \text{h.c.} \tag{6.20}$$

To calculate the radiative RHN masses, the tensor invariants can be used:[2]

$$\begin{aligned}I_1 &= \text{Tr}\left[\mathbb{M}\right] = M_1 + M_2 = \mathbb{M}_{11} + \mathbb{M}_{22},\\ I_2 &= \det\left[\mathbb{M}\right] = M_1 M_2 = \mathbb{M}_{11}\mathbb{M}_{22} - \mathbb{M}_{12}\mathbb{M}_{21},\end{aligned} \tag{6.21}$$

with $\mathbb{M}$ defined in Eq. (6.19) and approximately reads

$$\mathbb{M}_{ij}\Big|_{\mu=M_3} \simeq 4M_3 \log\left(\frac{M_3}{\Lambda}\right)\sum_{a,b} P^{(ba)}_{3i}P^{(ab)}_{3j}, \tag{6.22}$$

using that the second term in Eq. (6.19) is small. For RHN masses showing a hierarchy, the masses can be approximated by using the tensor invariants only:

$$\begin{aligned}M_2\Big|_{\mu=M_3} &\simeq I_1,\\ M_1\Big|_{\mu=M_3} &\simeq \frac{I_2}{I_1}.\end{aligned} \tag{6.23}$$

[2] Here, real-valued parameters are assumed, for complex parameters the corresponding invariants are found by using $I_1 = \text{Tr}\left[\mathbb{M}^\dagger\mathbb{M}\right] = M_1^2 + M_2^2$ and $I_2 = \det\left[\mathbb{M}^\dagger\mathbb{M}\right] = M_1^2 M_2^2$.

Since the quantum contributions proportional to M_3 dominate over the tree-level masses of N_1 and N_2, the mass eigenstates at the scale $\mu = M_3$ become:

$$M_2\Big|_{\mu=M_3} \simeq 4M_3 \sum_{a,b} \left(P_{31}^{(ab)} P_{31}^{(ba)} + P_{32}^{(ab)} P_{32}^{(ba)}\right) \log\left(\frac{M_3}{\Lambda}\right),$$
$$M_1\Big|_{\mu=M_3} \simeq 4M_3 \frac{\sum_{a,b,c,d} \left(P_{31}^{(ab)} P_{31}^{(ba)} P_{32}^{(cd)} P_{32}^{(dc)} - P_{31}^{(ab)} P_{31}^{(cd)} P_{32}^{(ba)} P_{32}^{(dc)}\right)}{\sum_{a,b} \left(P_{31}^{(ab)} P_{31}^{(ba)} + P_{32}^{(ab)} P_{32}^{(ba)}\right)} \log\left(\frac{M_3}{\Lambda}\right). \quad (6.24)$$

Both radiative masses are generically comparable in size as both arise at order $\mathcal{O}\big(P^{(ab)2}\big)$. The expression for $M_2|_{\mu=M_3}$ reproduces the result in Eq. (5.34), obtained in the one doublet case, by taking the limit $Y^{(2)} \to 0$, while $M_1|_{\mu=M_3}$ would vanish at the given order of perturbation theory, as expected. Instead of using the invariants, the 2×2 RHN mass matrix at the scale $\mu = M_3$ in Eq. (6.19) can also be diagonalized by $\mathbb{M} \simeq U_{\mathbb{M}} \mathrm{diag}(M_i, M_j) U_{\mathbb{M}}^T$, where

$$U_{\mathbb{M}}\Big|_{\mu=M_3} \simeq \frac{1}{\sqrt{\mathcal{P}_{31}^2 + \mathcal{P}_{32}^2}} \begin{pmatrix} \mathcal{P}_{32} & \mathcal{P}_{31} \\ -\mathcal{P}_{31} & \mathcal{P}_{32} \end{pmatrix}, \quad (6.25)$$

defining $\mathcal{P}_{3i} = P_{3i}^{(11)} + P_{3i}^{(22)}$.

To gain more analytical insight compared to the expressions in Eq. (6.24), a rank-1 scenario is considered not just for simplicity, but also as a proxy for the case of hierarchical neutrino Yukawa matrices. They can be cast in terms of their non-vanishing eigenvalues y_a and a tensor product of two vectors in flavor space $\vec{u}_L^{(a)}$, $\vec{u}_R^{(a)}$, which are normalized to unity:

$$Y^{(a)} = y_a \vec{u}_L^{(a)} \otimes \vec{u}_R^{(a)T}. \quad (6.26)$$

For the rank-1 symmetric RHN mass matrix, one can equivalently write:

$$M(\Lambda) = M_3 \, \vec{\omega} \otimes \vec{\omega}^T, \quad (6.27)$$

with $\|\vec{\omega}\| = 1$ also normalized to unity. From the three vectors in the RHN flavor space, $\vec{u}_R^{(a)}$, $\vec{\omega}$, and the two vectors in the left-handed neutrino flavor space, $\vec{u}_L^{(a)}$, four invariant scalar quantities can be constructed which are related by their relative orientations, namely $(\vec{u}_R^{(1)} \cdot \vec{\omega})$, $(\vec{u}_R^{(2)} \cdot \vec{\omega})$, $(\vec{u}_R^{(1)} \cdot \vec{u}_R^{(2)})$, and $(\vec{u}_L^{(1)} \cdot \vec{u}_L^{(2)})$. Furthermore, there are three eigenvalues: y_1, y_2 and M_3. The radiative RHN masses can be expressed solely in terms of these seven invariant quantities:

$$M_2\Big|_{\mu=M_3} \simeq -\frac{4M_3 \log\left(\frac{\Lambda}{M_3}\right)}{(16\pi^2)^2} \sum_{a,b} y_a^2 y_b^2 \left(\vec{u}_R^{(a)} \cdot \vec{\omega}\right) \left(\vec{u}_R^{(b)} \cdot \vec{\omega}\right) \left(\vec{u}_L^{(a)} \cdot \vec{u}_L^{(b)}\right)^2 \left[1 - \left(\vec{u}_R^{(a)} \cdot \vec{\omega}\right) \left(\vec{u}_R^{(b)} \cdot \vec{\omega}\right)\right],$$
$$M_1\Big|_{\mu=M_3} \simeq -\frac{4M_3 \log\left(\frac{\Lambda}{M_3}\right)}{(16\pi^2)^2} \frac{y_1^4 y_2^4 \left(\vec{u}_R^{(1)} \cdot \vec{\omega}\right)^2 \left(\vec{u}_R^{(2)} \cdot \vec{\omega}\right)^2 \left(\vec{\omega} \cdot \left(\vec{u}_R^{(1)} \times \vec{u}_R^{(2)}\right)\right)^2 \left[1 - \left(\vec{u}_L^{(1)} \cdot \vec{u}_L^{(2)}\right)^4\right]}{\sum_{a,b} y_a^2 y_b^2 \left(\vec{u}_R^{(a)} \cdot \vec{\omega}\right) \left(\vec{u}_R^{(b)} \cdot \vec{\omega}\right) \left(\vec{u}_L^{(a)} \cdot \vec{u}_L^{(b)}\right)^2 \left[1 - \left(\vec{u}_R^{(a)} \cdot \vec{\omega}\right) \left(\vec{u}_R^{(b)} \cdot \vec{\omega}\right)\right]}. \quad (6.28)$$

For vectors normalized to unity, the square of the triple product reads in detail:

$$\left(\vec{\omega} \cdot \left(\vec{u}_R^{(1)} \times \vec{u}_R^{(2)}\right)\right)^2 = 1 - \left(\vec{u}_R^{(1)} \cdot \vec{\omega}\right)^2 - \left(\vec{u}_R^{(2)} \cdot \vec{\omega}\right)^2 - \left(\vec{u}_R^{(1)} \cdot u_R^{(2)}\right)^2 + 2\left(\vec{u}_R^{(1)} \cdot \vec{\omega}\right)\left(\vec{u}_R^{(2)} \cdot \vec{\omega}\right)\left(\vec{u}_R^{(1)} \cdot u_R^{(2)}\right). \quad (6.29)$$

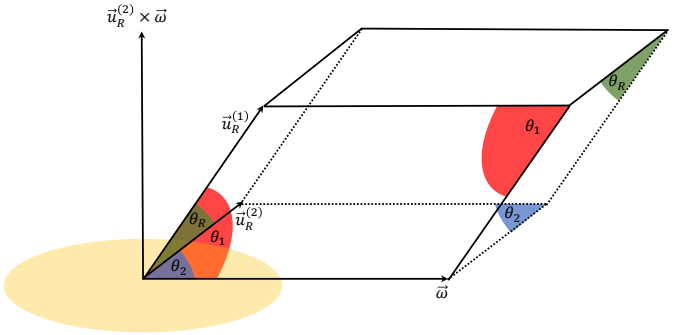

Figure 6.2: Sketch of the angles and vectors in the right-handed neutrino flavor space as well as the parallelepiped spanned by them.

In order to generate two non-vanishing RHN masses, the vectors in flavor space must fulfill certain properties, which can be inferred from the equations above:

- At least one of the $\vec{u}_R^{(a)}$ must be non-orthogonal to $\vec{\omega}$, to generate a non-vanishing M_2.
- Generating a non-vanishing M_1 needs the following conditions fulfilled at the same time:
  1. Both $\vec{u}_R^{(a)}$ must be non-orthogonal to $\vec{\omega}$.
  2. Both $\vec{u}_R^{(a)}$ and $\vec{\omega}$ are not coplanar.
  3. Both $\vec{u}_L^{(a)}$ must be non-orthogonal to each other.

Thus, generating M_2 needs at least two linearly independent directions in the RHN flavor space, while M_1 requires three independent directions in RHN flavor space plus two independent directions in the left-handed neutrino flavor space.

The global flavor group $U(3)_N \times U(3)_L$ is only broken down to nothing if there are enough directions in flavor space. If there is alignment between vectors in RHN flavor space, M_1 is vanishing due to a residual $U(1)_N$ group. In the case with only one Higgs doublet, a rank-2 neutrino Yukawa is necessary to generate two non-vanishing RHN masses, but the lightest is effectively only generated at the four-loop level. In the 2HDM it is possible to generate both at two-loop level because of more directions in flavor space.

The following angles are introduced as flavor-basis independent quantities:

$$\begin{aligned} \vec{u}_L^{(1)} \cdot \vec{u}_L^{(2)} &= \cos\theta_L, \\ \vec{u}_R^{(1)} \cdot \vec{u}_R^{(2)} &= \cos\theta_R, \\ \vec{u}_R^{(1,2)} \cdot \vec{\omega} &= \cos\theta_{1,2}, \end{aligned} \tag{6.30}$$

where the relationship among angles in the RHN flavor space is sketched in Fig. 6.2. With the parametrization above and the three eigenvalues (y_1, y_2, M_3), the physical RHN masses

read:

$$M_2\Big|_{\mu=M_3} \simeq -\frac{4y_1^2y_2^2}{(16\pi^2)^2}M_3\log\left(\frac{\Lambda}{M_3}\right)\left[\left(\frac{y_1}{y_2}s_1c_1\right)^2+\left(\frac{y_2}{y_1}s_2c_2\right)^2+2c_L^2c_1c_2\left(c_R-c_1c_2\right)\right],$$
$$M_1\Big|_{\mu=M_3} \simeq -\frac{4y_1^2y_2^2}{(16\pi^2)^2}M_3\log\left(\frac{\Lambda}{M_3}\right)\frac{c_1^2c_2^2\left(1-c_L^4\right)\left(1-c_1^2-c_2^2-c_R^2+2c_1c_2c_R\right)}{\left(\frac{y_1}{y_2}s_1c_1\right)^2+\left(\frac{y_2}{y_1}s_2c_2\right)^2+2c_L^2c_1c_2\left(c_R-c_1c_2\right)}, \quad (6.31)$$

with the shorthand notation $s_i = \sin\theta_i$ and $c_i = \cos\theta_i$ $(i = 1, 2, L, R)$. The quantum corrections between $\mu = M_3$ and the seesaw scale are small, therefore the physical mass scale of the RHNs N_1 and N_2 is determined by

$$M_0 \equiv \frac{4y_1^2y_2^2}{\left(16\pi^2\right)^2}M_3\log\left(\frac{\Lambda}{M_3}\right) . \quad (6.32)$$

Assuming that lepton number violation is introduced at the Planck scale, the expected mass scale is around

$$M_0 \sim 2\times10^{15}\,\text{GeV}\,y_1^2y_2^2\left(\frac{M_3}{1.2\times10^{19}\,\text{GeV}}\right)\log\left(\frac{M_3}{1.2\times10^{19}\,\text{GeV}}\right) , \quad (6.33)$$

and thus generically reproduces the well-known seesaw scale for neutrino Yukawa couplings of order $\mathcal{O}(1)$.

The analytical results are confirmed by a numerical scan in Fig. 6.3. The plot shows the ratio of the radiatively generated physical masses of $|M_2/M_1|$ against $|M_2|$. From numerically solving the RGEs between $\Lambda = M_P$ and $\mu = M_3$ for initial conditions $M_1 = M_2 = 0$, $M_3 = M_P/\sqrt{8\pi}$ and $y_1 = y_2 = 1$ and taking random angles in flavor space $\theta_L, \theta_R, \theta_{1,2}$ at scale Λ, the scatter plot was obtained. The two-loop quantum effects captured in the RGE generate two non-vanishing RHN masses, M_1 and M_2, both in the ballpark of $\mathcal{O}(10^{14})\,\text{GeV}$ and a mass hierarchy $|M_2/M_1|$ generically below $\mathcal{O}(100)$, similar to hierarchies in the up-quark sector.

The results of this section hold irrespective of the concrete tree-level masses of N_1 and N_2 or the hierarchy between M_1 and M_2 at the cut-off scale Λ, as long as the quantum contributions proportional to M_3 are dominating. Then, the wash-out effect due to the two-loop quantum corrections generically produces two RHN masses with a moderate hierarchy, $M_1|_{\mu=M_3} \sim M_2|_{\mu=M_3}$, which is expected to translate into a mild mass hierarchy for the active neutrinos.

6.4 Light Neutrino Masses in the General 2HDM Framework

Below the scale of the lightest right-handed neutrino mass, which is expected to be far above the electroweak scale for generic Yukawa couplings (see Eq. (6.32)), N_1 is integrated out. The resulting effective Lagrangian reads:

$$\mathcal{L}_{\text{eff}} \simeq -\frac{1}{2}\sum_{a,b}\sum_{\alpha,\beta}\kappa^{(ab)}_{\alpha\beta}\left(\overline{L_\alpha}\widetilde{\Phi}_a\right)\left(\widetilde{\Phi}_b^T L_\beta^c\right) + \text{h.c.}, \quad (6.34)$$

where the Wilson coefficients $\kappa^{(ab)}_{\alpha\beta}$ are evaluated at scale $\mu = M_1$:

$$\kappa^{(ab)}\Big|_{\mu=M_1} = \left(\mathbb{Y}^{(a)}\mathbb{M}^{-1}\mathbb{Y}^{(b)T}\right)\Big|_{\mu=M_1}, \quad (6.35)$$

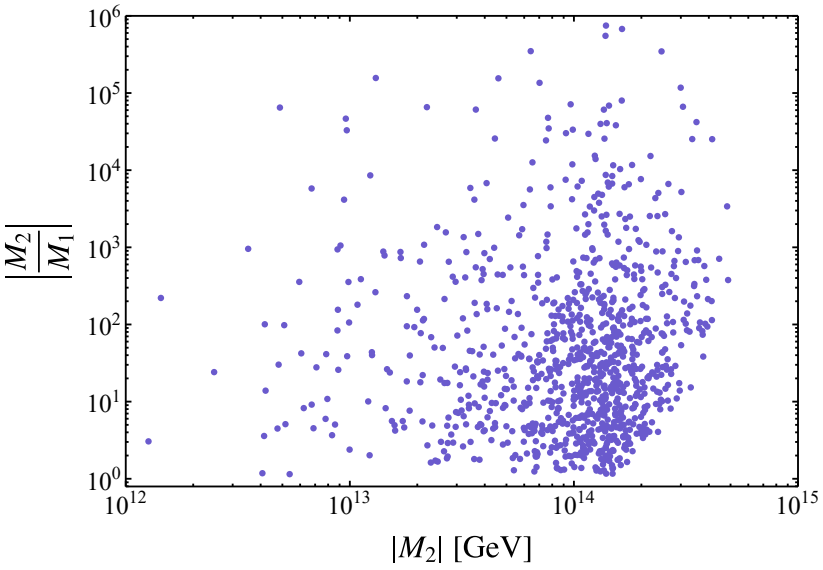

Figure 6.3: Scan plot from numerically solving the RGE, depicting the RHN mass hierarchy of the radiative masses $|M_2/M_1|$ vs. $|M_2|$ within the Planck-scale lepton number breaking framework in the 2HDM. The initial conditions at $\Lambda = M_P$ read: $M_3 = M_P/\sqrt{8\pi}$, $M_1 = M_2 = 0$, $y_1 = y_2 = 1$. The angles in flavor space take on random values between 0 and 2π.

with the double struck quantities defined as in Eq. (6.19) and neglecting the subdominant contribution suppressed by the heaviest RHN mass, M_3. Staying within the rank-1 ansatz for the neutrino Yukawas, the generated Wilson coefficients can be written as

$$\kappa^{(ab)}\Big|_{\mu=M_1} \simeq \frac{\vec{u}_L^{\,(a)} \otimes \vec{u}_L^{\,(b)T}}{\vec{u}_L^{\,(a)} \cdot \vec{u}_L^{\,(b)}} \sum_{i,j} \mathbb{P}_{ij}^{(ab)} \left(\mathbb{M}^{-1}\right)_{ij} \,, \tag{6.36}$$

with $i, j = 1, 2$ and $\mathbb{P}^{(ab)} \equiv \mathbb{Y}^{(a)T}\mathbb{Y}^{(b)}$. Using the notation introduced in Eqs. (6.26) and (6.32) one finds after some algebra,

$$\kappa^{(ab)}\Big|_{\mu=M_1} \simeq \frac{y_a y_b}{M_0} \frac{y_1^2 y_2^2}{y_a^2 y_b^2} \frac{\vec{u}_L^{\,(a)} \otimes \vec{u}_L^{\,(b)T}}{\cos\theta_a \cos\theta_b} \times \begin{cases} 1/(1-\cos^4\theta_L) & a = b, \\ -\cos^2\theta_L/(1-\cos^4\theta_L) & a \neq b\,. \end{cases} \tag{6.37}$$

The large separation between M_1 and the mass scale of the new scalar m_H can also lead to significant quantum corrections in the neutrino parameters and must therefore be considered to correctly describe the low-energy phenomenology. The dominant quantum contributions to the effective operator $\kappa^{(ab)}$ are captured in the energy-scale evolution [74, 105–107],

$$\frac{d\kappa^{(ab)}}{d\log\mu} = \beta_{\kappa^{(ab)}}\,, \tag{6.38}$$

where the beta function for the Wilson coefficients of the Weinberg operator reads at the one-loop level:

$$16\pi^2\beta_{\kappa^{(ab)}} = -3g_2^2\kappa^{(ab)} + \sum_{c,d=1}^{2} 4\lambda_{acbd}\kappa^{(cd)} + \sum_{c=1}^{2}\left(3\mathrm{Tr}\left(Y_u^{(a)}Y_u^{(c)\dagger}\right)\kappa^{(cb)} + 3\mathrm{Tr}\left(Y_u^{(b)}Y_u^{(c)\dagger}\right)\kappa^{(ac)}\right)\,, \tag{6.39}$$

with the quartic couplings λ_{acbd} as in Eq. (6.1). Here, the down-type quark and charged lepton Yukawa couplings have been neglected to focus on the dominant effects only. At the electroweak scale, in the leading-log approximation, the Wilson coefficient reads

$$\kappa^{(ab)}\Big|_{\mu=m_H} = \kappa^{(ab)}\Big|_{\mu=M_1} + \beta_{\kappa^{(ab)}} \log\left(\frac{m_H}{M_1}\right). \tag{6.40}$$

After EWSB, the Lagrangian in Eq. (6.34) yields the 3×3 active neutrino mass matrix

$$\mathcal{M}_\nu = -\frac{1}{2}\sum_{a,b} \kappa^{(ab)}\Big|_{\mu=m_H} v_a v_b, \tag{6.41}$$

which is observed at neutrino oscillation experiments. Effects of the RG running between the EW scale and the energy scale of the experiment are neglected as the relevant quantum effects occur between M_1 and the heavy scalar mass m_H.

The expected RG effects between the seesaw scale and the new scalar m_H can be categorized into three different cases:

- *Case 1*: Each of the tree-level Wilson coefficients $\kappa^{(ab)}$ receives corrections proportional to themselves, which are at most $\mathcal{O}(1)$. The tree-level contribution of $\kappa^{(ab)}$ to the active neutrino mass spectrum is then prevailing and the quantum correction does not lead to new qualitative features.

  This is generically the case for VEVs $v_1 \sim v_2$ and neutrino Yukawa couplings $y_1 \sim y_2$ in the same order of magnitude (staying within the rank-1 ansatz for neutrino Yukawas).

- *Case 2*: Through the RGEs in Eq. (6.39) different Wilson coefficients $\kappa^{(ab)}$ mix with each other. This mixing is induced by "Higgs exchanging interactions" through the Weinberg operators and is a characteristic feature of models with an extended scalar sector, introducing new qualitative features to the low-energy phenomenology [107–110].

  This is expected for hierarchical Higgs VEVs $v_1 \gg v_2 \simeq 0$ (*i.e.* choosing to work in the Higgs alignment limit) and $y_1 \sim y_2$.

- *Case 3*: The quantum effects lead to corrections to the tree-level Wilson coefficients which are proportional to themselves, but the operator mixing is suppressed due to tiny couplings to the second Higgs and thus leads to no new qualitative features.

  This is scenario is realized for a strong hierarchy between the neutrino Yukawa couplings $y_1 \gg y_2$, making the result identical to the one-Higgs doublet case, where the lightest right-handed mass is generated at four-loop level only (for a rank-2 Yukawa coupling) due to vanishing y_2 and is discussed in detail in chapter 5.

In the following, the first two cases are considered, which translate to a scenario in which the quantum effects from the running between M_1 and m_H can be neglected and one in which they can lead to important new phenomenology and thus must be considered.

6.4.1 Negligible Quantum Effects from the $\kappa^{(ab)}$ Running

Staying within the rank-1 hypothesis (see Eqs. (6.26) and (6.27)) for the neutrino Yukawas and the RHN mass matrix at the cut-off Λ, the active neutrino mass matrix at the scale

$\mu = M_1$ can be written as sum of four rank-1 matrices

$$\mathcal{M}_\nu \simeq \sum_{a,b} \mathfrak{m}_{ab}\, \vec{u}_L^{(a)} \otimes \vec{u}_L^{(b)T}, \tag{6.42}$$

with help of Eq. (6.37). Where mass parameters (similar to Eq. (5.43)) are introduced and defined as follows:

$$\mathfrak{m}_{ab} = \frac{(y_a v_a)(y_b v_b)}{2M_0} \frac{y_1^2 y_2^2}{y_a^2 y_b^2} \frac{1}{\cos\theta_a \cos\theta_b} \times \begin{cases} 1/(1-\cos^4\theta_L) & a = b, \\ -\cos^2\theta_L/(1-\cos^4\theta_L) & a \neq b. \end{cases} \tag{6.43}$$

By using the tensor invariants, the light neutrino masses can be extracted from the neutrino mass matrix:

$$\begin{aligned} I_1 &= \mathrm{Tr}\left[\mathcal{M}_\nu\right] = m_1 + m_2 + m_3 \,, \\ I_2 &= \frac{1}{2}\left(\mathrm{Tr}\left[\mathcal{M}_\nu\right]^2 - \mathrm{Tr}\left[\mathcal{M}_\nu^2\right]\right) = m_1 m_2 + m_1 m_3 + m_2 m_3 \,, \\ I_3 &= \det\left[\mathcal{M}_\nu\right] = m_1 m_2 m_3 \,, \end{aligned} \tag{6.44}$$

such that

$$\begin{aligned} I_1 &= \mathfrak{m}_{11} + \mathfrak{m}_{22} + (\mathfrak{m}_{12} + \mathfrak{m}_{21})\cos\theta_L, \\ I_2 &= \left(\mathfrak{m}_{11}\mathfrak{m}_{22} - \mathfrak{m}_{12}\mathfrak{m}_{21}\right)\sin^2\theta_L, \\ I_3 &= 0, \end{aligned} \tag{6.45}$$

follows from Eqs. (6.42) and (6.43). Note that $m_1 = 0$ exactly vanishes in the approximation made in Eq. (6.20). In general, m_1 will be of order $\mathcal{O}(10^{-6})\,\mathrm{eV}$ for M_3 close to the Planck scale. Quantum corrections to m_1 between M_1 and the heavy scalar mass m_H will be proportional to m_3, but two-loop suppressed [76–79]. Assuming a hierarchy between the non-vanishing active neutrinos, the invariants lead to:

$$\begin{aligned} m_3 \simeq I_1 &= m_0 \frac{y_1 y_2}{(1-\cos^4\theta_L)} \left[\frac{y_2}{y_1}\frac{\cos^2\beta}{\cos^2\theta_1} + \frac{y_1}{y_2}\frac{\sin^2\beta}{\cos^2\theta_2} - \frac{2\sin\beta\cos\beta\cos^3\theta_L}{\cos\theta_1\cos\theta_2}\right] , \\ m_2 \simeq \frac{I_2}{I_1} &= m_0 y_1 y_2 \sin^2\theta_L \left[\frac{y_2}{y_1}\frac{\cos^2\theta_2}{\sin^2\beta} + \frac{y_1}{y_2}\frac{\cos^2\theta_1}{\cos^2\beta} - \frac{2\cos\theta_1\cos\theta_2\cos^3\theta_L}{\sin\beta\cos\beta}\right]^{-1} , \end{aligned} \tag{6.46}$$

using Eq. (6.7), where $v_1 = v\cos\beta$ and $v_2 = v\sin\beta$. An active neutrino mass scale parameter is introduced as

$$m_0 = \frac{1}{2}\frac{v^2}{M_0} \,, \tag{6.47}$$

with M_0 defined in Eq. (6.32). Now, the overall mass scale can be estimated as

$$m_0 \simeq 0.05\,\mathrm{eV}\left(\frac{y_1}{0.7}\right)^{-2}\left(\frac{y_2}{0.7}\right)^{-2}\left(\frac{M_3}{1.2\times10^{19}\,\mathrm{GeV}}\right)^{-1} , \tag{6.48}$$

assuming that $\log(M_3/\Lambda) \simeq 1$. The numerical values are in the ballpark of the experiments if M_3 is around the Planck scale and the neutrino Yukawa couplings are of order $\mathcal{O}(1)$.

From the results in Eq. (6.46) it can be seen how misalignment in the LHN flavor space between $\vec{u}_L^{(1)}$ and $\vec{u}_L^{(2)}$ (*i.e.* $\sin\theta_L \neq 0$) is necessary in order to have two non-vanishing neutrino masses, otherwise $\mathcal{M}_\nu$ becomes rank-1.

The active neutrino mass scale of m_2 and m_3 is determined by the parameter defined in Eq. (6.47). For generic mixing angles in the left- and right-handed flavor space, similar-sized neutrino masses are expected. In detail, the mass hierarchy reads:

$$\left|\frac{m_3}{m_2}\right| \simeq \frac{\left(\frac{y_2\cos\theta_2\sin\beta}{y_1\cos\theta_1\cos\beta} + \frac{y_1\cos\theta_1\cos\beta}{y_2\cos\theta_2\sin\beta} - 2\cos^3\theta_L\right)^2}{\sin^2\theta_L\,(1-\cos^4\theta_L)}, \tag{6.49}$$

The predicted hierarchy and neutrino mass scale is independent of the charged lepton flavor space. So far, no restrictions have been imposed on the flavor structure of the charged lepton sector. Therefore, it is not possible to make predictions on the PMNS mixing matrix. Assuming generic misalignment angles at high energies, which are neither small nor maximal, as done throughout this chapter, will in general lead to an "anarchic" structure in the PMNS matrix. This is in qualitative agreement with the observed texture of the leptonic mixing matrix (see Eq. (2.13) and Fig. 2.4).

To confirm the analytical calculations, a numerical random scan is performed. For this, the two-loop RGE for the RHN mass matrix is solved above the scale M_1 as well as the one-loop RGE for the dimension-5 operator below scale M_1 (neglecting the effects of operator mixing in Eq. (6.39)). The initial conditions at the cut-off $\Lambda = M_P$ are $M_1 = M_2 = 0$, $M_3 = M_P/\sqrt{8\pi}$ and random angles in flavor space $(\theta_L, \theta_R, \theta_{1,2})$ between 0 and 2π. For the neutrino Yukawa couplings and Higgs misalignment angle β, three different realizations are considered: *i*) $y_1 = 1$ and $\tan\beta = 1$ (green points), *ii*) $y_1 = 1$ and $\tan\beta = 0.001$ (orange points), and *iii*) $y_1 = 0.001$ and $\tan\beta = 1$ (blue points).

As long as $y_2 \simeq y_1 \simeq 1$ and $\tan\beta \simeq 1$ (green points), the neutrino parameters are well within the ballpark of the observed values at neutrino oscillation experiments. However, if y_1/y_2 and/or $\tan\beta$ strongly deviate from 1, the resulting neutrino mass hierarchy is in general too large (neglecting the effects from operator mixing).

Even without considering effects from operator mixing below $\mu = M_1$, which typically milden the neutrino mass hierarchy in cases outlined below, the ballpark of the experimental values can be reproduced assuming reasonable $\mathcal{O}(1)$ parameters.

6.4.2 Non-negligible Quantum Effects from the $\kappa^{(ab)}$ Running

The second case under consideration is realized in the Higgs alignment limit, in which $\tan\beta = v_2/v_1 \simeq 0$, such that only one Higgs gets a non-zero VEV which resembles the Standard Model Higgs. The resulting active neutrino mass matrix in this limit reads

$$\mathcal{M}_\nu = -\frac{1}{2}\kappa^{(11)}v_1^2, \tag{6.50}$$

with $v_1 = v$. The corresponding Feynman diagram leading to the mass term can be seen in Fig. 6.5. Without the RG effects between scales M_1 and m_H a huge neutrino mass hierarchy would be expected (see Eq. (6.49) in the limit $\beta \to 0$). However, operator mixing induced by the "Higgs exchanging interactions" in Eq. (6.39) can lead to sizable quantum corrections to $\kappa^{(11)}$. The corresponding diagrams leading to operator mixing in Eq. (6.39) are shown in Fig. 6.6. Quantum corrections to the Wilson coefficient $\kappa^{(11)}$ at the scale m_H can be cast

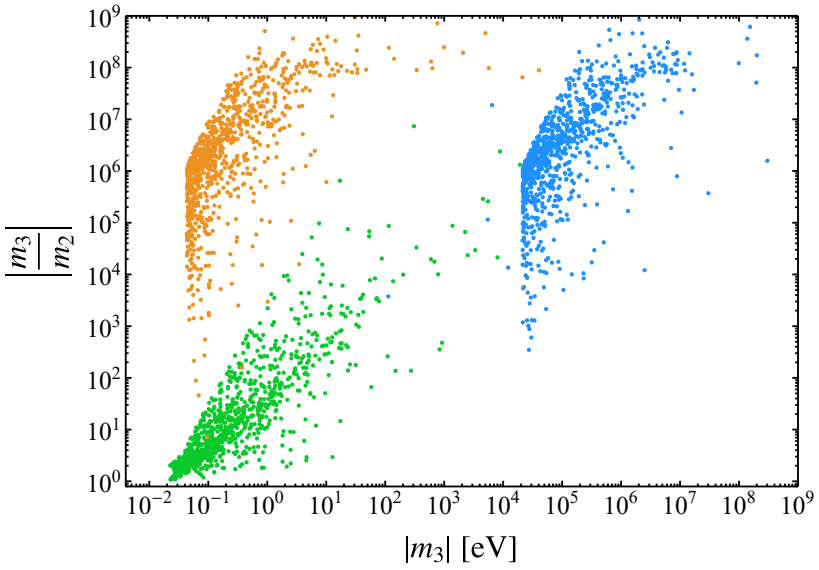

Figure 6.4: Numerical scan of the active neutrino mass hierarchy between the two heavier active neutrinos $|m_3/m_2|$ and $|m_3|$ in the Planck-scale lepton number breaking framework for two Higgs doublets and negligible RGE-induced operator mixing. Using the following parameters at $\Lambda = M_P$: $M_3 = M_P/\sqrt{8\pi}$, $y_2 = 1$, random flavor angles between 0 and 2π, and $y_1 = 1$, $\tan\beta = 1$ (green points), $y_1 = 1$, $\tan\beta = 0.001$ (orange points); $y_1 = 0.001$, $\tan\beta = 1$ (blue points).

as:

$$\kappa^{(11)}\Big|_{\mu=m_H} = \kappa^{(11)}\Big|_{\mu=M_1} + \delta\kappa^{(11)}, \tag{6.51}$$

where

$$\delta\kappa^{(11)} \simeq -\beta_{\kappa^{(11)}}\Big|_{\mu=M_1} \log\left(\frac{M_1}{m_H}\right) . \tag{6.52}$$

Following [108], the expression for the beta function can be written as:

$$\delta\kappa^{(11)} \simeq B_{1a}\kappa^{(a1)} + \kappa^{(1a)}B_{1a}^T + b\kappa^{(22)} , \tag{6.53}$$

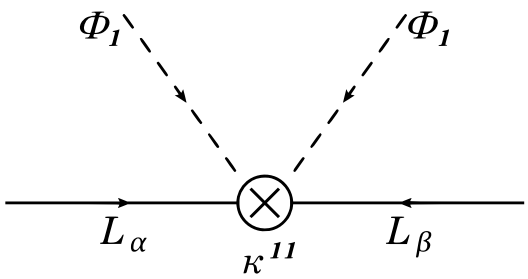

Figure 6.5: Feynman diagram for the effective operator $\kappa^{(11)}$ leading to active neutrino masses after EWSB.

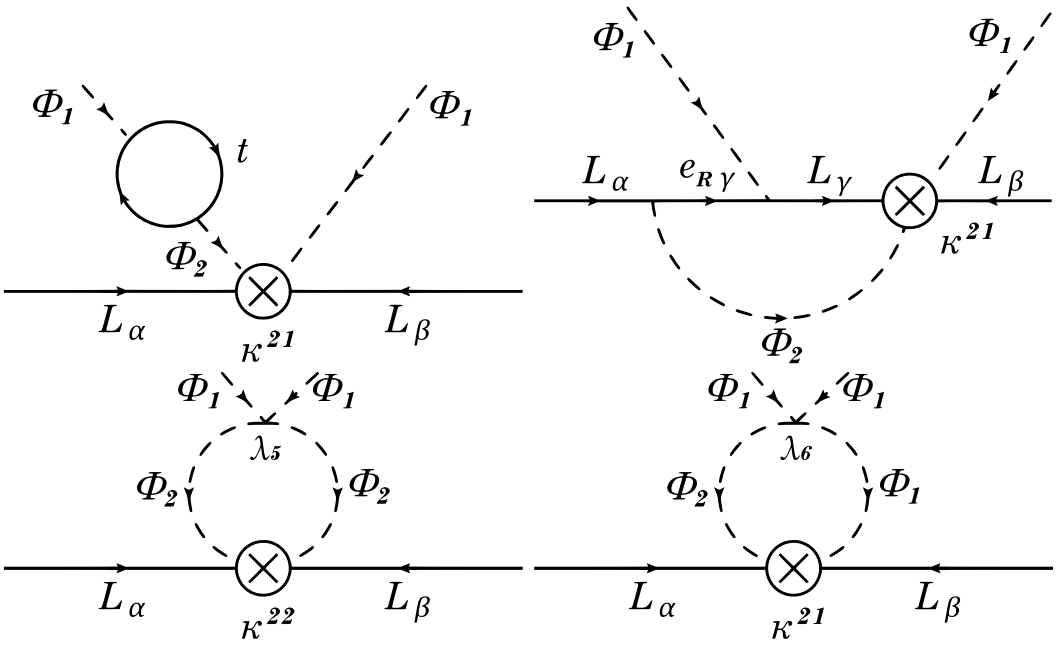

Figure 6.6: Corrections to the Wilson coefficients $\kappa^{(ab)}$ introducing operator mixing through the RG running.

showing the structure of the operator mixing from the energy-scale evolution, where the B_{1a} are 3×3 matrices and b is a number, which explicitly reads in the leading-log approximation:

$$b = -\frac{2\lambda_5}{16\pi^2}\log\left(\frac{M_1}{m_H}\right) \ , \tag{6.54}$$

depending on the λ_5 coupling in the scalar potential (see Eq. (6.2)). The loop-suppression is ameliorated through the large logarithm $\log(M_1/m_H)$ which comes from the separation between the seesaw scale M_1 and m_H. Assuming $\lambda_5 \sim \mathcal{O}(1)$ and heavy additional scalars $(\phi_2, \Phi_2^\pm, A_2)$ above the EW scale with $m_H \gg v$ one expects numerically,

$$b \simeq -0.3\,\lambda_5\,\log\left[\left(\frac{M_1}{10^{14}\,\text{GeV}}\right)\left(\frac{m_H}{10\,\text{TeV}}\right)^{-1}\right] \ . \tag{6.55}$$

The correction from the vertex renormalization term in Eq. (6.53) basically adds an additional term proportional to $b\,\vec{u}_L^{(2)} \otimes \vec{u}_L^{(2)T}$ to $\mathcal{M}_\nu$ in Eq. (6.50), enabling a mild neutrino mass hierarchy. The influence of the terms coming from the wave function renormalization in Eq. (6.53) is subdominant for a sizable λ_5 and neglected for the moment. The resulting active neutrino mass matrix $\mathcal{M}_\nu$ can be expressed in terms of mass parameters $\mathfrak{m}_{ab}$, similar to Eq. (6.42). For the alignment case $\tan\beta = 0$, they are:

$$\begin{aligned}
\mathfrak{m}_{11} &= -\frac{m_0}{(1-\cos^4\theta_L)}\frac{y_2^2}{\cos^2\theta_1}, \\
\mathfrak{m}_{22} &= -\frac{m_0}{(1-\cos^4\theta_L)}\frac{b\,y_1^2}{\cos^2\theta_2}, \\
\mathfrak{m}_{12} &= \mathfrak{m}_{21} = 0.
\end{aligned} \tag{6.56}$$

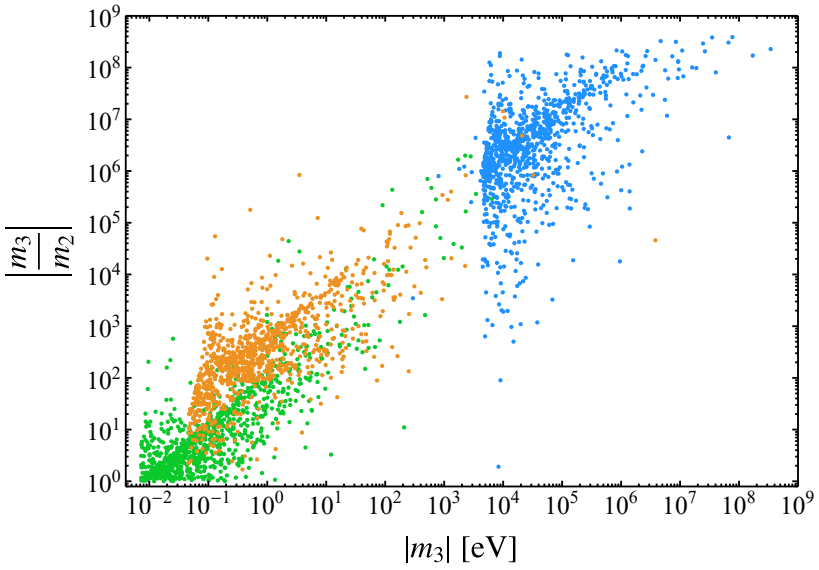

Figure 6.7: Same scenario as in Fig. 6.4, but considering the running between M_1 and $m_H = 10\,\text{TeV}$ for $\lambda_5 = 1$ while neglecting the influence of other couplings in Eq. (6.39). In this case the RG-induced operator mixing is clearly non-negligible.

Analogously to the previous section, the active neutrino masses can be obtained by using the tensor invariants in Eq. (6.44) and assuming a hierarchy between the mass eigenstates, such that

$$m_3 \simeq -m_0 \frac{y_1 y_2}{(1-\cos^4\theta_L)} \left[\frac{y_2}{y_1 \cos^2\theta_1} + \frac{b\, y_1}{y_2 \cos^2\theta_2}\right] , \tag{6.57}$$

which is proportional to the neutrino mass scale defined in Eq. (6.47), and can reproduce the observed values. The corresponding mass hierarchy reads:

$$\left|\frac{m_3}{m_2}\right| \simeq \frac{1}{\sin^2\theta_L} \left[\frac{y_2 \cos\theta_2}{\sqrt{b}\, y_1 \cos\theta_1} + \frac{\sqrt{b}\, y_1 \cos\theta_1}{y_2 \cos\theta_2}\right]^2 , \tag{6.58}$$

and is expected to be mild for similar-sized neutrino Yukawa couplings $y_1 \sim y_2$, generic misalignment angles in flavor space $\theta_1, \theta_2, \theta_L$, and assuming that $\lambda_5 \sim \mathcal{O}(1)$, such that $b \sim \mathcal{O}(1)$.

Including RG effects proportional to λ_5 mildens the overall neutrino mass hierarchy. The effect of the energy-scale evolution between M_1 and $m_H = 10\,\text{TeV}$ for $\lambda_5 = 1$ can be seen in Fig. 6.7, where otherwise the same choice of parameters is made as in Fig. 6.4.

In the case of a vanishing $\lambda_5 \ll 1$, a mild hierarchy can still be produced through RGE-induced operator mixing in Eq. (6.53) in the 3RHN scenario. A non-vanishing neutrino mass m_2 is generated beyond the leading-log approximation when solving the RGE in Eq. (6.38)

through the up-type Yukawa couplings. The corresponding mass parameters read,

$$\begin{aligned}
\mathfrak{m}_{11} &= -\frac{m_0}{(1-\cos^4\theta_L)}\frac{y_2^2}{\cos^2\theta_1}\left(1-\frac{6\tau y_t^2}{16\pi^2}+\frac{9\tau^2 y_t^4}{(16\pi^2)^2}\left(2+\cos^2\theta_t\right)\right),\\
\mathfrak{m}_{22} &= -\frac{m_0}{(1-\cos^4\theta_L)}\frac{y_1^2}{\cos^2\theta_2}\frac{9\tau^2 y_t^4}{(16\pi^2)^2}\cos^2\theta_t,\\
\mathfrak{m}_{12} = \mathfrak{m}_{21} &= -\frac{m_0}{(1-\cos^4\theta_L)}\frac{\cos^2\theta_L}{y_1 y_2\cos\theta_1\cos\theta_2}\frac{3\tau y_t^2}{16\pi^2}\left(1-\frac{6\tau y_t^2}{16\pi^2}\right)\cos\theta_t\,,
\end{aligned} \tag{6.59}$$

defining $\tau = \log\left(M_1/m_H\right)$ and neglecting contributions from quartic or gauge couplings. For simplification, both up-type Yukawa couplings $Y_u^{(a)}$ are assumed to be approximately rank-1 with similar-sized eigenvalues y_t and show misalignment characterized by the angle θ_t. With these assumptions $\mathrm{Tr}\left[Y_u^{(1)}Y_u^{(2)\dagger}\right] = y_t^2\cos\theta_t$. Using the tensor invariants in Eq. (6.44), the hierarchy between the active neutrino masses becomes:

$$\left|\frac{m_3}{m_2}\right| \simeq \frac{1}{\sin^2\theta_L(1-\cos^4\theta_L)}\left[\frac{y_2\cos\theta_2}{\sqrt{d}\,y_1\cos\theta_1}+\frac{\sqrt{d}\,y_1\cos\theta_1}{y_2\cos\theta_2}-2\cos^3\theta_L\right]^2, \tag{6.60}$$

where the lighter active neutrino is suppressed by

$$\begin{aligned}
d &\simeq \left(\frac{3y_t^2}{16\pi^2}\log\left(\frac{M_1}{m_H}\right)\cos\theta_t\right)^2,\\
d &\simeq 0.07\,y_t^2\left(\frac{\cos\theta_t}{0.6}\right)^2\log\left[\left(\frac{M_1}{10^{14}\,\mathrm{GeV}}\right)\left(\frac{m_H}{10\,\mathrm{TeV}}\right)^{-1}\right]^2,
\end{aligned} \tag{6.61}$$

which allows for mild mass hierarchies if the vectors in LHN flavor space are misaligned, while the up-type Yukawas lean towards alignment.

The analytical calculations are confirmed by numerical analysis. Fig. 6.8 shows that RGE-induced operator mixing with the up-type Yukawas $Y_u^{(a)}$ is able to ameliorate large neutrino mass hierarchies in the VEV alignment limit for vanishing λ_5 and aligned up-type Yukawa couplings. The effect is not as strong as from a sizable λ_5, but is still able to milden the hierarchy if the up-type Yukawas are aligned ($\cos\theta_t \simeq 1$) and have similar-sized eigenvalues.

6.5 Number of Physical Seesaw Parameters in the 2HDM

To determine the number of physical parameters in a scenario with an extended scalar sector, consider the following Lagrangian containing the RHNs (with family indices suppressed):

$$\mathcal{L}_N = \overline{L}i\not{\partial}L + \overline{e_R}i\not{\partial}e_R + \overline{N}i\not{\partial}N - \left(\overline{L}Y_e\Phi_1 e_R + \overline{L}Y^{(a)}\widetilde{\Phi}_a N + \frac{1}{2}\overline{N^c}MN + \mathrm{h.c.}\right), \tag{6.62}$$

which is invariant under $U(3)_N \times U(3)_L \times U(3)_e$ global transformations as long as $Y^{(a)} = Y_e = M = 0$ (with Higgs indices $a = 1, 2$). The charged leptons are assumed to couple only significantly to the Standard Model Higgs Φ_1 to simplify the discussion.

For general non-vanishing rank-1 Yukawas $Y^{(a)}$, a rank-1 RHN mass matrix, as well as a general Y_e matrix, the global $U(3)^3$ flavor symmetry is broken down to $U(1)_{\nu_1}$, when all

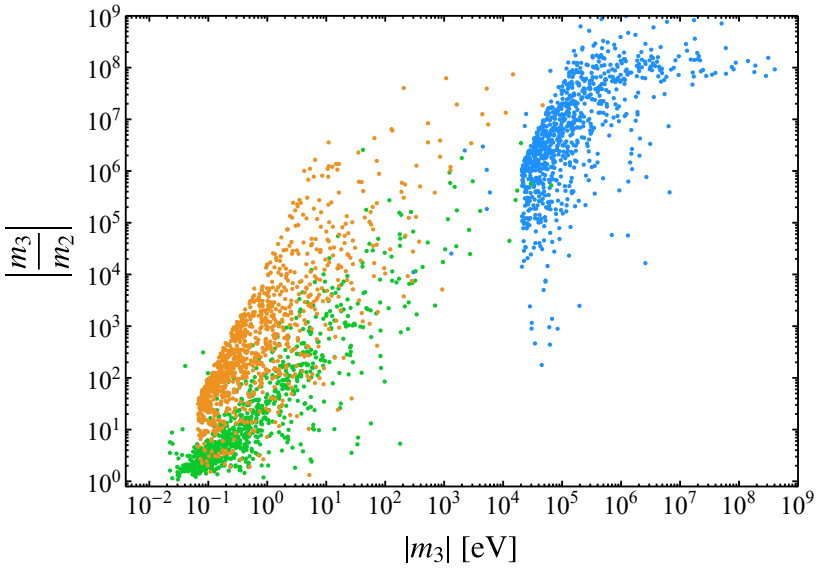

Figure 6.8: Parameter scan of the hierarchy of active neutrino masses $|m_3/m_2|$ against the largest active neutrino mass $|m_3|$ in the 2HDM, for parameter choices of y_2 and $\tan\beta$ as in Fig. 6.4. Mild neutrino mass hierarchies are possible for random misalignment angles, using $y_1 = 1$, $y_t = 1$, $\cos\theta_t = 1$ and $M_3 = M_P/\sqrt{8\pi}$ at $\Lambda = M_P$. Setting $\lambda_1 = \lambda_2 = 0.12$, while all other quartic couplings, including λ_5, are set to zero.

neutrinos, expect the lightest, become massive. (Neglecting the impact of quantum effects from the charged lepton and quark sector.)

At the high-energy scale, not all input parameters are necessarily physical parameters. The number of physical parameters can be found using the rule in Eq. (3.33). To employ this rule consider a general non-symmetric 3×3 rank-1 matrix which may be written as the tensor product of two different vectors

$$Y = \begin{pmatrix} a \\ b \\ c \end{pmatrix} \begin{pmatrix} d & e & f \end{pmatrix} = \begin{pmatrix} ad & ae & af \\ bd & be & bf \\ cd & ce & cf \end{pmatrix}, \tag{6.63}$$

where the following real parametrization can be introduced

$$\begin{aligned} a &= \sqrt{y}\cos\theta, & b &= \sqrt{y}\sin\theta\cos\phi, & c &= \sqrt{y}\cos\theta\sin\phi, \\ d &= \sqrt{y}\cos\vartheta, & e &= \sqrt{y}\sin\vartheta\cos\varphi, & f &= \sqrt{y}\cos\vartheta\sin\varphi, \end{aligned} \tag{6.64}$$

amounting to five real parameters $(y, \theta, \phi, \vartheta, \varphi)$. In the case of the rank-1 Majorana matrix, we have a general, symmetric 3×3 rank-1 matrix, which is just the tensor product of a vector with itself. Thus, for the rank-1 Majorana mass matrix there are only three parameters in a general basis (see Eq. (5.74)).

A general $U(n)$ matrix has $n(n-1)/2$ moduli, therefore breaking $U(3)^2 \to U(1)$ amounts to six broken real parameters. The number of physical parameters therefore becomes,

$$(9 + 5 + 5 + 3) \text{ parameters in total} - 9 \text{ broken real parameters} = 13 \text{ physical parameters}. \tag{6.65}$$

		rank $\left[Y_\nu^{(a)}\right]$		
		1	2	3
rank $[M]$	1	$U(1)_{\nu_1}$	nothing	nothing
	2	$U(1)_{\nu_1}$	nothing	nothing
	3	$U(1)_{\nu_1}$	nothing	nothing

Table 6.1: Residual groups after the breaking of the $U(3)_L \times U(3)_N$ flavor group by a non-vanishing neutral lepton sector in case of the 2HDM and 2ID1HDM (discussed in chapter 7) assuming generic misalignment. (Neglecting effects from the other SM fermion sectors.)

The calculation is in agreement with the identified parameters in the neutral lepton sector $(M_3, y_1, y_2, \theta_L, \theta_R, \theta_1, \theta_2)$, necessary to explain the active neutrino masses in the discussed 2HDM framework, plus parameters coming from the charged lepton sector (y_e, y_μ, y_τ) and three angles.

For each of the real parameters in $Y^{(a)}$, Y_e and M there can also be one phase. A general $U(n)$ matrix has $n(n+1)/2$ phases, therefore $U(3)^3$ has in total 18 complex phases. The residual symmetry $U(1)_{\nu_1}$ only has one phase. The number of physical phases amounts to

$$(9 + 5 + 5 + 3) \text{ phases in total} - 17 \text{ broken phase parameters} = 5 \text{ physical phases}, \quad (6.66)$$

which contains a Majorana phase and a CP violating phase from the neutral lepton sector and three CP violating phases coming from the charged lepton sector. A general overview of the $U(3)_N \times U(3)_L$ breaking, neglecting the couplings to other SM fermions, is given in Table 6.1.

6.6 Flavor-Changing Neutral Currents (FCNCs)

One generic feature of extending the Standard Model scalar sector with least one additional Higgs doublet are flavor-changing neutral currents (FCNCs) induced by the Yukawa couplings at tree-level [102]. FCNCs are tightly constrained and required to be small by observation. FCNCs are absent in the Standard Model since the diagonalization of the lepton and quark mass matrices also diagonalizes the respective Yukawa matrices.

In a general 2HDM, where quarks and leptons couple to both Higgs doublets via generic Yukawa interactions $Y_i^{(a)}$ (with $i = e, d, u, \nu$), both cannot be simultaneously diagonalized in general. Even if $Y_i^{(1)}$ is transformed into its flavor-diagonal frame, $Y_i^{(2)}$ will in general exhibit off-diagonal elements in the same frame. In general 2HDM scenarios, FCNCs are absent at tree-level if the Yukawa couplings fulfill the following commutator relations [111]:

$$\left[H^{(ab)}, H^{(cd)}\right] = 0, \qquad \left[F^{(ab)}, F^{(cd)}\right] = 0, \quad (6.67)$$

with $H^{(ab)} = Y_i^{(a)\dagger} Y_i^{(b)}$, $F^{(ab)} = Y_i^{(a)} Y_i^{(b)\dagger}$ and the Higgs indices $a, b, c, d = 1, 2$. Then, flavor is conserved at tree-level in the quark sector for $i = u, d$ and in the lepton sector for $i = e, \nu$. There are several other ways to circumvent tree-level FCNCs in two-Higgs doublet models without having Abelian H and F quantities which assume non-generic Yukawa structures. They are outlined briefly in the following:

- **Working in the alignment limit** [112], where both Yukawa couplings are aligned in the flavor space, such that $Y_i^{(1)} \propto Y_i^{(2)}$. In this way, the respective Yukawa interactions can be diagonalized simultaneously and FCNCs at tree-level are avoided. At higher loop-order, quantum corrections could still induce small flavor-changing neutral interactions. As shown in the calculations in Sec. 6.3, a certain amount of misalignment between the neutrino Yukawa couplings $Y^{(1)}$ and $Y^{(2)}$ is necessary to have sizable two-loop effects. The other Yukawa couplings in the theory could in principle still be aligned in flavor space if the *ad-hoc* assumption of alignment is maintained.

- **Working in the decoupling limit** [113], in which FCNCs are present at tree-level, but strongly suppressed and thus within the experimental bounds by setting the extra Higgs doublet far above the electroweak symmetry breaking scale. In this way, the heavy Higgs state decouples from the low-energy theory, but still can participate in the mass generation mechanism for the heavy right-handed neutrinos, where the decoupling limit does not apply. This scenario was considered in Sec. 6.4.

  FCNCs by the exchange of a Higgs at tree-level are then suppressed by $\mathcal{O}(v^2/m_H^2)$, where $v \simeq 246\,\text{GeV}$ is the electroweak scale and m_H is the scale of the heavy Higgs. After the heavy fields are integrated out, the light Higgs in the model behaves just like the Standard Model Higgs. No additional assumptions on Yukawa interactions or additional symmetries are necessary in order to suppress flavor effects within this framework.

- **Introducing inert Higgs doublets** that only couple to the right-handed neutrinos via Yukawa couplings by introducing an unbroken discrete Z_2 symmetry under which all Standard Model particles are left invariant. *Inert* because these doublets do not contribute to the spontaneous breaking of symmetry. One realization of this kind of model was introduced in order to explain the light neutrino masses via quantum effects and is well-known as the scotogenic model[3] [12]. In the next chapter, inert scalars charged under Z_2 (similar to [114]) are introduced which participate in the generation of radiative masses for the Z_2 charged right-handed neutrinos. The lightest particle stabilized by the unbroken discrete symmetry provides a dark matter candidate (the unbroken Z_2 also implies that both inert scalars do not acquire a vacuum expectation value).

[3] From the Greek word $\sigma\kappa\acute{o}\tau o\varsigma$, meaning darkness.

Chapter 7

Two-Loop Quantum Effects in Scotogenic Models

After discussing neutrino masses from Planck-scale lepton number breaking in the two-Higgs doublet model, an inert scalar scenario is considered. In order to have the same benefits of two scalars coupling to the right-handed neutrinos for the purpose of radiative generation of RHN masses, two new scalars are added to the SM particle spectrum. Following the philosophy of addressing more than one problem simultaneously with a single model, inert doublet models are intriguing because they also provide a viable dark matter candidate apart from explaining the origin of tiny neutrino masses.

7.1 The Two-Inert Doublet, One-Higgs Doublet Model

In this section, a set-up with neutrino-specific additional doublets η_a with the same gauge quantum numbers as the SM Higgs in the context of Planck-scale lepton number breaking is considered, following [4]. The SM symmetry group is extended by a discrete Z_2 symmetry under which all SM particles are even and the additional doublets η_a as well as the right-handed neutrinos N_i are odd:

$$\begin{aligned} \eta_a &\xrightarrow{Z_2} -\eta_a, \\ N_i &\xrightarrow{Z_2} -N_i, \\ \text{SM} &\xrightarrow{Z_2} +\text{SM}, \end{aligned} \tag{7.1}$$

where SM denotes all Standard Model fields, given in Table 2.1. The lightest Z_2-odd particle is then stabilized by the unbroken discrete symmetry and can be a viable WIMP (weakly interacting massive particle) dark matter candidate. This is similar to the well-known "scotogenic model" [12] which originally only involves one additional inert scalar η. For the dark matter phenomenology of the considered two-inert doublet, one-Higgs doublet model, see [115].

Typical for these kinds of models is that all lepton number violations involving SM particles only are absent at tree-level, but only occur at loop order. Adding one additional inert Z_2-odd scalar generically leads to milder neutrino mass hierarchies compared to the original realization [114, 116]. Since the additional doublets only couple to the RHNs in the Yukawa sector due to the discrete symmetry, FCNCs are also absent (see Sec. 6.6).

Field	Z_2	$U(1)_Y$	$SU(2)_L$	$SU(3)_c$
L_α	$+$	$-\frac{1}{2}$	$\underline{\mathbf{2}}$	$\underline{\mathbf{1}}$
e_{Ri}	$+$	-1	$\underline{\mathbf{1}}$	$\underline{\mathbf{1}}$
H	$+$	$\frac{1}{2}$	$\underline{\mathbf{2}}$	$\underline{\mathbf{1}}$
N_i	$-$	0	$\underline{\mathbf{1}}$	$\underline{\mathbf{1}}$
η_a	$-$	$\frac{1}{2}$	$\underline{\mathbf{2}}$	$\underline{\mathbf{1}}$

Table 7.1: Overview of the transformation behavior of the relevant fields in the scotogenic Planck-scale lepton number breaking scenario.

In the following, a concrete model involving two additional inert doublets and three right-handed neutrinos is studied. The three scalar doublets of the model and the three RHNs are reminiscent of the SM fermion sector's three family structure.

The scalar potential of the model can be separated into three parts:

$$V_{\text{pot}}(\Phi, \eta_1, \eta_2) = V_\phi(\Phi) + V_{\text{int}}(\Phi, \eta_1, \eta_2) + V_\eta(\eta_1, \eta_2), \tag{7.2}$$

where $V_\phi(\Phi)$ is the potential part of the SM scalar sector given in Eq. (2.5), $V_\eta(\eta_1, \eta_2)$ takes the same form as the most general 2HDM potential in Eq. (6.2), replacing Φ_a with η_a, and the interaction part takes the form:

$$\begin{aligned} V_{\text{int}}(\Phi, \eta_1, \eta_2) = &\frac{1}{2}\lambda_3^{(ab)} \left(\Phi^\dagger \Phi\right) \left(\eta_a^\dagger \eta_b\right) + \frac{1}{2}\lambda_4^{(ab)} \left(\Phi^\dagger \eta_a\right) \left(\eta_b^\dagger \Phi\right) \\ &+ \frac{1}{2}\lambda_5^{(ab)} \left[\left(\Phi^\dagger \eta_a\right) \left(\Phi^\dagger \eta_b\right) + \text{h.c.}\right], \end{aligned} \tag{7.3}$$

with dark scalar indices $a = 1, 2$. For the necessary and sufficient conditions on the quartic couplings for the existence of a stable vacuum for generic scalar potentials, see the algorithm presented in [117]. To ensure the Z_2 symmetry stays unbroken, the inert scalars must have a vanishing VEV: $\langle \eta_a \rangle = 0$.

The Lagrangian containing the newly introduced Z_2-odd particles reads:

$$\mathcal{L}_{\text{scoto}} = D_\mu \eta_a^\dagger D^\mu \eta_a + \frac{1}{2}\overline{N_i} i\partial\!\!\!/ N_i - \left(Y_{\alpha i}^{(a)} \overline{L_\alpha} N_i \widetilde{\eta}_a + \frac{1}{2} M_{ij} \overline{N_i^c} N_j + \text{h.c.}\right), \tag{7.4}$$

where N_i $(i = 1, 2, 3)$ are the RHN fields, L_α $(\alpha = e, \mu, \tau)$ are the lepton doublets and $\widetilde{\eta}_a = i\sigma_2 \eta_a^*$ denotes the charge conjugated dark scalar fields. The relevant particle content and its transformation behavior under the symmetries is summarized in Table 7.1.

The scalar sector of the model comprises of nine physical fields after the electroweak breaking of symmetry. Apart from the physical Standard Model Higgs h, there are two neutral and two charged scalar states for each of the inert scalars. If all the parameters in the scalar potential in Eq. (7.3) are assumed to be CP conserving, they must be real. A mixing between the CP-even η_{R_a} and CP-odd η_{I_a} parts of the neutral scalar field components $\eta_a^0 = (\eta_{R_a} + i\eta_{I_a})$ is absent in this case. Since both inert doublets share the same quantum

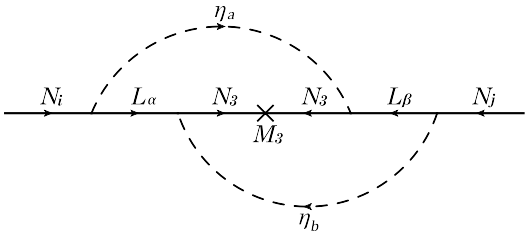

Figure 7.1: Leading two-loop diagram responsible for radiatively generating sizable right-handed neutrino masses in the inert doublet scenario.

numbers, changes of the basis leave the action invariant and it is possible, without loss of generality, to work in the basis where the mass matrix $(m_\eta)_{ab}$ is diagonal. In general, the 2×2 mass matrices for the real and imaginary neutral fields read after EWSB:

$$\left(M^2_{\eta_R}\right)_{ab} = \left(m^2_{\eta_a}\right)\delta_{ab} + \frac{v^2}{2}\left(\lambda_3^{(ab)} + \lambda_4^{(ab)} + \lambda_5^{(ab)}\right) = \left(M^2_{\eta^+}\right)_{ab} + \frac{v^2}{2}\left(\lambda_4^{(ab)} + \lambda_5^{(ab)}\right), \quad (7.5)$$

$$\left(M^2_{\eta_I}\right)_{ab} = \left(m^2_{\eta_a}\right)\delta_{ab} + \frac{v^2}{2}\left(\lambda_3^{(ab)} + \lambda_4^{(ab)} - \lambda_5^{(ab)}\right) = \left(M^2_{\eta^+}\right)_{ab} + \frac{v^2}{2}\left(\lambda_4^{(ab)} - \lambda_5^{(ab)}\right). \quad (7.6)$$

where M_{η^+} is the mass matrix of the charged inert scalars. Note that $M^2_{\eta_R} - M^2_{\eta_I} = v^2\lambda_5$. Using the simplifying assumption $m^2_{\eta_1}, m^2_{\eta_2} \gg v^2\lambda^{(ab)}_{3,4,5}$, two electrically neutral components have the mass m_{η_1} and another two have the mass m_{η_2}.

The right-handed neutrino mass matrix M is assumed to have a hierarchical mass spectrum at the cut-off Λ, $M_1 \ll M_2 \ll M_3$, such that it is well approximated by a rank-1 matrix. In this case, the tree-level masses of N_1 and N_2 at $\mu = \Lambda$ are effectively vanishing. Through two-loop quantum effects, the inert scalars produce non-vanishing masses for N_1 and N_2, proportional to M_3. The Feynman diagram responsible for these quantum corrections is given in Fig. 7.1. The generation of non-vanishing masses M_1 and M_2 in the inert scalar scenario is analogous to the one in the 2HDM case discussed in Sec. 6.3 and the resulting masses are given by Eq. (6.24).

7.2 Active Neutrino Masses in the Scotogenic Case

As in the previously investigated two-Higgs doublet model, the rank-1 ansatz for both neutrino Yukawa couplings $Y_\nu^{(1)}, Y_\nu^{(2)}$ in Eq. (7.4) is employed and the same parametrization as in Eq. (6.26) is used. Working with rank-1 couplings not just simplifies the analytical treatment, but can also be seen as a proxy for hierarchical Yukawa eigenvalues and demonstrates the predictivity of the considered models through parsimony in free parameters.

After the mass generation of the heavy right-handed neutrinos, all RHNs are integrated out at their respective mass scale. Below $\mu = M_1$ a Weinberg operator is obtained, corresponding to the neutrino mass generation diagram in Fig. (7.2) for the active neutrinos. The effective Lagrangian containing the dimension-5 operator reads:

$$\mathcal{L}_{\text{eff}} \simeq -\frac{1}{2}\sum_{\alpha,\beta}\kappa_{\alpha\beta}\left(\overline{L_\alpha}\widetilde{\Phi}\right)\left(\widetilde{\Phi}^T L^c_\beta\right) + \text{h.c.} \quad (7.7)$$

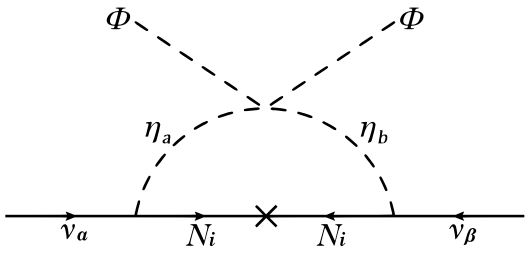

Figure 7.2: One-loop diagram responsible for the active neutrino masses in the scotogenic case with two inert doublets.

For multiple inert doublets, the coefficients of the effective operator take the following form

$$\kappa_{\alpha\beta} \simeq \sum_{a,b,k} \frac{Y^{(a)}_{\alpha k} Y^{(b)}_{\beta k} \lambda_5^{(ab)}}{16\pi^2} \frac{M_k}{m^2_{\eta_b} - M_k^2} \left\{ \frac{m^2_{\eta_b}}{m^2_{\eta_a} - m^2_{\eta_b}} \log\left(\frac{m^2_{\eta_a}}{m^2_{\eta_b}}\right) - \frac{M_k^2}{m^2_{\eta_a} - M_k^2} \log\left(\frac{m^2_{\eta_a}}{M_k^2}\right) \right\}, \tag{7.8}$$

working in the right-handed neutrino flavor basis in which the mass matrix M is diagonal. In general, the inert doublets are either lighter or heavier than the heavy radiative neutrino masses. In the generically expected case that $M_{1,2} \gg m_{\eta_{1,2}}$, the Wilson coefficients become

$$\begin{aligned} \kappa_{\alpha\beta} &\simeq -\sum_{a,b,k} \frac{Y^{(a)}_{\alpha k} Y^{(b)}_{\beta k} \lambda_5^{(ab)}}{16\pi^2} \frac{1}{M_k} \left\{ \frac{m^2_{\eta_b}}{m^2_{\eta_a} - m^2_{\eta_b}} \log\left(\frac{m^2_{\eta_a}}{m^2_{\eta_b}}\right) + \log\left(\frac{m^2_{\eta_a}}{M_k^2}\right) \right\}, \\ \kappa_{\alpha\beta} &\simeq -\sum_{a,b,k} \frac{Y^{(a)}_{\alpha k} Y^{(b)}_{\beta k} \lambda_5^{(ab)}}{16\pi^2} \frac{1}{M_k} \log\left(\frac{m^2_{\eta}}{M_0^2}\right), \end{aligned} \tag{7.9}$$

where in the second line, similar-sized inert doublet masses $m_{\eta_1} \simeq m_{\eta_2} = m_\eta$ are assumed and the radiative right-handed neutrino mass scale M_0, defined in Eq. (6.32), is used as an approximation for the generated masses M_1 and M_2 in the logarithm. After the electroweak breaking of the symmetry, Eq. (7.7) leads to the active neutrino Majorana mass term:

$$\mathcal{L}_{\text{eff}} \simeq -\frac{1}{2} \sum_{\alpha,\beta} (\mathcal{M}_\nu)_{\alpha\beta} \overline{\nu^c_\alpha} \nu_\beta + \text{h.c.}, \tag{7.10}$$

with[1]

$$(\mathcal{M}_\nu)_{\alpha\beta} \simeq \sum_{a,b,k} \frac{\lambda_5^{(ab)}}{32\pi^2} Y^{(a)}_{\alpha k} Y^{(b)}_{\beta k} \frac{v^2}{M_k} \log\left(\frac{m^2_\eta}{M_0^2}\right). \tag{7.11}$$

It is now straightforward to calculate the approximate expression for the largest active neutrino mass, using the rank-1 assumption for the Yukawa and RHN mass matrices, by following the same steps as in Sec. 6.4.1. The heaviest active neutrino mass becomes:

$$m_3 \simeq \text{Tr}(\mathcal{M}_\nu) \simeq -\frac{1}{4\pi^2} \frac{m_0 y_1 y_2}{(1 - \cos^4\theta_L)} \left(\frac{y_2 \lambda_5^{(11)}}{y_1 \cos^2\theta_1} + \frac{y_1 \lambda_5^{(22)}}{y_2 \cos^2\theta_2} - \frac{2\cos^3\theta_L \lambda_5^{(12)}}{\cos\theta_1 \cos\theta_2} \right) \log\left(\frac{m^2_\eta}{M_0^2}\right), \tag{7.12}$$

[1] The presented result differs from [12] and [114] by a factor of 2, which was noted in [118] and [116]. The convention for the VEV normalization used in [118] is $v = \langle\Phi\rangle$, whereas [116] uses $v = \langle\Phi\rangle/\sqrt{2}$, which this the same as used throughout this work. The obtained prefactor agrees with the one in [116].

which is proportional to the neutrino mass scale parameter in Eq. (6.47) and the one-loop suppression which is ameliorated by a large logarithm $\log(m_\eta^2/M_0^2)$. Assuming $\mathcal{O}(1)$ couplings for y_1, y_2 and $\lambda_5^{(ab)}$, m_3 in the ballpark of the experimentally observed values for generic misalignment angles. The corresponding neutrino mass hierarchy reads:

$$\left|\frac{m_3}{m_2}\right| \simeq \frac{[\mathrm{Tr}(\mathcal{M}_\nu)]^2}{\frac{1}{2}|\mathrm{Tr}(\mathcal{M}_\nu)^2 - \mathrm{Tr}(\mathcal{M}_\nu^2)|} \simeq \frac{\left[\frac{y_2}{y_1}\frac{\cos\theta_2}{\cos\theta_1}\lambda_5^{(11)} + \frac{y_1}{y_2}\frac{\cos\theta_1}{\cos\theta_2}\lambda_5^{(22)} - 2\cos^3\theta_L\lambda_5^{(12)}\right]^2}{\left[\lambda_5^{(11)}\lambda_5^{(22)} - \left(\lambda_5^{(12)}\right)^2\cos^4\theta_L\right]\sin^2\theta_L}\,. \tag{7.13}$$

Here, the same conclusions as in Sec. 6.4.1 hold, where misalignment in the LHN flavor space is necessary ($\sin\theta_L \neq 0$) to get a non-vanishing m_2. Apart from this, $\lambda_5^{(ab)}$ needs to have two non-vanishing eigenvalues, otherwise the neutrino mass matrix $\mathcal{M}_\nu$ stays rank-1. Interestingly, the inert scalars are not only the main ingredient for creating radiative masses for the heavy right-handed neutrinos via two-loop effects (see Fig. 7.1) in this model, but also participate in the radiative mass generation at one-loop level, see Fig. 7.2, for the left-handed neutrino sector.

The obtained analytical results are tested numerically by a random parameter scan, showing the hierarchy between the largest active neutrino masses $|m_3/m_2|$ vs. $|m_3|$ in Fig. 7.3. Assuming at the cut-off scale $\Lambda = M_P$: $M_3 = M_P/\sqrt{8\pi}$, $M_1 = M_2 = 0$ and $y_1 = y_2 = 1$. Taking $m_{\eta_1} = 100\,\mathrm{TeV}$ and $m_{\eta_2} = 2m_{\eta_1}$ for the inert doublet masses and $\lambda_5^{(11)} = \lambda_5^{(22)} = 1$, $\lambda_5^{(12)} = \lambda_5^{(21)} = 0$. The scan is performed over random angles between 0 and 2π in the flavor space.

Most points in the random scan are within $|m_3| = 0.01 - 0.1$ eV and the mass hierarchies are typically mild $|m_3/m_2| < 100$. It is thus possible to reproduce the experimentally observed neutrino parameters, making generic assumptions on the high-scale parameters.

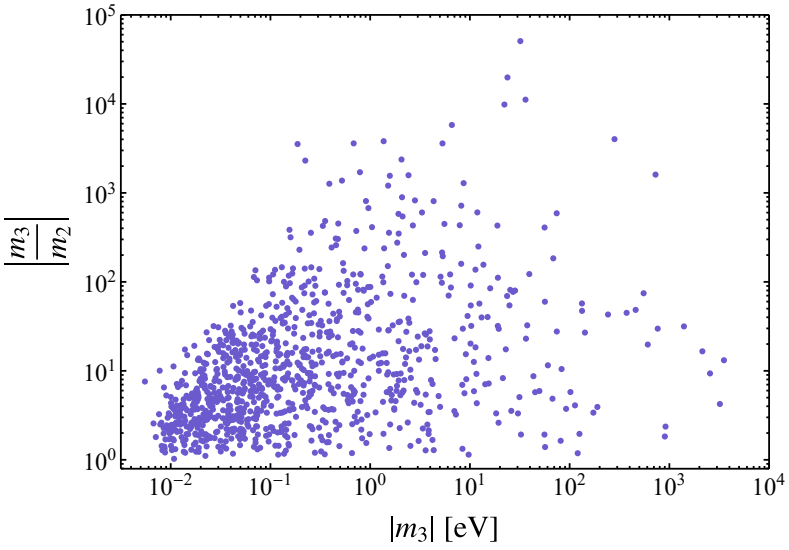

Figure 7.3: Numerical scan plot of the neutrino mass hierarchy of the two heavier active neutrinos $|m_3/m_2|$ vs. $|m_3|$ in the scotogenic Planck-scale lepton number breaking framework with two dark doublets. Taking at $\Lambda = M_P$: $M_3 = M_P/\sqrt{8\pi}$, $M_1 = M_2 = 0$, and assuming inert doublet masses $m_{\eta_1} = 100\,\text{TeV}$ and $m_{\eta_2} = 2m_{\eta_1}$. The neutrino Yukawa couplings have the eigenvalues $y_1 = y_2 = 1$ and the scan is performed over random misalignment angles in flavor space. For the quartic couplings $\lambda_5^{(11)} = \lambda_5^{(22)} = 1$ is assumed, setting all other quartic couplings to zero for simplicity.

Chapter 8

Conclusions

The origin of neutrino masses is one of the most important open questions of Particle Physics, requiring physics beyond the Standard Model. The overwhelming evidence from neutrino oscillation experiments shows that neutrino masses are tiny, albeit non-zero. This raises questions of the exact mechanism behind the generation as well as about their Dirac or Majorana nature. By introducing massive neutrinos into the SM, striking differences with respect to the rest of the fermion sector are observed in mass hierarchies between the particles and in the patterns of the mixing matrices (see chapter 2). All this suggests a different mass generation mechanism for neutrinos.

In this work, the idea of lepton number violation at a high-energy scale, like the Planck scale, was explored in different scenarios. Building on the type-I seesaw model (for a review see chapter 3), right-handed neutrinos with a hierarchical mass spectrum were introduced around the Planck scale. The lighter right-handed neutrino masses receive two-loop quantum corrections which dominate their tree-level masses. Introducing lepton number violation at Planck scale, the resulting quantum corrections can generate the well-known seesaw scale for sizable Yukawa couplings, avoiding the introduction of *ad-hoc* scales. These quantum corrections from the renormalization group evolution were analyzed in detail (see chapter 4) and shown that they can lead to a significant impact on the phenomenology within the type-I seesaw framework (independent of the scale at which the new physics is introduced). The leading-order quantum effects appear at the two-loop level, at which the corresponding beta functions have been studied. Usually, quantum corrections are expected to be small, but as a consequence of total lepton number violation by at least one massive right-handed neutrino, there is no protective symmetry for the lighter RHNs against large radiative corrections dominating their tree-level masses.

Within the Planck-scale lepton number violating scenario, at least one light neutrino mass within the ballpark of experimental values is predicted by making conservative assumptions. The lightest neutrino is suppressed by the Planck scale and is generically of order $\mathcal{O}(10^{-5})$ eV. In chapter 5, constraints on the high-energy parameters were worked out within a minimally extended SM, in order to reproduce the non-vanishing neutrino masses necessary to explain the neutrino oscillation data. In the most minimal scenario, one light neutrino is a pseudo-Dirac particle, while the others are Majorana, in order to be compatible with observations. If another sizable, right-handed neutrino mass is allowed, the light neutrinos can all be Majorana particles and explain the observations (see Sec. 5.2.1).

Furthermore, the two-loop quantum effects were investigated in two scenarios with an extended scalar sector. In the first scenario, one additional Higgs-like doublet (see chap-

ter 6) was considered and in the second, scotogenic scenario, the SM particle spectrum was extended by two inert scalar particles (see chapter 7). In both frameworks it was shown that two light neutrino masses in the ballpark of the experimental values and with the observed mild mass hierarchy can be generated, making reasonable assumptions on the high-scale parameters. For the extended scalar sector scenarios, the light neutrinos are Majorana particles. Flavor-changing neutral currents are avoided by either working within the decoupling limit or by making the newly introduced scalars inert. In the inert case, the dark doublets take part in two-loop generation of right-handed neutrino masses and in one-loop generation of the light-neutrino masses. One of the inert doublets provides a viable dark matter candidate.

Within the standard seesaw framework it is enough to have two right-handed neutrinos to explain the active neutrino masses, while the third RHN can be as heavy as the Planck scale. Through two-loop effects, the mass scale of the heaviest RHN and the lighter RHN masses, responsible for the active neutrino mass scale, are closely related when tree-level contributions are dominated by quantum corrections proportional to M_3. Through the washing-out of tree-level masses due to dominant radiative corrections, the effective number of parameters is reduced. The result is a higher overall predictivity of the model. The most minimal set-ups explaining the experimental observations for each scenario were explored in the spirit of parsimony. Since no assumptions on the flavor structures at high-energies are made, the expected mixing in the leptonic sector is neither small nor maximal, in accordance with experimental observations.

At least one light neutrino within the experimental ballpark $m_3 \simeq (16\pi^2)^2 v^2/M_P \simeq \mathcal{O}(0.1)\,\text{eV}$ with $\mathcal{O}(1)$ Yukawa couplings is predicted by the type-I seesaw with Planck-scale lepton number breaking scenario. Furthermore, by minimally extending the scalar sector, a mild hierarchy between the atmospheric and solar neutrino mass scale is generically expected. This suggests a possible link between Planck-scale physics and low-energy neutrino observables. The assumption of introducing lepton number violation at the Planck scale, as well as some possible motivations – apart from neutrino masses – are discussed in Sec. 5.5.

Solar and atmospheric neutrino oscillation experiments have shown that neutrino masses are non-vanishing and provide solid evidence for physics beyond the Standard Model. This work illustrates how the Planck scale is a phenomenologically viable option for the right-handed neutrino mass scale in seesaw models to explain the light neutrino masses observed in experiments. The general relevance of two-loop effects on RHN masses for the low-energy neutrino phenomenology is pointed out. The methods and models presented in this work may not only be of interest for the discussed Planck-scale lepton number violating framework, but may find broader applications and may also be incorporated into other models making use of the seesaw mechanism.

Acknowledgments

Above all, I would like to express my gratitude to my supervisor Prof. Alejandro Ibarra for giving me the opportunity to write my PhD thesis at his chair and for his ever kind support as well as countless helpful discussions and guidance over the years working together.

A special thank you also goes to all the people I've had the pleasure collaborating with: Takashi Toma, César Bonilla, and Johannes Herms. I am indebted to you for all the fruitful discussions, shared insightful expertise, and great working atmosphere.

Further, I want to thank my ever helpful and great colleagues at the T30d chair over the years, in particular Franz Zimma, Anja Brenner, Xabier Marcano, Andreas Rappelt, Sebastian Ingenhütt and Gonzalo Herrera-Moreno for sharing this time with me, as well as all my colleagues from the other theory chairs and from the SFB 1258. Another special thank you for her helpful administrative support and kindness goes to Karin Ramm.

My time during the doctoral studies would have not been the same without my great office mates over the years, Juan Cruz, Wenyuan Ai, Stephan Kürten, Philip Lüghausen, Nico Gubernari and Stefan Lederer, as well as all the people at the Physics Department I've come know on a personal level over the years and all the friendships that will last well beyond academia. On a personal level, I want to thank Julian Fischer and Matthias Stock, which I know since the first semester of my Physics studies for the great time.

Last but not least, I want to thank my parents, Georg and Waltraud as well as my dear brother Alexander for their support and love during my studies.

This work was supported by the collaborative research center SFB 1258.

Bibliography

[1] P. Strobl, *Mechanism of neutrino mass generation by Planck-scale lepton number breaking*, *Master's thesis, Technical University of Munich* (2018) .

[2] A. Ibarra, P. Strobl and T. Toma, *Neutrino masses from Planck-scale lepton number breaking*, *Phys. Rev. Lett.* **122** (2019) 081803 [1802.09997].

[3] A. Ibarra, P. Strobl and T. Toma, *Two-loop renormalization group equations for right-handed neutrino masses and phenomenological implications*, *Phys. Rev. D* **102** (2020) 055011 [2006.13584].

[4] C. Bonilla, J. Herms, A. Ibarra and P. Strobl, *Neutrino parameters in the Planck-scale lepton number breaking scenario with extended scalar sectors*, *Phys. Rev. D* **103** (2021) 035010 [2012.11567].

[5] K.S. Babu and R.N. Mohapatra, *Predictive neutrino spectrum in minimal $SO(10)$ grand unification*, *Phys. Rev. Lett.* **70** (1993) 2845 [hep-ph/9209215].

[6] D.-G. Lee and R.N. Mohapatra, *Automatically R-conserving supersymmetric $SO(10)$ models and mixed light Higgs doublets*, *Phys. Rev. D* **51** (1995) 1353–1361 [hep-ph/9406328].

[7] B. Bajc, G. Senjanović and F. Vissani, *$b-\tau$ Unification and Large Atmospheric Mixing: A Case for a Noncanonical Seesaw Mechanism*, *Phys. Rev. Lett.* **90** (2003) [hep-ph/0210207].

[8] Y. Grossman and M. Neubert, *Neutrino masses and mixings in non-factorizable geometry*, *Phys. Lett. B* **474** (2000) 361–371 [hep-ph/9912408].

[9] S.J. Huber and Q. Shafi, *Seesaw mechanism in warped geometry*, *Phys. Lett. B* **583** (2004) 293–303 [hep-ph/0309252].

[10] K. Agashe, S. Hong and L. Vecchi, *Warped seesaw mechanism is physically inverted*, *Phys. Rev. D* **94** (2016) [1512.06742].

[11] S. Dodelson and L.M. Widrow, *Sterile neutrinos as dark matter*, *Phys. Rev. Lett.* **72** (1994) 17–20 [hep-ph/9303287].

[12] E. Ma, *Verifiable radiative seesaw mechanism of neutrino mass and dark matter*, *Phys. Rev.* **D73** (2006) 077301 [hep-ph/0601225].

[13] P.-H. Gu, H.-J. He and U. Sarkar, *Dirac neutrinos, dark energy and baryon asymmetry*, *JCAP* **2007** (2007) 016–016 [0705.3736].

[14] L. Amendola, M. Baldi and C. Wetterich, *Quintessence cosmologies with a growing matter component*, *Phys. Rev. D* **78** (2008) 023015 [0706.3064].

[15] M. Fukugita and T. Yanagida, *Barygenesis without grand unification*, *Phys. Lett. B* **174** (1986) 45.

[16] V. Kuzmin, V. Rubakov and M. Shaposhnikov, *On anomalous electroweak baryon-number non-conservation in the early universe*, *Phys. Lett. B* **155** (1985) 36.

[17] G. Ballesteros, J. Redondo, A. Ringwald and C. Tamarit, *Standard Model—axion—seesaw—Higgs portal inflation. Five problems of particle physics and cosmology solved in one stroke*, *JCAP* **2017** (2017) 001–001 [1610.01639].

[18] E. Ma, T. Ohata and K. Tsumura, *Majoron as the QCD axion in a radiative seesaw model*, *Phys. Rev. D* **96** (2017) [1708.03076].

[19] P. Minkowski, $\mu \to e\gamma$ *at a Rate of One Out of* 10^9 *Muon Decays?*, *Phys. Lett.* **67B** (1977) 421.

[20] T. Yanagida, *Horizontal gauge symmetry and masses of neutrinos*, *Conf. Proc.* **C7902131** (1979) 95.

[21] R.N. Mohapatra and G. Senjanović, *Neutrino Mass and Spontaneous Parity Nonconservation*, *Phys. Rev. Lett.* **44** (1980) 912.

[22] J. Schechter and J.W.F. Valle, *Neutrino Masses in* $SU(2) \times U(1)$ *Theories*, *Phys. Rev.* **D22** (1980) 2227.

[23] M.D. Schwartz, *Quantum Field Theory and the Standard Model*, Cambridge University Press (2014).

[24] E.K. Akhmedov, *Do charged leptons oscillate?*, *JHEP* **2007** (2007) 116–116 [0706.1216].

[25] P. de Salas, D. Forero, S. Gariazzo, P. Martínez-Miravé, O. Mena, C. Ternes et al., *2020 Global reassessment of the neutrino oscillation picture*, 2006.11237.

[26] K. Abe, J. Amey, C. Andreopoulos, M. Antonova, S. Aoki, A. Ariga et al., *Combined Analysis of Neutrino and Antineutrino Oscillations at T2K*, *Phys. Rev. Lett.* **118** (2017) [1701.00432].

[27] S. Abe, T. Ebihara, S. Enomoto, K. Furuno, Y. Gando, K. Ichimura et al., *Precision Measurement of Neutrino Oscillation Parameters with KamLAND*, *Phys. Rev. Lett.* **100** (2008) [0801.4589].

[28] L. Whitehead, *Neutrino oscillations with MINOS and MINOS+*, *Nucl. Phys. B* **908** (2016) 130–150 [1601.05233].

[29] A.Y. Smirnov, *The MSW effect and solar neutrinos*, hep-ph/0305106.

[30] W. Grimus, *Neutrino Physics - Theory, from Lectures on Flavor Physics*, Springer Berlin Heidelberg (2004), DOI:10.1007/b98411, [hep-ph/0307149].

[31] Particle Data Group collaboration, *Review of Particle Physics*, *Phys. Rev. D* **98** (2018) 030001.

[32] I. Esteban, M.C. Gonzalez-Garcia, A. Hernandez-Cabezudo, M. Maltoni and T. Schwetz, *Global analysis of three-flavour neutrino oscillations: synergies and tensions in the determination of θ_{23}, δ_{CP}, and the mass ordering*, *JHEP* **2019** (2019) [1811.05487].

[33] F. Capozzi, E. Di Valentino, E. Lisi, A. Marrone, A. Melchiorri and A. Palazzo, *Global constraints on absolute neutrino masses and their ordering*, *Phys. Rev. D* **95** (2017) [1703.04471].

[34] C. Jarlskog, *A Basis independent formulation of the connection between quark mass matrices, CP violation and experiment*, *Z. Phys. C* **29** (1985) 491.

[35] C. Giganti, S. Lavignac and M. Zito, *Neutrino oscillations: The rise of the PMNS paradigm*, *PPNP* **98** (2018) 1–54 [1710.00715].

[36] B. Kayser, *Majorana neutrinos and their electromagnetic properties*, *Phys. Rev. D* **26** (1982) 1662.

[37] G. Barbiellini and G. Cocconi, *Electric Charge of the Neutrinos from SN1987A*, *Nature* **329** (1987) 21.

[38] M. Diwan, V. Galymov, X. Qian and A. Rubbia, *Long-Baseline Neutrino Experiments*, *Annu. Rev. of Nucl.* **66** (2016) 47–71 [1608.06237].

[39] C. Giunti and T. Lasserre, *eV-Scale Sterile Neutrinos*, *Annu. Rev. of Nucl.* **69** (2019) 163–190 [1901.08330].

[40] MiniBooNE collaboration, *Significant Excess of Electronlike Events in the MiniBooNE Short-Baseline Neutrino Experiment*, *Phys. Rev. Lett.* **121** (2018) 221801 [1805.12028].

[41] IceCube collaboration, *Searches for Sterile Neutrinos with the IceCube Detector*, *Phys. Rev. Lett.* **117** (2016) 071801 [1605.01990].

[42] G. Mangano, G. Miele, S. Pastor, T. Pinto, O. Pisanti and P.D. Serpico, *Relic neutrino decoupling including flavour oscillations*, *Nucl. Phys. B* **729** (2005) 221–234 [hep-ph/0506164].

[43] N. Aghanim, Y. Akrami, M. Ashdown, J. Aumont, C. Baccigalupi, M. Ballardini et al., *Planck 2018 results*, *A&A* **641** (2020) A6 [1807.06209].

[44] M. Archidiacono, S. Gariazzo, C. Giunti, S. Hannestad, R. Hansen, M. Laveder et al., *Pseudoscalar—sterile neutrino interactions: reconciling the cosmos with neutrino oscillations*, *JCAP* **2016** (2016) 067–067 [1606.07673].

[45] C. Kraus, B. Bornschein, L. Bornschein, J. Bonn, B. Flatt, A. Kovalik et al., *Final results from phase II of the Mainz neutrino mass search in tritium β decay*, *Eur. Phys. J. C* **40** (2005) 447–468 [hep-ex/0412056].

[46] E.W. Otten and C. Weinheimer, *Neutrino mass limit from tritium β decay*, *Rept. Prog. Phys.* **71** (2008) 086201 [0909.2104].

[47] KATRIN collaboration, *Improved Upper Limit on the Neutrino Mass from a Direct Kinematic Method by KATRIN*, *Phys. Rev. Lett.* **123** (2019) 221802 [1909.06048].

[48] J. Formaggio, *Project 8: Using Radio-Frequency Techniques to Measure Neutrino Mass*, *Nucl. Phys. B* **229-232** (2012) 371–375 [1101.6077].

[49] M. Galeazzi, F. Gatti, M. Lusignoli, A. Nucciotti, S. Ragazzi and M.R. Gomes, *The Electron Capture Decay of 163-Ho to Measure the Electron Neutrino Mass with sub-eV Accuracy (and Beyond)*, 1202.4763.

[50] K. Abazajian, K. Arnold, J. Austermann, B. Benson, C. Bischoff, J. Bock et al., *Neutrino physics from the cosmic microwave background and large scale structure*, *Astropart. Phys.* **63** (2015) 66–80 [1309.5383].

[51] S.R. Choudhury and S. Hannestad, *Updated results on neutrino mass and mass hierarchy from cosmology with Planck 2018 likelihoods*, *JCAP* **2020** (2020) 037–037 [1907.12598].

[52] M.J. Dolinski, A.W. Poon and W. Rodejohann, *Neutrinoless Double-Beta Decay: Status and Prospects*, *Annu. Rev. Nucl.* **69** (2019) 219–251 [1902.04097].

[53] M. Agostini, M. Allardt, A. Bakalyarov, M. Balata, I. Barabanov, L. Baudis et al., *Background-free search for neutrinoless double-β decay of ^{76}Ge with GERDA*, *Nature* **544** (2017) 47.

[54] KamLAND-Zen collaboration, *Search for Majorana Neutrinos Near the Inverted Mass Hierarchy Region with KamLAND-Zen*, *Phys. Rev. Lett.* **117** (2016) 082503 [1605.02889].

[55] S. Weinberg, *Baryon- and Lepton-Nonconserving Processes*, *Phys. Rev. Lett.* **43** (1979) 1566.

[56] W. Konetschny and W. Kummer, *Nonconservation of total lepton number with scalar bosons*, *Phys. Lett. B* **70** (1977) 433.

[57] T.P. Cheng and L.-F. Li, *Neutrino masses, mixings, and oscillations in $SU(2) \times U(1)$ models of electroweak interactions*, *Phys. Rev. D* **22** (1980) 2860.

[58] G. Gelmini and M. Roncadelli, *Left-handed neutrino mass scale and spontaneously broken lepton number*, *Phys. Lett. B* **99** (1981) 411.

[59] R. Foot, H. Lew, X.-G. He and G.C. Joshi, *See-saw neutrino masses induced by a triplet of leptons*, *Z. Phys. C* **44** (1989) 441.

[60] E. Ma, *Pathways to Naturally Small Neutrino Masses*, *Phys. Rev. Lett.* **81** (1998) 1171–1174 [hep-ph/9805219].

[61] B. Bajc and G. Senjanović, *Seesaw at LHC*, *JHEP* **2007** (2007) 014–014 [hep-ph/0612029].

[62] L. Wolfenstein, *Different varieties of massive Dirac neutrinos*, *Nucl. Phys. B* **186** (1981) 147.

[63] A. Baldini, Y. Bao, E. Baracchini, C. Bemporad, F. Berg, M. Biasotti et al., *Search for the lepton flavour violating decay $\mu^+ \to e^+\gamma$ with the full dataset of the MEG experiment*, *Eur. Phys. J. C* **76** (2016) 434 [1605.05081].

[64] A. Broncano, M. Gavela and E. Jenkins, *The effective Lagrangian for the seesaw model of neutrino mass and leptogenesis*, *Phys. Lett. B* **552** (2003) 177 [hep-ph/0210271].

[65] A. Santamaria, *Masses, mixings, Yukawa couplings and their symmetries*, *Phys. Lett. B* **305** (1993) 90–97 [hep-ph/9302301].

[66] J. Casas and A. Ibarra, *Oscillating neutrinos and $\mu \to e, \gamma$*, *Nucl. Phys. B* **618** (2001) 171–204 [hep-ph/0103065].

[67] A. Aparici, J. Herrero-Garcia, N. Rius and A. Santamaria, *On the Nature of the Fourth Generation Neutrino and its Implications*, *JHEP* **07** (2012) 030 [1204.1021].

[68] J. Casas, J. Espinosa, A. Ibarra and I. Navarro, *Naturalness of nearly degenerate neutrinos*, *Nucl. Phys. B* **556** (1999) 3–22 [hep-ph/9904395].

[69] J. Casas, J. Espinosa, A. Ibarra and I. Navarro, *General RG equations for physical neutrino parameters and their phenomenological implications*, *Nucl. Phys. B* **573** (2000) 652–684 [hep-ph/9910420].

[70] M.E. Machacek and M.T. Vaughn, *Two-loop renormalization group equations in a general quantum field theory (II). Yukawa couplings*, *Nucl. Phys. B* **236** (1984) 221.

[71] Y. Pirogov and O. Zenin, *Two-loop renormalization group restrictions on the standard model and the fourth chiral family*, *Eur. Phys. J. C* **10** (1999) 629–638 [hep-ph/9808396].

[72] F. Staub, *SARAH*, 0806.0538.

[73] F. Staub, *SARAH 4: A tool for (not only SUSY) model builders*, *Comp. Phys. Comm.* **185** (2014) 1773–1790 [1309.7223].

[74] K. Babu, C. Leung and J. Pantaleone, *Renormalization of the neutrino mass operator*, *Phys. Lett. B* **319** (1993) 191–198 [hep-ph/9309223].

[75] S. Antusch, M. Drees, J. Kersten, M. Lindner and M. Ratz, *Neutrino mass operator renormalization revisited*, *Phys. Lett. B* **519** (2001) 238–242 [hep-ph/0108005].

[76] S. Davidson, G. Isidori and A. Strumia, *The Smallest neutrino mass*, *Phys. Lett. B* **646** (2007) 100 [hep-ph/0611389].

[77] D. Choudhury, R. Gandhi, J. Gracey and B. Mukhopadhyaya, *Two-loop neutrino masses and the solar neutrino problem*, *Phys. Rev. D* **50** (1994) 3468 [hep-ph/9401329].

[78] K. Babu and E. Ma, *Natural Hierarchy of Radiatively Induced Majorana Neutrino Masses*, *Phys. Rev. Lett.* **61** (1988) 674.

[79] S. Petcov and S. Toshev, *Conservation of lepton charges, massive Majorana and massless neutrinos*, *Phys. Lett. B* **143** (1984) 175.

[80] J.A. Casas, A. Ibarra and F. Jiménez-Alburquerque, *Hints on the high-energy seesaw mechanism from the low-energy neutrino spectrum*, *JHEP* **2007** (2007) 064–064 [hep-ph/0612289].

[81] A. de Gouvêa and J.W.F. Valle, *Minimalistic neutrino mass model*, *Phys. Lett. B* **501** (2001) 115–127 [hep-ph/0010299].

[82] E.K. Akhmedov, Z.G. Berezhiani and G. Senjanovic, *Planck scale physics and neutrino masses*, *Phys. Rev. Lett.* **69** (1992) 3013 [hep-ph/9205230].

[83] V. Berezinsky, M. Narayan and F. Vissani, *Low scale gravity as the source of neutrino masses?*, *JHEP* **04** (2005) 009 [hep-ph/0401029].

[84] S.B. Giddings and A. Strominger, *Loss of incoherence and determination of coupling constants in quantum gravity*, *Nucl. Phys. B* **307** (1988) 854.

[85] S. Coleman, *Black holes as red herrings: Topological fluctuations and the loss of quantum coherence*, *Nucl. Phys. B* **307** (1988) 867.

[86] R.N. Mohapatra, *Physics of the neutrino mass*, *New J. Phys.* **6** (2004) 82–82 [hep-ph/0411131].

[87] L.M. Krauss and F. Wilczek, *Discrete gauge symmetry in continuum theories*, *Phys. Rev. Lett.* **62** (1989) 1221.

[88] L.F. Abbott and M.B. Wise, *Wormholes and Global Symmetries*, *Nucl. Phys.* **B325** (1989) 687.

[89] R. Kallosh, A. Linde, D. Linde and L. Susskind, *Gravity and global symmetries*, *Phys. Rev. D* **52** (1995) 912–935 [hep-th/9502069].

[90] S.W. Hawking, *Particle creation by black holes*, *Commun. Math. Phys.* **43** (1975) 199.

[91] R. Barbieri, J. Ellis and M.K. Gaillard, *Neutrino masses and oscillations in $SU(5)$*, *Phys. Lett. B* **90** (1980) 249.

[92] Y. Chikashige, R. Mohapatra and R. Peccei, *Are there real goldstone bosons associated with broken lepton number?*, *Phys. Lett. B* **98** (1981) 265.

[93] G. Ballesteros, J. Redondo, A. Ringwald and C. Tamarit, *Unifying Inflation with the Axion, Dark Matter, Baryogenesis, and the Seesaw Mechanism*, *Phys. Rev. Lett.* **118** (2017) [1608.05414].

[94] N. Okada and Q. Shafi, *Observable Gravity Waves From $U(1)_{B-L}$ Higgs and Coleman-Weinberg Inflation*, 1311.0921.

[95] N. Okada, V.N. Şenoğuz and Q. Shafi, *The observational status of simple inflationary models: an update*, *Turk. J. Phys.* **40** (2016) 150 [1403.6403].

[96] T. Higaki, R. Kitano and R. Sato, *Neutrinoful universe*, *JHEP* **2014** (2014) [1405.0013].

[97] U.J. Saldaña-Salazar, *The flavor-blind principle: A symmetrical approach to the Gatto-Sartori-Tonin relation*, *Phys. Rev. D* **93** (2016) 013002 [1509.08877].

[98] A. Masiero, S.K. Vempati and O. Vives, *See-saw and lepton flavour violation in SUSY SO(10)*, *Nucl. Phys. B* **649** (2003) 189–204 [hep-ph/0209303].

[99] A. Vicente, *Higgs Lepton Flavor Violating Decays in Two Higgs Doublet Models*, *Front. in Phys.* **7** (2019) [1908.07759].

[100] L. Fromme, S.J. Huber and M. Seniuch, *Baryogenesis in the two-Higgs doublet model*, *JHEP* **2006** (2006) 038–038 [hep-ph/0605242].

[101] J.M. Cline, K. Kainulainen and A.P. Vischer, *Dynamics of two-Higgs-doublet CP violation and baryogenesis at the electroweak phase transition*, *Phys. Rev. D* **54** (1996) 2451–2472 [hep-ph/9506284].

[102] G. Branco, P. Ferreira, L. Lavoura, M. Rebelo, M. Sher and J.P. Silva, *Theory and phenomenology of two-Higgs-doublet models*, *Phys. Rept.* **516** (2012) 1 [1106.0034].

[103] I.F. Ginzburg and I.P. Ivanov, *Tree-level unitarity constraints in the most general two Higgs doublet model*, *Phys. Rev. D* **72** (2005) [hep-ph/0508020].

[104] P. Ferreira and D. Jones, *Bounds on scalar masses in two Higgs doublet models*, *JHEP* **2009** (2009) 069–069 [0903.2856].

[105] P.H. Chankowski and Z. Płuciennik, *Renormalization group equations for seesaw neutrino masses*, *Phys. Lett. B* **316** (1993) 312 [hep-ph/9306333].

[106] S. Antusch, M. Drees, J. Kersten, M. Lindner and M. Ratz, *Neutrino mass operator renormalization in two Higgs doublet models and the MSSM*, *Phys. Lett. B* **525** (2002) 130 [hep-ph/0110366].

[107] W. Grimus and L. Lavoura, *Renormalization of the neutrino mass operators in the multi-Higgs-doublet standard model*, *Eur. Phys. J.* **C39** (2005) 219 [hep-ph/0409231].

[108] A. Ibarra and C. Simonetto, *Understanding neutrino properties from decoupling right-handed neutrinos and extra Higgs doublets*, *JHEP* **11** (2011) 022 [1107.2386].

[109] W. Grimus and H. Neufeld, *3-Neutrino mass spectrum from combining seesaw and radiative neutrino mass mechanisms*, *Phys. Lett. B* **486** (2000) 385–390 [hep-ph/9911465].

[110] A. Ibarra and A. Solaguren-Beascoa, *Lepton parameters in the see-saw model extended by one extra Higgs doublet*, *JHEP* **11** (2014) 089 [1409.5011].

[111] F.J. Botella, F. Cornet-Gomez and M. Nebot, *Flavor conservation in two-Higgs-doublet models*, *Phys. Rev. D* **98** (2018) 035046.

[112] A. Pich and P. Tuzón, *Yukawa alignment in the two-Higgs-doublet model*, *Phys. Rev. D* **80** (2009) [0908.1554].

[113] J.F. Gunion and H.E. Haber, *CP-conserving two-Higgs-doublet model: The approach to the decoupling limit*, *Phys. Rev. D* **67** (2003) [hep-ph/0207010].

[114] D. Hehn and A. Ibarra, *A radiative model with a naturally mild neutrino mass hierarchy*, *Phys. Lett.* **B718** (2013) 988 [1208.3162].

[115] V. Keus, S.F. King, S. Moretti and D. Sokolowska, *Dark matter with two inert doublets plus one Higgs doublet*, *JHEP* **2014** (2014) [1407.7859].

[116] P. Escribano, M. Reig and A. Vicente, *Generalizing the Scotogenic model*, *JHEP* **07** (2020) 097 [2004.05172].

[117] I.P. Ivanov, M. Köpke and M. Mühlleitner, *Algorithmic boundedness-from-below conditions for generic scalar potentials*, *Eur. Phys. J. C* **78** (2018) [1802.07976].

[118] A. Merle and M. Platscher, *Running of radiative neutrino masses: the scotogenic model — revisited*, *JHEP* **11** (2015) 148 [1507.06314].